

# Molecular Engineering of Multifunctional Metallophthalocyanine-Containing Framework Materials

Aylin Aykanat, Zheng Meng, Georganna Benedetto, and Katherine A. Mirica\*

Burke Laboratory, Department of Chemistry, Dartmouth College, Hanover, New Hampshire 03755, United States

**ABSTRACT:** The recent development of metallophthalocyanine (MPc)-based frameworks has opened the door to a new class of promising multifunctional materials with emergent electrical, magnetic, optical, and electrochemical properties. This perspective article outlines the process of molecular engineering—which uses the strategic selection and combination of molecular components to guide the assembly of materials and achieve target function—to demonstrate how the choice of MPc-based molecular components combined with the toolkit of reticular chemistry leads to the emergence of structure–property relationships in this class of materials. The role of complexity and emergence as core principles of molecular engineering of functional materials are discussed. Subsequent illustration of the molecular design criteria that stem from the unique optical, electrical, magnetic, and electrochemical features of MPc monomers sets the stage for achieving emergent function on the basis of the underlying properties of the constituent molecular building blocks. The review of strategies available for the controlled assembly of MPc monomers employing the principles of self-assembly and reticular chemistry serves as a guide for the attainment of enhanced control over relative position, orientation, and aggregation of MPcs building blocks, while creating opportunities to discover new emergent properties. The central focus on the advances in MPc-based framework materials shows how the electronic, photophysical, magnetic, and electrochemical properties in these materials emerge from molecular design principles that build on the initial properties embedded in MPc-based building blocks. Concluding remarks summarize accomplishments and pave the way for future directions.

## INTRODUCTION

**Complexity and Emergence as Core Features of Molecular Engineering.** Innovations in materials have shaped the development of civilizations. Each historical step towards mastery over stone, copper, bronze, iron, silicon, and organic matter has introduced tools and methods that have surmounted societal challenges and increased the technological complexity of the society.<sup>1, 2, 3</sup> Today, innovation in materials design for targeted applications continues to be critically important for ensuring sustainability of our global resources and safeguarding the health and longevity of the human population.<sup>4</sup>

Historically, chemistry has aimed to predict and direct the properties of molecules and materials for specific functions.<sup>5</sup> Many initial efforts in controlling properties of materials have largely relied on top-down approaches for sculpting and modifying existing bulk structures.<sup>6, 7, 8</sup> However, recent efforts based on molecular engineering—the process of constructing materials from atoms and molecules with targeted function—hold promise for controlling the structure–function relationships in new materials with atomic precision. Molecular engineering of new materials requires understanding of factors that influence the organization of structural components across a number of length scales—from atomic to macroscopic—coupled with the understanding of the structure–function relationships that *emerge* from the increased *complexity* of the materials architecture relative to its constituent components (Figure 1). Thus, utilizing the principles of molecular design and engineering for the advancement of

materials, where optimization of performance toward functional systems can be rationally attained from atomically precise molecular components, has the potential to develop complex, emergent and multifaceted function.

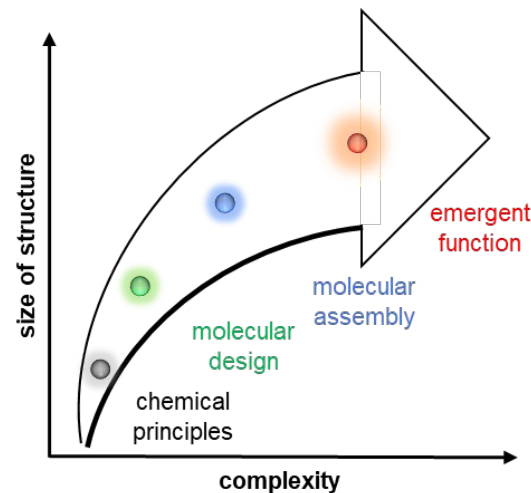


**Figure 1.** Molecular engineering requires mastery of complexity and emergence with the goal of programming and controlling structure–function relationships in materials and devices.

Since increasing complexity is an established strategy for achieving emergence of novel properties,<sup>9</sup> molecular engineering requires mastery of complexity<sup>5</sup> and emergence<sup>9</sup> with the goal of predicting and controlling structure–function relationships in materials and devices. A complex system is one in which the number of independent

1 interacting components is sufficiently large to achieve  
 2 emergence of function, and one whose function is very  
 3 sensitive to small structural perturbations.<sup>5</sup> In functional  
 4 materials, complexity often scales with size; therefore,  
 5 emergent function of materials is expected to be size-  
 dependent (**Figure 1**).

6 Currently, the principles of molecular engineering for  
 7 achieving one desired structure–property relationship at a  
 8 time in certain classes of materials are relatively well-  
 9 established.<sup>10, 11, 12, 13, 14</sup> For instance, the molecular design  
 10 criteria for band gap engineering in graphene<sup>15</sup> and in  
 11 conductive polymers,<sup>12, 14, 16</sup> for improvement of energy  
 12 conversion technology,<sup>17</sup> crystal engineering of stability in  
 13 explosives,<sup>18</sup> semiconductor spintronics,<sup>19</sup> design of  
 14 topology and porosity in network solids,<sup>20</sup> enhancement of  
 15 electrocatalysis,<sup>21</sup> and integration of conductivity in hybrid  
 16 systems<sup>22</sup> have established principles for achieving and  
 17 optimizing structure–property correlation in a material.  
 18 However, molecular engineering of multifunctional  
 19 materials, where more than one property is designed to co-  
 20 exist for fine-tuning specific function, are significantly less  
 21 developed. Our overarching goal in this perspective is to  
 22 illustrate—through several examples—how molecular  
 23 engineering of multifunctional materials can be achieved by  
 24 starting with multifunctional molecular precursors.  
 25 Although extending such principles to further attain  
 26 rationally designed emergent function in devices becomes  
 27 more difficult to achieve as the role of material/device  
 28 interfaces, defects, impurities, and sensitivity to other  
 29 physical parameters may be more difficult to predict and  
 30 control, recent examples suggest that rigorous and  
 31 systematic studies in this area can lead to transformative  
 32 outcomes.

**General Process of Molecular Engineering.** The process of molecular engineering is grounded in the fundamental understanding of chemical principles at the interfaces of organic, inorganic, and physical chemistry. Beginning this process requires an understanding of electronic structure and principles of chemical synthesis in order to facilitate an emergent system. Armed with these tools on the molecular level, the process proceeds to the molecular design of desired structure–property correlations through strategic perturbations to the molecular structure. The path towards emergent function follows through the tools available for molecular assembly beyond the molecule, such as molecular self-assembly or chemical synthesis with nanoscale control (**Figure 1**). Emergent function of the resulting assembly is then tested in reference to the initial molecular precursors in terms of the structure–function correlations. In this perspective article, we show examples of how attaining multifunctional emergent function can be achieved by starting with multifunctional molecular building blocks.

**Molecular Design and Self-assembly as Critical Steps Toward Emergent Properties.** While designing and selecting precursors to engineer a multifunctional material, it is necessary to decide on the chemical and physical properties one aims to introduce within the material, and how both the chosen building blocks and their combination can lead to the emergence of those properties. Once a target material with chosen properties is designed, one can harness fundamental chemical principles, such as self-assembly, coordination chemistry or dynamic covalent chemistry, to direct the assembly and embed desired functionalities with synergistic and adjustable metrics required for emergent function (**Figure 2**).

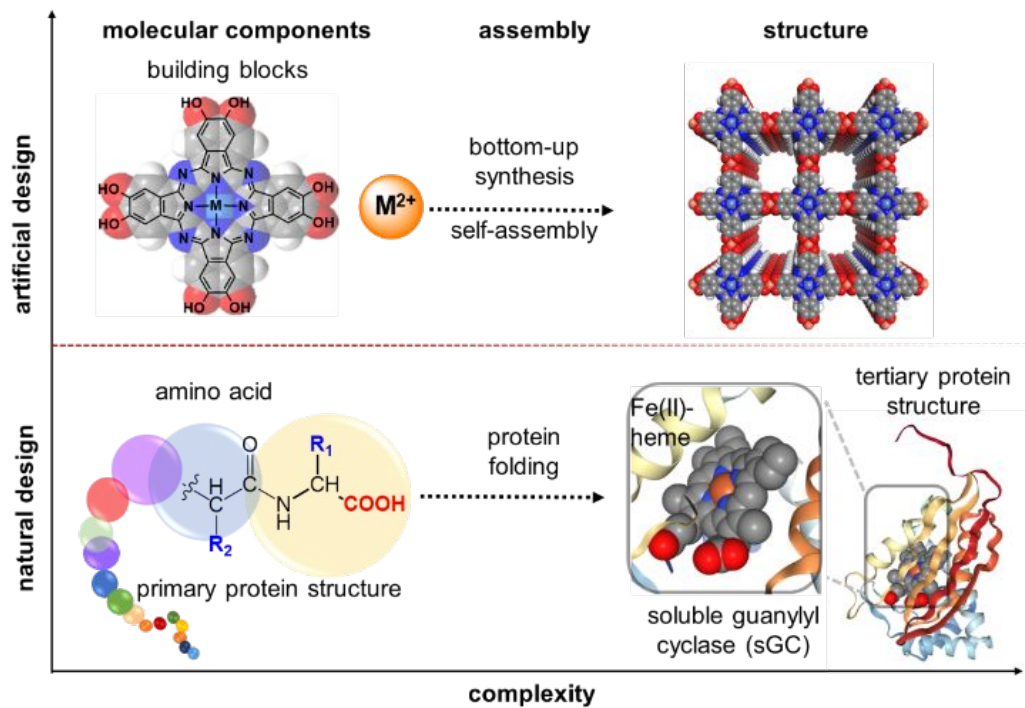


**Figure 2.** Comparison of using the principles of rational design and molecular engineering to embed desired structure–property relationships to design principles employed by nature.

Molecular self-assembly is the organization of components in which atoms or molecules arrange themselves into ordered structures through relatively weak and reversible intermolecular interactions.<sup>23</sup> This complex phenomenon plays a central role in many biological processes such as cellular mitosis and the folding of proteins (**Figure 2**).<sup>23</sup> The use of self-assembly to generate synthetic materials requires judicious choice of their molecular building blocks and their functional heteroatoms.<sup>24, 25</sup> This technique for the fabrication of functional nano-systems is beginning to be used more frequently, as it offers relatively straightforward routes to complex systems through design and synthetic execution. The functionalization and rational substitution of organic linkers enable the use of non-covalent interactions, such as hydrogen-bonding, van der Waals, electrostatic, or coordination bonding.<sup>23, 26</sup> Different types of hierarchical self-assemblies, from nano- to microscopic scales, including oligomers, D-A conjugates, wires, columns, and liquid-crystalline blends, have also been demonstrated using these techniques.<sup>27, 28, 29, 30</sup>

**Scope and Aims of this Perspective.** This perspective highlights recent trends in molecular engineering of multifunctional framework materials: metal-organic frameworks (MOFs) and covalent organic frameworks (COFs). Although crystal engineering principles have provided a solid foundation to investigate topological and morphological control over MOFs and COFs by variation of the geometrical orientations of the building blocks,<sup>31</sup> the tailored design and emergence of multifunctional performance characteristics within the final structure is still in development. The use of reticular synthesis, first defined by Yaghi *et al.* in 2003,<sup>25</sup> has made it possible to implement molecular design principles and strategic selection of secondary building units to direct the assembly of frameworks with ordered structures. In contrast to initial reports of framework materials that have largely focused on the engineering of their porosity, recent discoveries of redox active and conductive framework materials have enabled the synergistic integration of reticular synthesis with bottom-up design of conductive and ordered polymeric structures, where sensing,<sup>32, 33, 34</sup> catalytic function,<sup>35, 36</sup> gas capture, and charge storage capacity<sup>37</sup> can be controlled electronically leading to emergence of multifunctionality. The molecular design of such multifunctional framework materials has largely relied on molecular building blocks that have the characteristics of being planar, highly conjugated, and redox active. One of such molecular building blocks that has been successfully embedded within frameworks to generate a synergistic combination of multifunctional and electrochemically active materials is metallophthalocyanine (MPc).

This class of molecular building blocks constitutes an important category of multifunctional materials and has the

potential to draw on bioinspired design principles based on structural similarity between MPcs (**Figure 3**) and metalloporphyrins (MPys). As MPys are ubiquitous in nature as multifunctional redox-active molecular recognition systems, they have been adapted in synthetic systems to mimic biological systems through functions in light harvesting,<sup>38</sup> chemical sensing,<sup>39</sup> and catalysis.<sup>40</sup> This perspective outlines the general progress of molecular engineering with distinct components of molecular design, molecular assembly, and assessment of emergent function in the context of MPc-based functional materials. We select MPc-based framework materials as a representative class of multifunctional materials for demonstrating the principles of molecular engineering because these materials can be constructed from the bottom up using atomically precise, yet extremely modular multifunctional building blocks (**Table 1**).

We focus on the emergence of conductivity and electrochemically active function in MPc-containing framework materials with increasing complexity of the system in the context of multifaceted applications. Towards this goal, this perspective aims to: (1) summarize molecular design criteria for achieving structure-function relationships using MPc building blocks and highlight strategies for achieving complexity and emergence using these structural units in the context of light-matter interactions, charge transport, magnetism, electronically transduced chemical sensing, and catalytic function within electrochemically active systems; (2) discuss the unique physical and chemical properties of MPc-based molecular materials as a function of their molecular structure, supramolecular assembly, and reticular organization as well as illustrate how reticular chemistry can capitalize on these intrinsic properties to amplify MPc's utility as functional materials through complexity and emergence; (3) generalize these findings to illustrate how the principles of molecular engineering can enable the design of multifunctional frameworks materials. We conclude by pointing out gaps in the fundamental understanding of MPc-based materials and offering a perspective on the future direction in the molecular engineering of MPc-containing framework materials.

This perspective excludes ideas of molecular engineering of framework materials focused primarily on pore size control for optimizing gas storage or uptake. Although extremely promising examples of MPc post-synthetically modified frameworks and composite materials<sup>41</sup> exist, they are outside the scope of this perspective. Readers who are interested in MPc-based molecular materials are encouraged to refer to the following reviews and books for authoritative views on synthetic access to MPcs,<sup>42, 43, 44</sup> MPc-based hybrid composite materials with carbon nanostructures,<sup>26</sup> and their use in various applications.<sup>30, 45, 46, 47</sup>

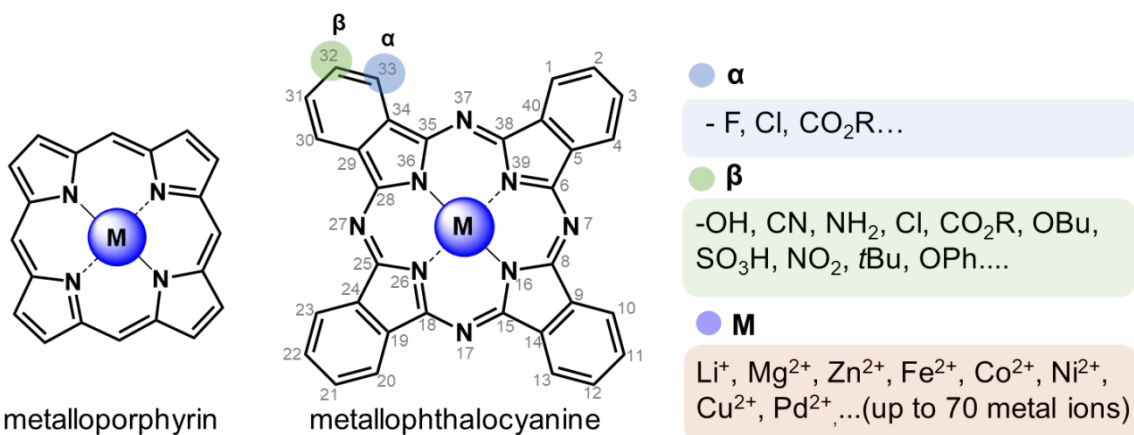


**Figure 3.** Chemical structures of metalloporphyrin and metallophthalocyanine and possible substitution positions and functional groups.

**Unique Features of MPcs.** MPcs are structurally analogous to MPys and have a highly conjugated 18  $\pi$ -electron system with four isoindole units linked together through nitrogen atoms (Figure 3). The combination of aromaticity in an extended  $\pi$ -system endows MPcs with exceptional electronic, optical, and redox properties, which have been harnessed in a wide range of applications in electronic devices,<sup>48, 49</sup> photodynamic therapy,<sup>50</sup> artificial photosynthesis,<sup>51, 52</sup> and catalysis.<sup>53</sup> MPcs have important electronic and photophysical properties that result from  $\pi \rightarrow \pi^*$  (HOMO to LUMO) electronic transitions. As a result, MPcs exhibit intense Q absorption bands centered at 600–800 nm<sup>54</sup> and moderate HOMO–LUMO gap of around 2 eV.<sup>55</sup> The use of metal ions with unpaired electrons can endow MPcs with a magnetic moment,<sup>56</sup> leading to fascinating magnetic properties, such as long-range ferromagnetic coupling.<sup>57</sup> Remarkably, considerable optimization over the optical, electronic, and physical properties at the molecular level can be achieved by numerous chemical modifications of MPcs (Figure 3), through the addition of peripheral substitution with electron withdrawing/donating groups, exchanging the metal center, and addition of sterically bulky or long hydrocarbon chains.<sup>46</sup> MPcs have  $D_{4h}$  symmetry, which predetermines their commonly adopted square or cubic type arrangements in the solid state.<sup>58</sup> The strong  $\pi$ – $\pi$  interactions resulting from the large aromatic system of MPcs can lead to cofacial stacking (H-aggregate) or head-to-tail arrangement (J-aggregates).<sup>26, 28</sup> The unique molecular symmetry, together with the planar aromatic skeleton of MPc, allows predictable control of their spatial position and orientation with atomic precision. The incorporation of MPc-based building blocks into materials does not solely add up the unique chemical and physical properties that molecular MPcs possess; their arrangement by supramolecular interactions, coordination bonds, and covalent bonds in two- and three-dimensions can further enhance those properties and generate emergent multifunctionality.<sup>59</sup>

Although MPcs have been utilized as the analogs of MPys, MPcs possess several unique features and advantages. *First*, MPcs are more synthetically accessible than MPys and can be made in large quantities through the

cyclotetramerization of various phthalic acid derivatives including phthalonitrile, diiminoisoindole, phthalic anhydride, and phthalimides.<sup>44</sup> Synthetic availability and tunability of MPc is an important prerequisite for fundamental investigation of structure–property relationships of molecular systems and strategic design of more complex materials with emergent function. *Second*, MPcs generally have higher thermal stability than MPys, which may be related to their additional benzene ring peripherally fused over each of the four pyrrole units, giving a larger conjugated aromatic structure and more rigid conjugated structure. This feature is also advantageous for their use in devices that require high temperature operation.<sup>30, 60</sup> *Third*, MPcs' larger aromatic structure can lead to relatively low HOMO–LUMO gaps and wider absorption in the visible and near-infrared regions.<sup>46, 49, 61, 62</sup> The aforementioned features in MPcs are particularly advantageous for the fabrication of small band gap and photovoltaic materials. *Fourth*, MPcs have stronger propensity to adopt horizontal orientations on substrates than MPys, leading to high charge–carrier mobility and relatively longer exciton diffusion length in devices. This phenomenon can be ascribed to the strong tendency for MPcs to cofacially stack (H-aggregate),<sup>63</sup> in contrast MPys can exhibit head-to-tail molecular stacking (J-aggregate) that leads to energy migration.<sup>64, 65</sup>

**Unique Features of MPc-based Framework Materials.** Framework systems have become one of the most actively investigated materials that have found potential in multiple disciplines including gas storage, catalysis, and more recently, gas sensing.<sup>66</sup> Self-assembled MOF and COF systems built from the bottom up allow for the insertion of these multifunctional properties through the strategic choice of their constituent building blocks. Many initial MOF systems were built using principles of reticular chemistry using secondary building units (SBUs) of a given geometry and connectivity that strongly coordinated to benzene based carboxylates, imidazoles, catechols and thiol functionalized linkers<sup>67</sup> to direct the structure, composition and topology. The original application of these highly porous and rigid framework structures were mainly gas storage and separation,<sup>68</sup> where

much focus has been dedicated to pore volume engineering and functionalization of internal surface chemistries<sup>66</sup> to improve separation and retention of specific gases.<sup>68</sup> Isolation of graphene in 2004 has catalyzed research activity in multifunctional 2D materials, and has led to a profound recognition that synthetic access to new conjugated linkers that could lead to the self-assembly of graphene analogs through coordination bonds. Soon after, researchers were able to gain access and establish unique multifunctional properties within 2D framework materials, such as conductivity,<sup>66, 69</sup> electrocatalytic activity,<sup>69</sup> photocatalysis,<sup>70</sup> light harvesting capabilities<sup>71</sup> and enhanced selectivity in gas sequestration.<sup>72</sup> Already hailed for their optical, electronic, and redox-active properties coupled with great synthetic modularity and established ability to undergo self-assembly and engage in coordination bonds, triphenylene (TP)-based<sup>73, 74, 75</sup> and benzene-based<sup>78</sup> linkers, have found their way into framework materials to generate remarkable conductivity coupled with catalytic, sensing, and energy storage function.<sup>22, 69, 76, 77</sup> Computational studies have calculated that the bulk material of multi-layered TP-based MOFs possess metallic conductivity, similar to graphene,<sup>78</sup> where increasing interlayer spacing can induce changes in band structure.<sup>69</sup> Subtle changes in the composition of the ligand and metal can also dramatically influence the physical and chemical properties of the frameworks (i.e., stacking of layers and presence of interfaces and defects within the bulk), which can in turn affect their electronic properties.<sup>22, 69, 77</sup>

As MPcs themselves possess several multifunctional features as those described above, it seems reasonable to

assume that these building blocks will form frameworks with exceptional and synergistic multifunctional properties. Amongst tunable 2D MOFs and COFs, MPc-based frameworks exhibit several competitive metrics and features, with great potential for further refinement. These features largely stem from the fact that the bulk, thin film, and nanowire forms emerging from MPc-based molecular architectures exhibit remarkable properties—unique light-matter interactions,<sup>45</sup> charge transport,<sup>55</sup> magnetism,<sup>57</sup> and electrocatalytic function<sup>79</sup>—with established molecular design principles for modulating these properties through straightforward changes in molecular structure (Table 1).<sup>80, 81</sup> The ability of MPc-frameworks to acquire, for instance, unique light harvesting capacity is due to their preference for stacked orientation and excellent  $\pi$ - $\pi$  overlap of the MPc units. In fact, many of the emergent properties (low HOMO-LUMO gap, fine tunable optical absorbance, and photoconductivity) arise from MPc's tendency to form aggregates and stacks through  $\pi$ - $\pi$  aromatic interactions in an eclipsed fashion to accommodate extended  $\pi$ -systems and to enable out of plane charge transfer.<sup>43, 47, 82</sup> Capitalizing on the established design principles by embedding MPc multifunctional building blocks into novel architectures within framework materials presents a unique opportunity for fundamental studies of complexity and emergence.

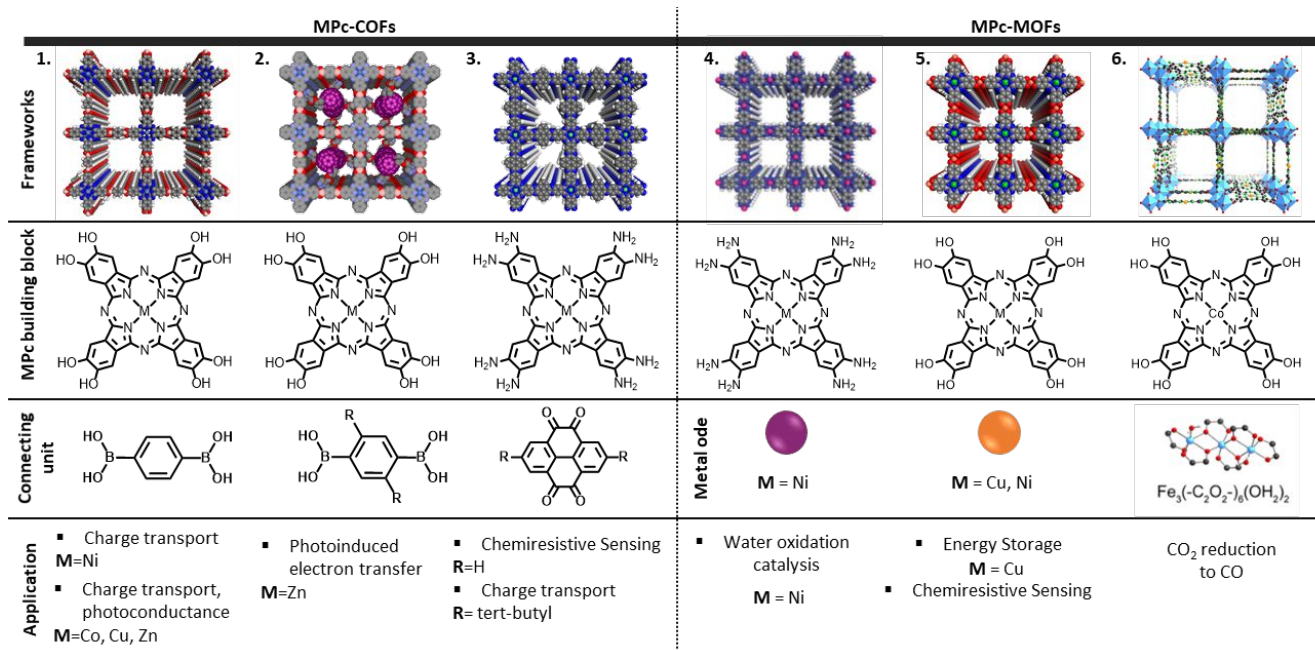


**Table 1.** Highlight of several MPc-COF and MPc-MOFs showcased in this perspective. References for structures reprinted or adapted from the following: Structure 1. adapted with permission from references<sup>83</sup> Copyright 2010 Springer Nature. 2. Reprinted with permission from reference<sup>84</sup> Copyright 2014 American Chemical Society. 3. Reprinted with permission from reference<sup>33</sup> Copyright 2019 American Chemical Society. 4. Reproduced with permission from reference<sup>85</sup> Copyright 2017

Royal Chemistry. 5. Reprinted with permission from reference <sup>34</sup> Copyright 2019 American Chemical Society. 6. Reprinted with permission from reference <sup>36</sup>. Copyright 2019 American Chemical Society.

## STRUCTURE-FUNCTION RELATIONSHIPS OF MPC-BASED MOLECULAR MATERIALS

As a result of their 18  $\pi$ -electron planar aromatic structure, MPCs possess intriguing optical, electronic, and magnetic properties that can be harnessed in various applications, such as electronics devices,<sup>49</sup> magnetics,<sup>57</sup> chemical sensing,<sup>86</sup> and catalysis.<sup>47, 53</sup> The versatile functionalization of MPCs allows further refinement or adjustment of these properties.<sup>26, 42</sup> For a functional solid-state material, these basic properties are related to both the fundamental chemical structures of the MPC units and their supramolecular arrangement into an assembled state. Controlling the structure of MPCs across different length scales is the key to harnessing their full potential as multifunctional building units.

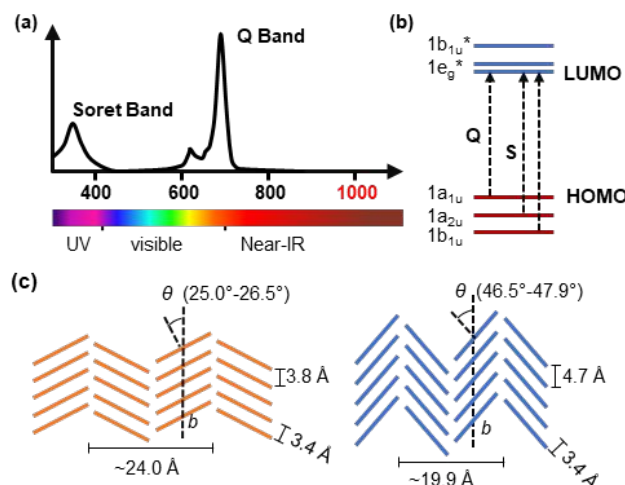


**Figure 4.** (a) A typical absorption spectrum of MPC and the corresponding electronic transition. (b)  $\pi$ - $\pi^*$  transitions in the HOMO and LUMO gap of MPCs (c) Schematic stacking of the herringbone  $\alpha$ - and  $\beta$ -phases.  $\theta$  is the angle between the  $z$  axis of the molecule and the  $b$  axis of the crystal structure. (a and b) Adapted with permission from ref <sup>46</sup> Copyright 2008 Wiley InterScience. (c) Adapted with permission from ref <sup>87</sup> Copyright 2014 Springer-Verlag Berlin Heidelberg

**Optical Properties in MPC-based molecular units.** MPCs exhibit beautiful and intense blue and green colors that have been historically applied and been very successful as industrial dyes and pigments.<sup>49</sup> These optical properties result from MPCs absorbing in the visible and near-IR region and are capitalized in various fields, such as organic solar cells,<sup>88</sup> photodynamic therapy of cancer,<sup>89</sup> nonlinear optical devices,<sup>90</sup> heat absorbers,<sup>91</sup> and near-IR imaging.<sup>41</sup> A typical electronic absorption spectrum of MPC is shown in **Figure 4a**. The strongest and most well-resolved absorption band in a vast number of MPCs is the Q-band, lying in the visible region at wavelengths between

620 to 720 nm, which is ascribed to the  $1a_{1u} \rightarrow 1e_g^*$  transition (**Figure 4b**).

Many optical applications utilize this Q-band absorption, the fine-tuning of the Q-band is, thus, of great importance. There are generally three approaches for tailoring the absorbance of MPCs in the near-IR region at the molecular level. The first method is incorporation of a suitable metal cavity. The choice of different metal cavities leads to changes of the electronic structure and causes the Q-band shift within a range of ca. 100 nm (620–720 nm) as a function of the metal size, coordination environment, and oxidation state.<sup>44</sup> MPCs with closed-shell metal ions (e.g., LiPc, MgPc, ZnPc) show Q-band absorptions around 670 nm;<sup>92</sup> while those with open-shell metal ions can interact strongly with the phthalocyanine ring (e.g., FePc, CoPc, RuPc) and have Q-bands around 630 to 650 nm.<sup>93</sup> MnPc has been reported with strongly red shifted Q band around 808 and 828 nm.<sup>94</sup> The second method relies on extending the electronic  $\pi$ -conjugation by expanding the macrocycle or oligomerizing MPCs, which results in a decrease in the separation between the HOMO and LUMO energies and leads to a red shift of the Q-band.<sup>46</sup> Naphthalocyanine, in which naphthalene moieties are used instead of benzene groups, have Q-band peaks red-shifted by 80 to 100 nm compared to those of similar phthalocyanine compounds, exhibiting peaks at 750 and 840 nm.<sup>95</sup> The third approach relies on the introduction of substituents with different electron-donating or -withdrawing characteristics. In general, electron-withdrawing groups cause a red shift of the Q-band, while electron-donating substituents have a minimal effect on the Q-band absorption maxima.<sup>46</sup> However, these effects still depend on particular substituent, as well as substituting number and position.<sup>46, 96</sup>

The optical properties of MPCs in the solid state are more complicated and difficult to control compared to the solution phase. Weak intermolecular  $\pi$ -electron and van der Waals interactions between MPCs give rise to various crystalline phases. MPC molecular units exhibit different type of stacking modes with the central metal atoms forming one-dimensional columns giving rise to different polymorphs, the most abundant being  $\alpha$  and  $\beta$ -phases (**Figure 4c**).<sup>46, 49</sup> Distinct phases absorb in different regions of the electromagnetic spectrum, which is likely due to different intermolecular interactions coupling with the HOMO-LUMO transitions of single MPC molecule. For example, in the  $\beta$  phase of ZnPc, the Q-band peak is found at 700 nm, which red-shifts to 750 nm in  $\alpha$  phase.<sup>97</sup>

The behavior and self-organization of MPCs reflects their optical and electronic properties, and can cause complications in some applications, such as in pigments and in organic solar cells, where undesirable aggregation on surfaces must be controlled.<sup>47, 49</sup> However, the current methods toward the control of the selective generation of

specific phases, including temperature control, post treatments by solvent or inorganic salts, integration into nanoparticles, are still empirical.<sup>98</sup>

### Charge transport in MPc-based molecular units.

Charge transport properties in MPc-based molecular materials are governed by the identity of specific MPc and their supramolecular arrangement. Thus, these properties are influenced by a wide range of chemical and physical parameters, such as the identity of metal cavity,<sup>99</sup> substituent groups, structural packing,<sup>46</sup>  $\pi$ - $\pi$  overlap, and presence of dopants or impurities.<sup>100</sup> Most MPcs are found to be p-type semiconductors<sup>43, 101</sup> and have been studied for use in organic field effect transistors (OFETs),<sup>102</sup> solar cells,<sup>103</sup> light emitting diodes,<sup>104</sup> and optical switching.<sup>45, 105</sup>

Solid-state molecular MPcs exhibit intrinsic conductivities at low to moderate levels, and depending on the different metal cavities, these values range from  $10^{-14}$  to  $10^{-7}$  S cm<sup>-1</sup>.<sup>46</sup> The intrinsically low conductivities in MPcs can be ascribed to their solid-state arrangement, which do not allow an appropriate overlap of  $\pi$ -orbitals to form a conduction band. In MPc materials, charge carriers undergo hopping mechanisms, as they "hop" from one localized energy level into another, which requires large activation energies.<sup>106</sup> However, some MPcs have been known to exhibit higher conductivities when in the form of a single crystal, such as the case for LiPc, which has been reported to have conductivities as high as  $2 \times 10^{-3}$  S cm<sup>-1</sup>.<sup>107, 108</sup> This was found to be related to the presence of the structural disorders and defects in LiPc crystals. MPcs can also reach high conductivities through the addition of chemical dopants, such as oxidants (Figure 5a).<sup>106, 109</sup> Doping with iodine or other oxidants can promote the emergence of metallic conductivity in MPc crystals<sup>110</sup> and polycrystalline films<sup>109</sup> by increasing the concentration of holes as charge carriers<sup>111</sup> or creating extra charge transfer pathways.<sup>109</sup>

Charge transport behavior can also be modified through the introduction of substituent groups to MPcs. For

instance, a fully fluorinated CuPc ( $F_{16}CuPc$ ) presents n-type characteristics with an electron mobility comparable to the hole mobility of its unsubstituted counterpart, CuPc.<sup>112</sup> Introducing electron-withdrawing or -donating functionalities can also lead to their integration into multicomponent systems as electron- (D-A) complexes for energy related systems.<sup>46</sup> For example, MPcs covalently linked to fullerenes,<sup>46, 88, 113</sup> are excellent electron-acceptor systems for photo-induced charge transfer and separation<sup>46</sup>

Lastly, supramolecular self-assembly of MPcs into one dimensional (1D) columnar structures by  $\pi$ - $\pi$  interaction, which is sometimes aided by the introduction of functionalities at  $\beta$ -positions (e.g., crown ethers<sup>114</sup> or long hydrocarbon chains)<sup>115</sup> to provide additional peripheral intermolecular interactions,<sup>43, 46</sup> can give rise to electron delocalization along the *c*-axis.<sup>116</sup> Measurements of electrical conductivity on such morphologically distinct materials (i.e., crystals, nanoribbons, polycrystalline films, and nanowires)<sup>117</sup> can greatly vary, indicating the influence of morphology and grain boundaries on electrical behavior.

In summary, the electronic properties of MPc-based materials are not only dependent on their chemical composition, such as identity of the metal cavity, oxidation state,  $\pi$ -conjugated system, and presence of substituent groups on their periphery, but also on their self-organization into solid state structures. The tools of chemical synthesis and structural engineering can impart great tunability over MPc charge dynamics through high-level of control of MPc self-assembly to generate materials with remarkable and controllable electronic properties. Initial investigations using the principles of supramolecular chemistry have demonstrated precedent on achieving this level of control on the nanoscale, however extending this level of control into 3D self-organized structures using strong linkages can afford stable and functional solid-state materials.

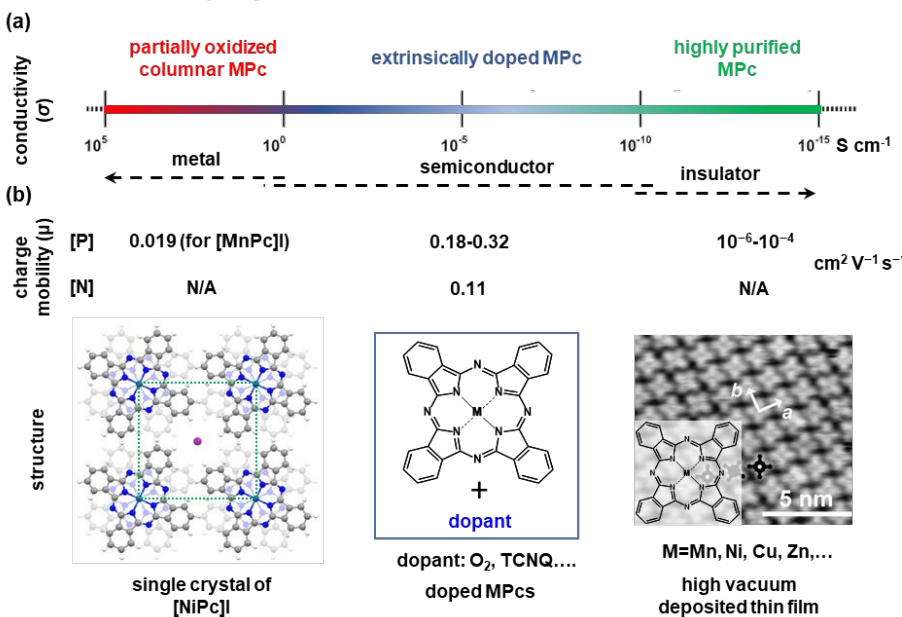


**Figure 5.** (a) Conductivities<sup>46, 49, 109, 118</sup> and (b) charge mobilities<sup>48, 119, 120</sup> of MPcs that are influenced by a wide range of chemical and physical parameters ([p] hole mobilities, [n] electron mobilities). (b) Reprinted with permission from ref<sup>118</sup>. Copyright 2015 Elsevier.

#### Magnetic properties of MPc-based molecular units.

The design and fabrication of materials that exhibit semiconducting and magnetic properties for spintronics and quantum computing is an attractive but long-standing challenge.<sup>121</sup> MPc materials, in sharp contrast with common organic compounds, which are typically diamagnetic, are notable exceptions and have served as prototypical systems to study the magnetic properties of transition metals embedded in a tunable ligand sphere.<sup>87, 122</sup> Firstly, magnetic properties of MPcs depends on the electronic ground state of the metal used in the center of the phthalocyanine (Pc) ring, which, in turn, is largely determined by the surrounding ligand sphere.<sup>87</sup> The total spin value of MPc units is determined by the electronic configuration in the d orbitals of the metal (Figure 6a), which usually can be identified as a square-planar ligand-field due to the  $D_{4h}$  symmetry of MPc unit.<sup>87</sup> MPcs with transition metal centers, including Ti, V, Cr, Mn, Fe, Co, Ni and Cu, have been intensely investigated in molecular magnetism studies, compared to other MPcs.<sup>87</sup> The magnetic moments of MPcs follow the order of MnPc ( $4.8 \mu_B$ ) > CrPc ( $4 \mu_B$ ) > VPc ( $3 \mu_B$ ) > TiPc ( $2 \mu_B$ ) = FePc ( $2 \mu_B$ ) > CuPc ( $1 \mu_B$ ) = CoPc ( $1 \mu_B$ )  $\approx$  ScPc ( $0.99 \mu_B$ )  $\approx$  AgPc ( $0.95 \mu_B$ ) > CaPc ( $0 \mu_B$ ) = ZnPc ( $0 \mu_B$ ),<sup>122</sup> indicating that magnetic strength can be controlled at a molecular level through the choice of the metal.

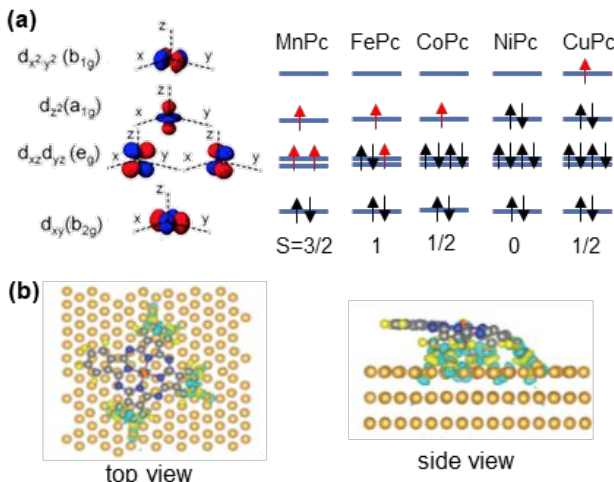


**Figure 6.** (a) d orbitals of metal in MPc molecules (notation as irreducible representations in  $D_{4h}$  symmetry and blue and red identify the different wave function phases) and representation of electron configuration in the d orbitals of MnPc, FePc, CoPc, NiPc, and CuPc.<sup>87</sup> (b) Top and side views of the differential charge density induced by MPc bonding to the substrate.<sup>123</sup> (a) Reprinted with permission from ref<sup>87</sup>. Copyright 2014 Springer-Verlag Berlin Heidelberg. (b) Reprinted with permission from ref<sup>123</sup>. Copyright 2015 American Physical Society.

In the solid state of some MPcs, strong intrachain and weak interchain coupling between metal atoms result in anisotropic magnetic properties.<sup>87</sup> However, most of the

bulk solid-state MPcs remain paramagnetic down to the lowest achievable temperatures in experimental testing because the intermolecular magnetic exchange interactions are not strong enough to sustain long range order.<sup>124, 125, 126</sup> Only  $\beta$ -MnPc<sup>127, 128</sup> and  $\alpha$ -FePc<sup>129, 130</sup> polymorphs exhibit long range ferromagnetism below an ordering temperature ( $T_c = 8.3$  K for  $\beta$ -MnPc and  $T_c = 10$  K for  $\alpha$ -FePc) ascribed to relatively stronger interchain interactions.

When MPc molecules are deposited on a metallic substrate, the hybridization of the  $3d_{z^2}$  states of the metal center in the MPc and the electronic states of the substrate can influence the position of the metal center on the substrate, while the orientation of MPc is mostly influenced by the interaction of the N atoms and the surface.<sup>131</sup> This interaction between the orbitals of MPc and conducting substrates, also called the Kondo effect, can modify the value of total spin of the molecule.<sup>132, 133</sup> Thus, the substrate on which MPc is adsorbed can influence its magnetic state depending on specific interaction between the substrate and the MPc molecules. When MPc molecules assemble into clusters, the intermolecular interactions may compete with the Kondo effect and the molecules may change their magnetic state.<sup>87</sup>

The molecular spin state of MPcs can also be manipulated by the adsorption of the small molecules on MPcs, such as organic ligands and gaseous molecules, that can change the electronic configuration upon their interaction with MPcs.<sup>134, 135, 136, 137, 138</sup> For example, the magnetic state of MnPc molecules on a Bi(110) surface can be modified when the  $Mn^{2+}$  center coordinates to CO molecules adsorbed, and reduces the spin of the adsorbed MnPc from  $S = 1$  to  $S = 1/2$ .<sup>137</sup> Usually the modification of the spin state is reversible, thus this property is appealing for molecular spintronic devices.

In summary, the magnetic properties of MPc molecules are strongly related with the electronic ground state of the central metal atom hybridized with the ligand states.<sup>87</sup> For solid-state MPc-based materials, intermolecular exchange interactions between magnetic metal cavities and the electronic coupling to the supporting substrate regulates their magnetic properties. These initial studies are inspiring and provide the platform to understand the structure-property relationships that influence magnetic moments in MPc compounds and further the development of controlling the alignment of MPc molecules on substrates to maximize intermolecular exchanges. These developments can lead to advances in single molecule magnetic switching, toward information storage and processing, and magnetic-based sensors.<sup>87</sup>

**Chemical sensing.** Inspired by the central role of MPys in biological systems for regulating various physiological processes, significant effort has been devoted to the use of MPcs as functional units in selective chemical sensors.<sup>139, 140</sup> The coordination of a ligand along the axial site can modify

the electronic properties of MPcs and cause changes that may be detectable through various methods of signal transduction, such as alteration of conductivity, mass, and optical properties.<sup>86, 116, 139</sup> Consequently, there has been strong interest in integrating MPcs into multiple sensing architectures that span field-effect transistors (Figure 7a),<sup>141</sup> chemiresistors,<sup>142</sup> electrochemical sensors<sup>143</sup>, quartz crystal microbalance,<sup>144, 145</sup> surface acoustic-wave,<sup>146</sup> and colorimetric sensors.<sup>147, 148, 149</sup> Well documented examples have illustrated the utility of MPc sensors towards gaseous analytes such as NO,<sup>150</sup> NO<sub>2</sub>,<sup>151</sup> NH<sub>3</sub>,<sup>152</sup> Cl<sub>2</sub>,<sup>153</sup> H<sub>2</sub>,<sup>154</sup> and O<sub>2</sub>.<sup>155</sup>,<sup>156</sup> MPc-based sensors have also been utilized for the determination of volatiles<sup>157, 158, 159</sup>, ions,<sup>160</sup> and biomolecules.<sup>161, 162, 163, 164, 165</sup>

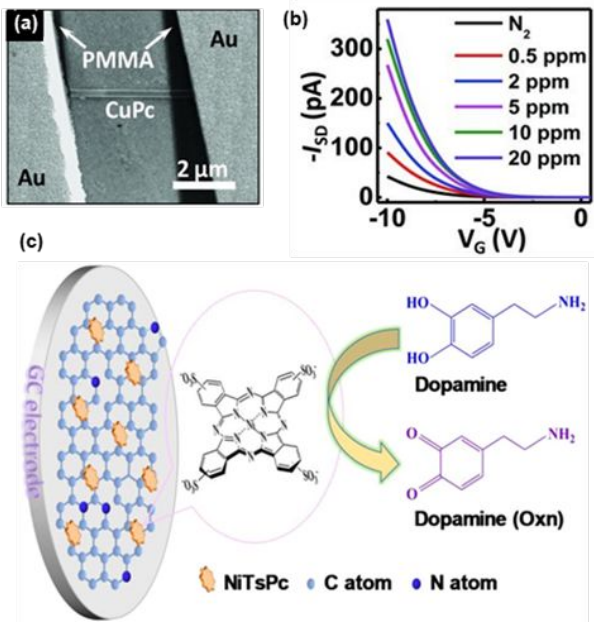


**Figure 7.** (a) SEM image of a FETs based on CuPc nanowire<sup>166</sup> and (b) the transfer characteristics of the FET to various SO<sub>2</sub> concentration (0-20 ppm) at room temperature. (c) Schematic representation of the N-G/NiTsPc/GC electrode toward DA oxidation.<sup>167</sup> (a and b) Reprinted with permission from ref <sup>166</sup> Copyright 2013 Wiley-VCH Verlag. (<https://creativecommons.org/licenses/by/4.0/>) (c) Reprinted with permission from ref <sup>167</sup> Copyright 2016 Elsevier.

**Chemiresistive sensing.** The impact from both intrinsic (identity of the metal cavity, peripheral substituent, etc.) and extrinsic parameters (material morphology and substrate/electrode contacts) can profoundly affect the sensing performances across different sensing architectures. Speaking first to intrinsic parameters, Bohrer *et al.* investigated sensing responses across CoPc and H<sub>2</sub>Pc thin films and found that the central metal cavity, presence of surface bound O<sub>2</sub>, and Lewis basicity of the analyte strongly influenced responses across sensing films.<sup>168</sup> Indeed other experiments have shown the electron donor/acceptor abilities of analyte and different binding affinities of the metal in MPcs significantly influence the sensing response.<sup>139, 168, 169</sup> Consistently, theoretical

studies have demonstrated the effects of metal variants (M = Mg, Mn, Co, Ni, and Zn) on MPcs sensitivity towards volatile organic compounds, which showed strong correlations between Mullikan electronegativity values of the analytes and sensitivity of the MPcs.<sup>170</sup> The influence of peripheral substituents on the sensing response has also been investigated.<sup>80, 170</sup> For example, a ZnPc thin film showed negligible response to reducing gas NH<sub>3</sub>; however, the addition of strong electron-withdrawing peripheral substituents (-F), which significantly increased ZnPcs sensitivity toward NH<sub>3</sub>.<sup>171</sup>

As analyte binding interactions occur primarily at the surface of the sensing material (**Figure 7b**), different methods of thin film deposition (thermal evaporation, solvent-casting, self-assembled monolayers or Langmuir-Blodgett) are known to affect sensitivity of MPcs towards various gases.<sup>81</sup> Other extrinsic parameters such as crystal morphology, degree of crystallinity, crystallite size, presence of grain boundaries,<sup>172</sup> film thickness, and structural order<sup>81</sup> of MPc-based materials on the surfaces of substrates also play a vital role, as the availability of active sites for chemical sensing also influence the sensitivity of the gas sensors.<sup>169</sup> Nevertheless, MPc-based sensors have shown high sensitivity for a wide range of gaseous and volatile analytes with sub-ppm to ppb level limit of detections (LODs), such as for NO<sub>2</sub> (LOD: 40-100 ppb)<sup>172,173</sup> NO (LOD<20 ppm, **Figure 7c**),<sup>174</sup> NH<sub>3</sub> (LOD: 0.7-1 ppm),<sup>175, 176</sup> H<sub>2</sub>S (LOD: 100 ppb),<sup>144</sup> and SO<sub>2</sub> (0.5 ppm).<sup>166</sup> Although cross sensitivity among different analytes still remain,<sup>86, 168</sup> they may be potentially overcome using linear discriminant analysis (LDA). Troglar and co-workers demonstrated that single sensor normalization of analyte concentration leads to excellent discrimination and identification of analytes with 95.1% classification accuracy using MPcs (M=Co, Ni, Cu, Zn, and H<sub>2</sub>).<sup>177</sup>

In most cases, sensing devices made using thermally evaporated MPc films display low conductivities and require high driving voltages (e.g., 8-100 Volts).<sup>177, 178, 179</sup> Methods to overcome these limitations are made through combining MPcs with conductive materials like graphene and carbon nanotubes (**Figure 7d**).<sup>180, 181, 182, 183, 184, 185</sup> In addition, high operating temperatures (100–200 °C) are often required to optimize sensitivity and reduce response and/or recovery times.<sup>139</sup> Although these limitations are mainly due to MPcs physiochemical properties, extensive work in this field has demonstrated the utility of MPcs as sensitive and selective sensors to specific gases.

**Electrochemical sensing.** MPcs (M= Fe, Co, Cu, Zn and Ni), have also been extensively used as liquid phase electrochemical sensors, where their rigid, planar and extended  $\pi$ -systems allow them the ability to undergo fast redox processes with minimal reorganizational energies.<sup>186, 187, 188</sup> In this medium, MPcs usually serve as redox mediators that bring the overpotential to moderate or low values so that possible interferences are minimized, increasing the electrode activity. In this regard, CoPc and CuPc are the two most frequently used MPcs for electrochemical sensing, likely due to their high electrochemical activity under general test conditions.<sup>86</sup>

1 MPcs have also been used as dopants in electrochemical  
2 systems to amplify sensitivity and enhance selectivity  
3 towards specific analytes.<sup>150, 189, 190</sup>

4 MPcs have been utilized for electrochemical sensing of  
5 various biologically important analytes such as  
6 dopamine,<sup>162, 191</sup> catecholamines,<sup>192</sup> amino acids,<sup>193</sup> ascorbic  
7 acid, and uric acid,<sup>164, 165</sup> where they are usually combined  
8 with a conductive matrix, such as graphene<sup>165, 189</sup> and  
9 carbon nanotubes,<sup>194, 195</sup> to form a composite material that  
10 provides the optimized microenvironment for the  
11 electroactive species, as well as enhances electron transfer  
12 rates between electroactive species and the electrode. MPcs  
13 can also be directly deposited onto glassy carbon  
14 electrodes, as shown by Schoenfisch and coworkers for the  
15 detection of nitric oxide (NO).<sup>150</sup> This work highlights the  
16 use of Fe(II)Pc, Co(II)Pc, Ni(II)Pc, and Zn(II)Pc as probes for  
17 NO sensing under both differential pulse voltammetry  
18 (DPV) and constant potential amperometry (CPA), where  
19 MPcs provided signal sensitivity amplification ( $\sim 1.5x$ ).  
20 Intriguingly, FePc exerted the most specific catalytic activity  
21 toward NO over  $\text{NO}_2$ , while CO exhibited no measurable  
22 activity for bare or MPc-modified electrodes.

23 Currently, optical and chromatographic sensors are  
24 the state-of-the-art instruments for detection of analytes  
25 with high accuracy,<sup>196, 197</sup> but these instruments are difficult  
26 to miniaturize and provide real-time analysis of the  
27 chemical environment. Material-based gas sensors (CO,  $\text{CO}_2$ ,  
28 humidity, etc.) can enable fast response times and low  
29 LODs,<sup>198</sup> however, some limitations that remain are cross-  
30 sensitivity, stability and selectivity.<sup>198</sup> For  
31 commercialization of material-based sensors, certain  
32 considerations must be taken into account, such as  
33 accuracy, response times, power consumption, scalability  
34 and costs. In this regard, MPcs possess useful properties,  
35 modularity, and synthetic accessibility can help address  
36 some of these challenges.

37 **Catalysis** Arguably the most investigated application  
38 of MPcs thus far has been in catalysis where, as in sensing,  
39 researchers draw inspiration from the extensive catalytic  
40 applications of porphyrin complexes to propose reasonable  
41 reactions for which MPcs can catalyze. MPy complexes are  
42 often active sites of biological enzymes responsible for the  
43 oxidation and reduction of various compounds. For  
44 instance, the heme group, an iron containing porphyrin, is  
45 an imperative cofactor for cytochrome P-450 that reduces  
46 dioxygen in different metabolic pathways.<sup>53</sup> This catalytic  
47 pathway is mirrored in the use of MPcs in oxygen reduction  
48 reactions (ORRs).

49 MPcs have been used as both homogeneous and  
50 heterogeneous catalysts for a wide range of organic  
51 reactions like the oxidation of alkanes, olefins, aromatic  
52 compounds, alcohols, and sulfur-containing compounds,  
53 the preparation of nitrogen-containing compounds, and C-C  
54 bond formation.<sup>53</sup> Sulfonated CoPcs are used in industrial  
55 processes, such as the Merox process, which involves the  
56 oxidation of mercaptans for the desulfurization of  
57 petroleum.<sup>199</sup> MPcs also serve as electrochemical catalysts  
58 for the oxidation of thiols, NO, nitrite, hydrazine,  
59 hydroxylamine, catecholamines, glucose and other sugars

60 as well as the reduction of molecular oxygen.<sup>188</sup> Neither  
photocatalytic applications of MPcs, nor detailed  
description of all the above reactions will be discussed in  
this perspective, but there are extensive reviews on these  
topics available in literature.<sup>53, 188, 199, 200</sup> The efficiency of the  
catalysts depends on the supporting media for the MPc,  
metal center identity, Pc substitution which influences  
electron density, along with multiple other factors, such as  
pH and phase of the reaction that are beyond the scope of  
this review.<sup>53</sup>

With organic reactions, heterogeneous MPc-based catalysts have the advantage of recyclability and increased adsorption of substrates when compared to homogeneous MPc-based catalysts.<sup>53</sup> There are multiple methods for incorporating MPcs into a heterogeneous catalyst namely covalent anchoring, physical adsorption, grafting, electrostatic interaction and encapsulation into a support system.<sup>53</sup> Parton *et. al.* encapsulated FePc in zeolite Y (FePcY) and supported the complex on a polydimethylsiloxane (PDMS) membrane to form a catalyst for oxidation of cyclohexane with 'BuOOH.<sup>201</sup> The catalyst was 18.5 wt% FePcY with a turnover rate of 3.3 min<sup>-1</sup> and saw a 300-fold catalytic increase compared to other zeolite complexes. The zeolite support enabled the FePc active site to assume the optimal transition state due to the steric strain induced. Another study by Parton *et. al.* using zeolite encapsulated nitro-substituted FePc had a turn over number (TON) of 6000 for the oxidation of cyclohexane whereas the homogeneous catalyst was rendered ineffective by oxidative self-destruction.<sup>53</sup> These studies show how the tuning of solid support varies the catalytic efficacy by providing the optimal orientation of the binding site and the optimized concentration of adsorbent.

Water oxidation, or oxygen evolution reaction (OER), has important applications in energy storage and conversion such as fuel cells and batteries.<sup>202</sup> In 1981, a series of different sulfonated MPcs (M=Cr, Mn, Ni, Al, Cu, Zn, Fe and Co) were investigated as homogeneous catalysts for the oxidation of water by a ruthenium (III) trisbipyridyl compound.<sup>203</sup> Solution concentrations varied from  $1 \times 10^{-5}$  M to  $2 \times 10^{-5}$  M of MPc catalysts with  $\text{Ru}(\text{bpy})_3(\text{ClO}_4)_3$ . At room temperature, the sulfur substituted CoPc catalyst performed the best with a 62% yield of  $\text{O}_2$ , while sulfur substituted FePc had a 47% and NiPc had a 18% yield. Years later, FePc's and NiPc's performance for OER was improved by integration onto multi-walled carbon nanotubes (MWCNTs) to form heterogeneous catalysts.<sup>204</sup> Comparisons between MPc loading on the MWCNTs and the current densities ( $j$ ), in which a higher  $j$  is indicative of a more reactive catalyst, revealed that the FePc/MWCNT catalyst was best in both acidic and basic conditions with a loading of 7:1 of MWCNT:FePc. At this loading,  $j$  was about 0.2 mA/cm<sup>2</sup> for acidic conditions and about 5.5 mA/cm<sup>2</sup> for basic conditions. The NiPc/MWCNT catalyst was most effective at a 2:1 ratio MWCNT:NiPc. The MWCNTs aided in catalytic function due to their non-covalent  $\pi$ - $\pi$  interactions with the MPcs that aided in stability and charge transfer.<sup>204</sup> At this loading,  $j$  was about 0.1 mA/cm<sup>2</sup> for acidic conditions and about 5.5 mA/cm<sup>2</sup> for basic conditions. Comparative

1 studies were done by contrasting ratios of  $j$  of modified  
 2 electrodes to  $j$  of the bare electrode ( $j_m/j_b$ ). In acidic  
 3 conditions, the  $j_m/j_b$ s for the electrodes modified with NiPc,  
 4 FePc, MWCNT, NiPc/MWCNT, and FePc/MWCNT were,  
 5 respectively, 5.39, 12.30, 7.99, 60.90, and 143.53. It was  
 6 seen that the OER activity increased synergistically with the  
 7 incorporation of MPcs on MWCNTs to form a heterogeneous  
 catalyst.

8 For ORRs it is important, especially in fuel cell  
 9 applications, to develop a catalyst that promotes a 4-  
 10 electron transfer transition instead of a 2-electron  
 11 transition state, which results in less released energy.<sup>205</sup>  
 12 The pathway is dependent on the metal center and Pc  
 13 substituent identities. MPc (M=Co, Ni, Cu) electrodes result  
 14 in a two electron transfer mechanism to produce hydrogen  
 15 peroxide, while Fe and Mn electrodes result in a four  
 16 electron transfer to produce water.<sup>188</sup> Catalytic activity of  
 17 the MPc electrode is directly correlated to the M(III)/M(II)  
 18 redox potential since there is a direct linear relationship  
 19 between log of the current and the M(III)/M(II) redox  
 20 potential.<sup>188</sup> As corroborated with calculation studies by Shi  
 21 and Zhang, the best catalyst is FePc followed by CoPc at  
 22 room temperature.<sup>206</sup> Better catalytic activity is associated  
 23 with higher ionization potential (IP) and oxygen binding  
 24 energy ( $E_{bo_2}$ ). The sum of IP and  $E_{bo_2}$  for CoPc and FePc was  
 25 6.82 eV and 7.00 eV, respectively. In addition to metal  
 26 center type, Pc substituent character can influence electron  
 27 density on the metal center and therefore influence binding  
 28 and catalysis. For instance, perfluorinated CoPc adsorbed  
 29 on ordinary pyrolytic graphite had the most positive redox  
 30 potential, which helps rationalize why it was the best  $O_2$   
 31 reduction catalyst.<sup>188</sup> Many theoretical calculations and  
 32 experiments aid in understanding the influence of the MPc  
 metal centers and substituents' identity on mechanism  
 pathway and efficacy.

33 Experimental studies verified the theoretical findings  
 34 that the metal center and substituents on the  
 35 phthalocyanine ring altered the catalytic ability of MPcs for  
 36 ORR. In acid, catalytic efficiency of MPc-based catalysts  
 37 followed the following trend: Fe > Co > Ni > Cu.<sup>207</sup> This can  
 38 be explained by the Pauling model where  $d_{z^2}$  orbitals of the  
 39 central metal interact with the  $sp^2$  orbitals on the dioxygen.  
 40 The electron density on Fe was optimal for this interaction.  
 41 In the same study, the catalytic activity for the cobalt series  
 42 was as follows: CoPc(NH<sub>2</sub>)<sub>4</sub> > CoPc > CoPcCl<sub>4</sub>.<sup>207</sup> The series  
 43 shows that an increase in substituent electron donor  
 44 capacity increased catalytic activity by donating more  
 45 electron density to the bond between the Pc central metal  
 46 and oxygen analyte. Hebié *et. al.* performed ORRs with  
 47 different MPc on carbon supports in alkaline solution. FePc  
 48 was found to be the best catalyst supported by the following  
 49 data of half wave potential, number of electrons involved in  
 50 the reaction, and limiting current density: FePc/C (0.96 V,  
 51 4.0, -79.4 mA/cm<sup>2</sup>).<sup>208</sup> The MPc-based catalysts can be  
 52 tuned by varying properties like metal center and  
 53 substituent identities to develop the most effective catalyst.

54 Historically, reports indicate that the CoPc performed  
 55 best catalytically compared to other MPcs for the  
 56 electrochemical reduction of CO<sub>2</sub>.<sup>209</sup> While we will be

5 focusing on the electrochemical reduction, there is  
 6 extensive research on the photoreduction of CO<sub>2</sub> using  
 7 MPcs.<sup>210, 211</sup> An electrochemical homogeneous CO<sub>2</sub>  
 8 reduction catalyst used by Hiratsuka *et. al.* was  
 9 tetrasulfonated MPc (MTSPc) dissolved in Clark-Lubs  
 10 buffer.<sup>212</sup> During exposure to CO<sub>2</sub>, CoTSPc and NiTSPc were  
 11 seen to be active with first reduction waves around -0.8 V  
 12 vs SCE and the second around -1.2 V vs SCE. MTSPc  
 13 lowered the overpotential for CO<sub>2</sub> reduction by about 0.2-  
 14 0.4 V at 1 mA/cm<sup>2</sup>. For heterogeneous catalysts,  
 15 Christensen *et. al.* studied CoPc-coated edge graphite  
 16 electrodes in the presence of KH<sub>2</sub>PO<sub>4</sub> and a NaOH buffer.<sup>213</sup>  
 17 The second reduction of the MPc resulted in the  
 18 electroreduction of CO<sub>2</sub>. More recently, Shibata *et. al.*  
 19 simultaneously reduced CO<sub>2</sub> and NO<sub>3</sub> using gas-diffusion  
 20 electrodes in which CoPc and NiPc performed the best.<sup>214</sup>  
 21 The electrode consisted of MPc and carbon black and  
 22 polytetrafluoroethylene. In this instance, NiPc saw selective  
 23 reduction of only CO<sub>2</sub>, not NO<sub>3</sub>, and CO formation reached a  
 24 maximum of 95% at -1.5 V. There are some MPc catalysts  
 25 that can selectively reduce CO<sub>2</sub> and electronic properties of  
 26 the monomers can help elucidate mechanistic information.

27 MPc-based catalysts are an extensively researched  
 28 field especially more recently in ORR and CO<sub>2</sub> reduction for  
 29 fuel cells and renewable energy solutions. The tunability of  
 30 the MPc's heterogeneous support, metal center, and ligand  
 31 substituents allows for optimization of catalytic yield  
 32 whether in the organic or electrochemical applications. The  
 33 catalytic dependence on the MPc's electronic properties  
 34 bodes well for future applications of MPc-based  
 35 frameworks for catalysis.

36 **Energy storage and conversion.** To achieve energy  
 37 storage from renewable sources and to meet the high  
 38 demands for batteries for use in telecommunication,  
 39 electric-vehicles, portable electronics and computing,  
 40 energy storage solutions, such as batteries and  
 41 supercapacitors, have seen significant optimization in  
 42 recent years.<sup>215, 216</sup> Energy storage devices require the use  
 43 of materials that can convert stored chemical energy to  
 44 electrical energy with high efficiency, thus many different  
 45 anode and cathode materials have been explored as  
 46 possible constituents.<sup>215, 217, 218</sup> Many attempts have been  
 47 made to push the relevant energy storage and conversion  
 48 properties of materials to achieve high efficiency.<sup>215</sup> In this  
 49 context, MPc-based electrode materials have been  
 50 investigated as possible alternatives to energy storage or  
 51 conversion systems such as Li<sup>+</sup>-intercalated graphite  
 52 materials, usually paired with Li<sub>x</sub>(CoO<sub>2</sub>)<sub>y</sub>,<sup>217</sup> or (ORR)  
 53 catalysts for polymer electrolyte membrane fuel cells  
 54 (PEMFCs).<sup>219</sup> MPcs exhibit several excellent characteristics  
 55 that would prove useful when used as active materials for  
 56 batteries, such as wide range of operational temperatures,  
 57 high capacity, long term stability, and propensity to stack in  
 58 layers for high intercalation capacity.<sup>217</sup> Li *et. al.* took  
 59 advantage of substituted FePcs stability in harsh oxygen  
 60 reducing environments to create nonprecious metal  
 catalytic sites for fuel cells that were stable up to 1000  
 cycles (Figure 8b).<sup>219</sup> Other studies have demonstrated the  
 promising performances of MPcs as non-precious metal

cathode materials, where improvements in capacity, cycling, and coulombic efficiency have been observed.<sup>217</sup> Much of this precedent combines MPC units with carbon-based materials, likely to increase the electronic conductivity.<sup>220</sup>

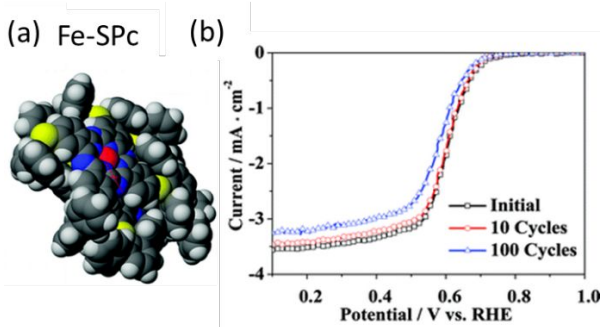


**Figure 8.** Space filling model of ferrous 2,9,16,23-tetra(2',6'-diphenylphenthioether) phthalocyanine and (b) initial activity along with activity observed after 10 and 100 potential sweeps in oxygen saturated electrolyte. Curves were obtained at a sweep rate of 10 mV/s and an electrode rotation speed of 400 rpm. Reprinted with permission from reference<sup>219</sup> Copyright 2010 American Chemical Society.

The incorporation of MPCs into lithium-thionyl chloride (Li/SOCl<sub>2</sub>) batteries with high discharge voltages and energy densities are abundant in precedent.<sup>221 222</sup> This type of battery consists of a lithium anode, a carbon cathode and thionyl chloride, which acts as a catalytic reducing agent.<sup>222</sup> It has been well documented that doping the cathode with MPC complexes improves the relative energy density,<sup>222</sup> cell voltage, rate of discharge and the lifetime of Li/SOCl<sub>2</sub> batteries.<sup>223</sup> Xu et. al. investigated the influence of the electronic configuration of the metal in MPC on the catalytic activity of Li/SOCl<sub>2</sub> batteries.<sup>222</sup> The group observed increases in the energy of Li/SOCl<sub>2</sub> batteries increases by 63-106% when the electrolyte contains MPCs-tetrasulfonic acid (MpCTs) (M-Mn<sup>2+</sup>, Ni<sup>2+</sup>), where the central metals with an electronic configuration of d<sup>9</sup> were inactive, while those with d<sup>5</sup> and d<sup>8</sup> exhibited high catalytic activity due to their strong tendency to form square planar complexes during the reduction process. In 2016, Yang *et al.* also demonstrated that a series of metal 2,9,16,23-tetraaminophthalocyanines (TAPcM, M = Cu(II), Ni(II), Zn(II), Fe(II), Mn(II)) combined with multi-walled carbon nanotubes (MWCNTs) can dramatically improve the capacity of Li/SOCl<sub>2</sub> batteries by improvement of their electrocatalytic performances, a process that depends on both competitive and cooperative process of forming metal-ligand-SOCl<sub>2</sub> adducts.<sup>224 221</sup> This study found that all of the TAPcM compounds improved the ceiling voltage of the batteries above 3.1 V and the overall capacity by 82.6% and 59.5% from 2,9,16,23-TAPcMn(II) and 2,9,16,23-TAPcNi(II), respectively. The order of the electrocatalytic activities of the F-MWCNTs modified with MPCs is Mn(II) > Ni(II) > Zn(II) > Fe(II) > Cu(II), which further corroborates the influence of electronic configuration of the metal ions in MPC. Compton and coworkers also demonstrated the potential advantages of using MWCNTs combined with MPCs as electrode materials for the development of

supercapacitors.<sup>225</sup> This group observed the superior performance of MWCNT-NiTAPc (maximum power density of  $700 \pm 1 \text{ W kg}^{-1}$ , a maximum specific energy of  $134 \pm 8 \text{ Wh kg}^{-1}$  and excellent stability of over 1500 charge-discharge continuous cycling) compared to MWCNTs modified with unsubstituted NiPc or nickel(II) tetra-tert-butylphthalocyanine, possibly due to the participation of the additional nitrogen-containing groups on the NiPc in the electrochemistry.

Lithium-air batteries are also desirable alternatives to Li-ion batteries due to their theoretical high energy density ( $3500 \text{ Wh kg}^{-1}$ )<sup>218</sup> and low cost.<sup>226</sup> The structure of Li-O<sub>2</sub> batteries are similar to that of Li-ion, except that the cathodes are exposed to atmospheric oxygen, which is used to store and convert energy through the oxidation of lithium metal to Li<sup>+</sup>, which then migrates to the cathode.<sup>218</sup> At the cathode, Li<sup>+</sup> combines with O<sub>2</sub> and 2 electrons to form Li<sub>2</sub>O<sub>2</sub>. Some of the disadvantages of this cycle has been poor rate capability due to the slow rate of oxygen reduction and evolution reaction mechanism and slow mass transport to the cathode, a challenge that has been attempted to be solved with new cathode materials to facilitate kinetic processes.<sup>218</sup> Abraham and coworkers prepared CoPc-containing carbon black electrodes at 600 °C to facilitate the oxygen reduction reactivity at the porous carbon electrode.<sup>226</sup> This study determined that the rate-determining step in the ORR of CoPc catalyzed Li-air cell was the formation of the superoxide O<sup>2-</sup>, which is stabilized by the CoPc catalyst through lowering the activation energy barrier for O<sub>2</sub> reduction and increasing the voltage of the cell.

The potential use of MPCs in energy storage devices can improve stability, charge/discharge cycles, energy densities, and increase capacities.<sup>217</sup> The influence of the electronic configuration and the metal cavities have also been investigated, where electronic state of the metal cavities can render that MPC catalytically active or inactive toward Li/LOCl<sub>2</sub> batteries.<sup>222</sup> Although preliminary studies have explored the mechanisms of electron transfer of MPC-based energy storage devices, the synergistic effects of including these materials into cathode devices can increase the energy of batteries up to 80%.<sup>227</sup>

As a kind of multifunctional building block, MPCs show their unique and modular optical, electronic, and magnetic properties and their capability in chemical sensing and catalysis. Utilizing these properties must rely not only on structure engineering of MPCs at molecular level, such as modification of the metal cavities, substitution, and π-system expansion. However, to fully capitalize on their full potential, we must also rely on our capability in arranging those functional building blocks in a controllable and rational way into three dimensional space, because the property of the condensed matter is a combination of the assembly of molecular building blocks. Self-assembly of MPCs driven by supramolecular interactions have already shown the potential for the improvement of charge transport and magnetic properties by control the stacking of the MPCs. Reticular synthesis by using MPCs as key functional building blocks, with the involvement of other

1 building units, are expected to provide a new level of control  
 2 of their spatial arrangement and greater tunability of the  
 3 chemical properties in the resulting solid-state materials.

### 4 STRATEGIES FOR CONTROLLED ASSEMBLY OF MPC

5 **BUILDING BLOCKS** The control over spatial orientation  
 6 and long range order of MPcs into highly-ordered structures  
 7 can enhance certain functional properties and enable  
 8 effective interfacing of MPcs within semiconductor  
 9 devices.<sup>82</sup> As previously discussed, MPcs have already  
 10 demonstrated great technological potential as field effect  
 11 transistors, solar cells, and sensors, but the ability to  
 12 develop and manipulate well-defined structures—either on  
 13 surfaces or as bulk materials—are needed to achieve  
 14 optimized electrical and optical performances. Thus, much  
 15 research has focused on organizing MPcs using the bottom-  
 16 up approaches to control the assembly of monomers in a  
 17 precise fashion.<sup>82</sup>

18 The  $\pi$ - $\pi$  stacking ability of MPc monomers allows for  
 19 their self-organization into supramolecular structures on  
 20 surfaces. Moreover, symmetrical or asymmetrical  
 21 structural modifications to the periphery sites can facilitate  
 22 and direct this self-assembly<sup>82</sup> through noncovalent  
 23 interactions such as hydrogen bonding, van der Waals  
 24 interactions, and  $\pi$ - $\pi$  stacking.<sup>82</sup> In many cases, high-  
 25 resolution scanning tunneling microscopy (HR-STM) has  
 26 allowed direct visualization of the distinct phases in the  
 27 aggregated state and the relative orientations of MPcs at  
 28 interfaces.<sup>82,228, 229</sup> Applying the principles of reticular  
 29 chemistry to MPc molecular systems can precisely control  
 30 the relative orientations and positions while providing the  
 31 foundations to investigate emergent properties.

32 **Self-assembly of MPcs on surfaces.** The self-assembly  
 33 of MPcs on various types of surfaces (e.g., Au, HOPG, Ir) to  
 34 control their bidimensional organization is of paramount  
 35 importance in MPc-based devices utilized for gas-sensing,  
 36 photocurrent generation, and light emission because these  
 37 performances depend on the organization of the molecules  
 38 at the nanoscale—with each other and interacting with the  
 39 surface. MPcs can be deposited onto substrates using a  
 40 variety of methods including chemical vapor deposition,<sup>230</sup>  
 41 thermal evaporation,<sup>228</sup> and Langmuir-Blodgett (L-B)  
 42 deposition.<sup>231</sup> Numerous intrinsic and extrinsic factors,  
 43 such as substrate composition, deposition mode and  
 44 conditions (e.g., solvent, temperature, concentration),<sup>231,232,</sup>  
 45 <sup>233</sup> and intermolecular interactions,<sup>234</sup> can influence the  
 46 formation of different crystallographic phases. These  
 47 distinct phases can affect certain properties of MPcs, such  
 48 as electronic and optical properties. For example, on six-  
 49 fold symmetric Au(111), planar CuPc with  $D_{4h}$  symmetry  
 50 assembled into a square lattice structure (**Figure 9a, 9e**).<sup>229</sup>  
 51 The CuPc's strong interaction with the Au(111) surface lead  
 52 to a slight deviation of the HOMO (-1.5 eV) of CuPc. When  
 53  
 54  
 55  
 56  
 57  
 58  
 59  
 60

adsorbed on a Dirac material such as graphene, CuPc  
 molecules self-assembled into parallel perpendicular chain-  
 like structure (**Figure 9b, 9f**), and shifted the HOMO level of  
 CuPc to -1.3 V.<sup>229,235</sup> A slight reduction of the HOMO-LUMO  
 gap of CuPc can be observed as compared to that on  
 Au(111) substrate. The MPc-substrate interaction also  
 seems to be related to the identity of the metal center. Dou  
*et al.* observed that on the surfaces of graphene on Ni(111),  
 Ni, Cu and Zn MPc exhibited weak interactions while FePc  
 and CoPc had much stronger coupling interactions  
 attributed to the nature of the d-band.<sup>236</sup>

Influencing the kinetics and thermodynamics of the self-  
 assembly process can lead to different structural  
 architectures in MPcs. For example, three distinct ordered  
 phases have been reported by using titanyl phthalocyanine  
 (TiOPc) monolayer on the surface of Au (111) through the  
 control of the deposition flux. The kinetically accessible  
 hexagonal phase is shown in **Figure 8c, 8g**.<sup>234</sup> The  
 intermolecular interactions can also be used to construct  
 highly organized two- and three-dimensional structures on  
 surfaces with the participation of the other building  
 blocks.<sup>237</sup> For example, multiple intermolecular hydrogen  
 bonds between the H atom of neighboring chloroaluminium  
 phthalocyanine molecule and the peripheral F atom on  
 perfluoropentacene can be used form a stable ordered  
 square network in molecular ratio of 2 : 1 (**Figure 9d,**  
**9h**).<sup>238</sup>

These precedents suggest that it is important to  
 understand the many parameters involved in self-assembly  
 of MPc structures on the surfaces of substrates in order to  
 control their orientation and alignment, where both the  
 adsorbate–substrate, adsorbate–adsorbates interaction, as  
 well as the self-assembly dynamics can affect the  
 aggregation state of MPcs on surfaces.<sup>26</sup> It is important to  
 note that these interactions will also influence the electrical  
 properties of MPcs on surfaces.

**Supramolecular Self-Assembly and Covalent  
 Linkage of Substituted MPcs.** Considerable effort has been  
 devoted to the functionalization of MPcs to influence their  
 supramolecular nanoarchitectures into organized  
 structures and investigate their emergent properties.<sup>28, 82</sup>  
 Some of these complexes include “shish-kebab” type 1D  
 polymers (**Figure 10a**) and sandwich-like  
 bis(phthalocyaninato)lanthanide(III) complexes (**Figure  
 10b**). The biaxially coordinated MPc structures were  
 initially developed to influence cofacial stacking  
 arrangements and influence small interplanar distances to  
 allow  $\pi$ - $\pi$  overlap and enhance conductivities (0.1 S/cm).<sup>239</sup>  
 The strategy of controlled orientation of MPc polymers can  
 attain good conductivities without oxidative doping, and  
 can be

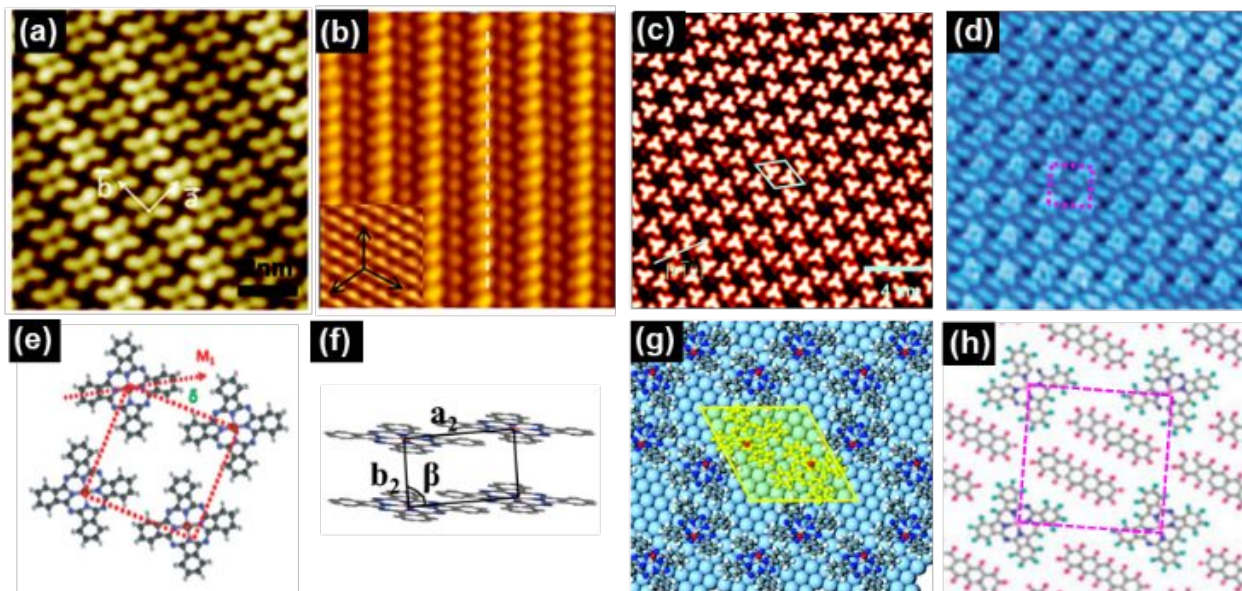


**Figure 9.** STM images of (a) CuPc with a tetrameric unit cell on Au(111)<sup>229</sup> (b) the second layer of CuPc films consisting of parallel standing-up CuPc chains<sup>235</sup> (c) a full monolayer of TiOPc with honeycomb phase on Ag (111),<sup>234</sup> and (d) a ordered square binary molecular network formed by chloroaluminium phthalocyanine molecule and perfluoropentacene in a molecular ratio of 2:1 on HOPG.<sup>238</sup> (e)-(h) are the corresponding structural model for (a)-(d), respectively. Figures (a and b) reproduced with permission from reference<sup>235</sup>. Copyright 2017 MDPI. (<http://creativecommons.org/licenses/by/4.0/>). Figures (e and f) were reprinted from reference<sup>229</sup>. Copyright 2008 American Chemical Society. Figures (c, d and h) were reproduced with permission from reference<sup>234</sup>. Copyright 2019 The Royal Society of Chemistry. Figure (g) reprinted with permission from<sup>238</sup>. Copyright 2014 American Chemical Society.

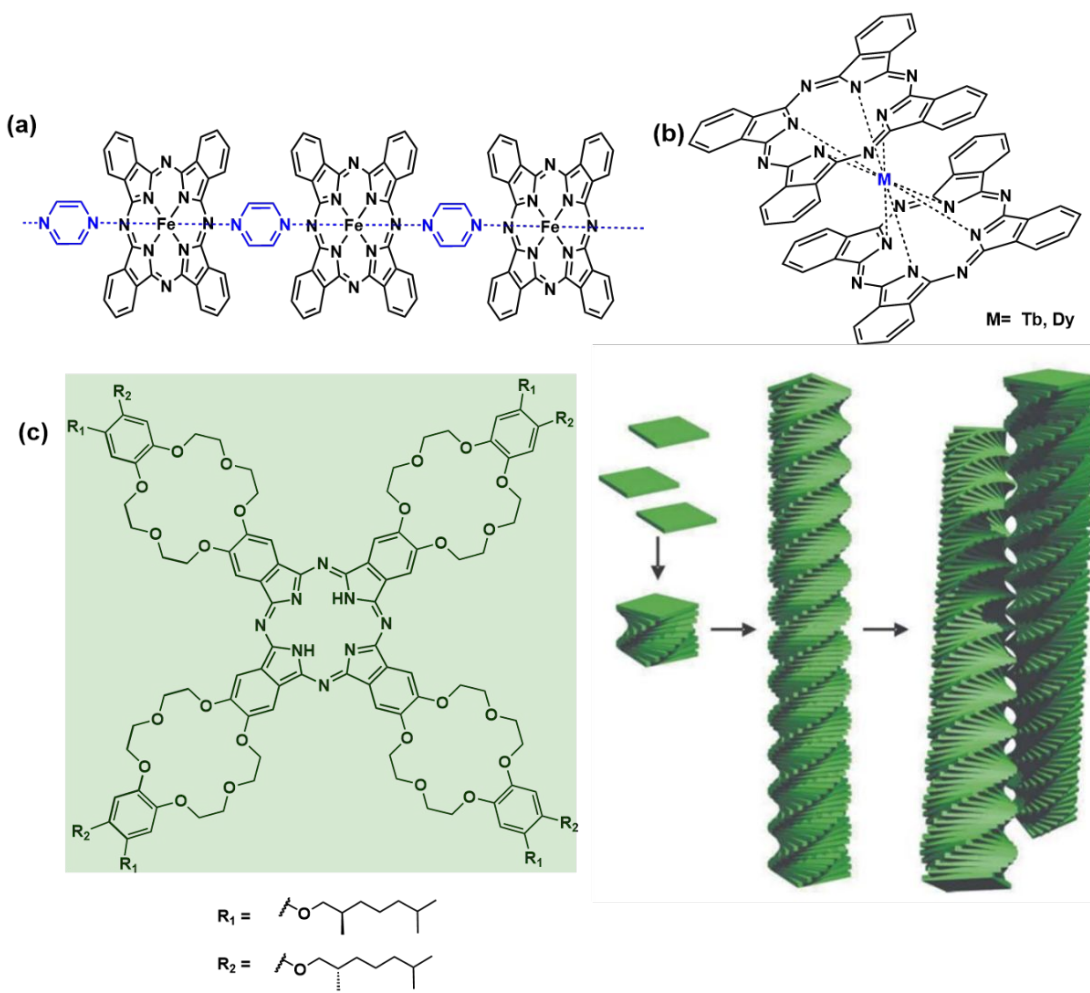


**Figure 10.** (a) Structure of phthalocyaninato(p-pyrazine)iron(II).<sup>239</sup> (b) phthalocyanine double-decker complexes, (M=Tb, Dy)<sup>240</sup> (c) Crown ether phthalocyanine<sup>114</sup> (a) Adapted with permission from reference<sup>239</sup> Copyright 1988 Elsevier (b) Adapted with permission from reference<sup>240</sup> Copyright 2003 American Chemical Society and (c) Reprinted with permission from reference<sup>114</sup> Copyright 1999 AAAS.

prepared by means of connecting the central metal cavities through bivalent bridges with compounds such as bipyridine (bpy) or 1,4-diisocyanobenzene (dib), (Figure 10a).<sup>239</sup> The combinations of different metal cavities and π-electron containing bridging ligands can also change the electrical, magnetic and optical properties observed in these polymers.<sup>239</sup> The sandwich-like MPc complexes (Figure 10b) can demonstrate interesting magnetic properties when integrated with lanthanide elements. Kaizu and coworkers observed slow magnetization relaxation as single molecular property in Tb<sup>3+</sup> or Dy<sup>3+</sup> substituted MPcs, where the origin of the magnetism is from both orbital and spin angular momentums of a single lanthanide ion.<sup>240</sup>

The structural modification to the periphery of MPcs can be used to improve this intrinsic self-organization into columnar structures. A seminal example of this influence has been observed through functionalization of metal-free phthalocyanines with crown ethers, where Nolte, Rowan and coworkers attached micrometer-long chiral tails to the periphery of MPcs, which then self-assembled to form

helical coiled-coil aggregates when dissolved in chloroform (Figure 10c).<sup>114</sup> The group observed a self-organization of MPcs into right-handed helical columns that further assemble into left-handed twisted bundles (Figure 10c)<sup>47, 114, 241</sup> Such control over chirality may be valuable for optoelectronic applications, where optically active chiral fibers are desirable candidates for use as nonlinear optical materials and as components in sensor devices for the detection of alkali metal ions through complexation between crown ether moieties.

Alternatively, greater levels of control over supramolecular assembly may be achieved through covalent linkage of D-A systems. Considerable effort has been devoted to creating new active materials for organic photovoltaic devices that convert solar to electrical energy with high efficiency.<sup>242</sup> These materials, generally made by combining one electronically rich and one electronically deficient material, so called D-A systems, must use photons to create free charge carriers that are efficiently separated and collected at separate electrodes. One method to fabricate D-A systems using MPcs is through covalently

linking them to electron acceptors, such as carbon nanotubes, porphyrins, perylenediimides (PDIs), and fullerenes.<sup>243</sup>

Covalently linked systems can offer several advantages over supramolecular assembled ones, such as closer proximities and modulation of electronic properties in the ground and excited states.<sup>244</sup> The relative distances of the D-A moieties, orientation, aggregation and electronic coupling of covalently linked D-A complexes have also been known to crucially affect the yields and kinetics of charge transfer in D-A systems.<sup>245-246</sup>

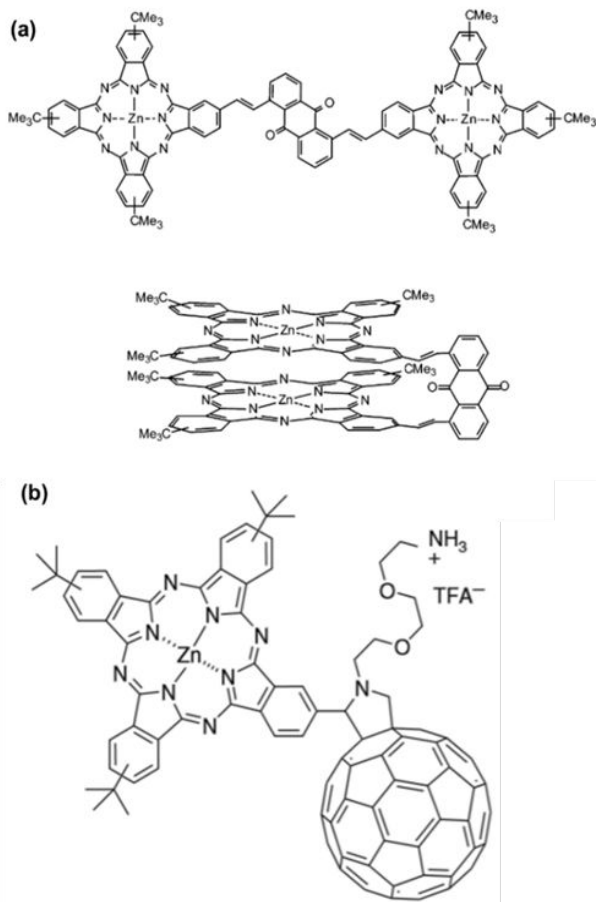


**Figure 11 (a)** Examples of covalently attached D-A systems (a) ZnPc- anthraquinone -ZnPc triad<sup>245</sup> (b) Zinc phthalocyanine (ZnPc) and C<sub>60</sub> dyad<sup>247</sup> (a) Reprinted with permission from reference <sup>245</sup> Copyright 2006 American Chemical Society. (b) Reprinted with permission from <sup>247</sup>. Copyright 2005 American Chemical Society.

PDIs have had central roles as electron acceptors in artificial photosynthesis and D-A systems due to their interesting properties,<sup>248</sup> stability, and ability to extend charge separation lifetimes.<sup>244</sup> Guldi and coworkers observed that modifications of two ZnPcs to the positions of a central anthraquinone (Figure 11a) changed the aggregation status of the triads which altered the kinetics of these electron transfer reactions.<sup>245</sup> Additionally, fullerenes have been extensively used as electron acceptors covalently linked to MPcs because they can potentially act as electron accumulators, have favorable reduction potentials, and can

absorb in different regions of the spectrum (ZnPc at  $\lambda \sim 550$  to 750 nm and C<sub>60</sub> at  $\lambda \sim 420$  to 470 nm).<sup>249-249</sup> As such, Guldi *et al.* described the self-organization of ZnPc and C<sub>60</sub> (Figure 11b) into nanostructured 1-D nanotubes and presented ultrafast charge separation (i.e.,  $\sim 10^{12}$  s<sup>-1</sup>) and ultraslow charge recombination (i.e.,  $\sim 10^3$  s<sup>-1</sup>).<sup>247</sup> The observed ZnPc<sup>+</sup>-C<sub>60</sub><sup>-</sup> lifetime of 1.4 ms, relative to that of the monomeric ZnPc-C<sub>60</sub> ( $\sim 3$  ns) was found to be an impressive stabilization of 6 orders of magnitude.

The synthetic substitution, covalent linkage and assembly of substituted MPcs make promising, highly ordered architectures and materials by applying the fundamental principles of supramolecular assembly. The insertion of functional groups on the peripheral or axial sites of MPcs will influence their kinetic or thermodynamic states during hierarchical assembly and can shift their final chemical and physical properties to new territories. The covalent linkage of D-A constituents provides new developments of photophysical systems along with foundational studies to build on our understanding of the kinetics of charge transfer and the parameters that affect photo-induced charge separation lifetimes. Although only a few examples were mentioned here, there are many examples of covalently linking MPcs to electron acceptors, and the effects of structural modification on their supramolecular assembly and charge dynamics.<sup>26</sup>

## DESIGN, SYNTHESIS AND ASSEMBLY OF MPC-FRAMEWORKS

**Reticular chemistry in manipulating framework architectures.** Reticular chemistry utilizes the relatively strong coordination and covalent bonds to make crystalline open frameworks and significantly expanded the scope of chemical compounds and useful materials.<sup>187, 250, 251</sup> This bottom-up approach for the construction of framework materials involves the assembly of molecular components with well-defined structure, geometry, and pre-embedded functionalities, usually driven under thermodynamic conditions, to afford structures that exceed the simple sum of different molecular components.<sup>252, 253</sup> Compared with top-down fabrication, bottom-up approaches are more versatile, more precise, and can provide extensive structural diversity. The trademark advantage of MOF/COF frameworks is their modular design, structural diversity, and synthetic access to custom ligands that allow for rationally designed structures with functionalized pores and surfaces.<sup>254</sup>

Yaghi and coworkers demonstrated how self-assembly principles may be used to direct the synthesis of MOFs using metal-carboxylate type bonds to enable rigid structures with permanent porosity and large surface areas.<sup>255</sup> This revolution in crystalline material design and synthesis has provided a diverse toolkit for coordination-driven self-assembly.<sup>256</sup> The geometry and symmetry of the precursors are used, in addition to topology, to direct the final topology of the frameworks and can lead to control over useful functional properties such as topology, porosity, dimensionality and surface chemistry. The reported novel frameworks propelled the field of reticular chemistry and led to the development of thousands of new framework

1 structures for applications such as gas storage and  
2 separation, catalysis, optoelectronics, chemical sensing,  
3 etc.<sup>256</sup>

4 The synthesis of both MOFs and COFs require  
5 thoughtful reflection on the appropriate functionalities  
6 upon the molecular components that would enable the final  
7 desired topology and properties. As much of this precedent  
8 has been carried out for existing frameworks structures  
9 using available synthetic chemistry, functional group  
10 incorporation on MPc building blocks has naturally built on  
11 this existing precedent that broadly incorporates  
12 coordination or dynamic covalent chemistry.

### 13 Synthetic development of MPc Frameworks.

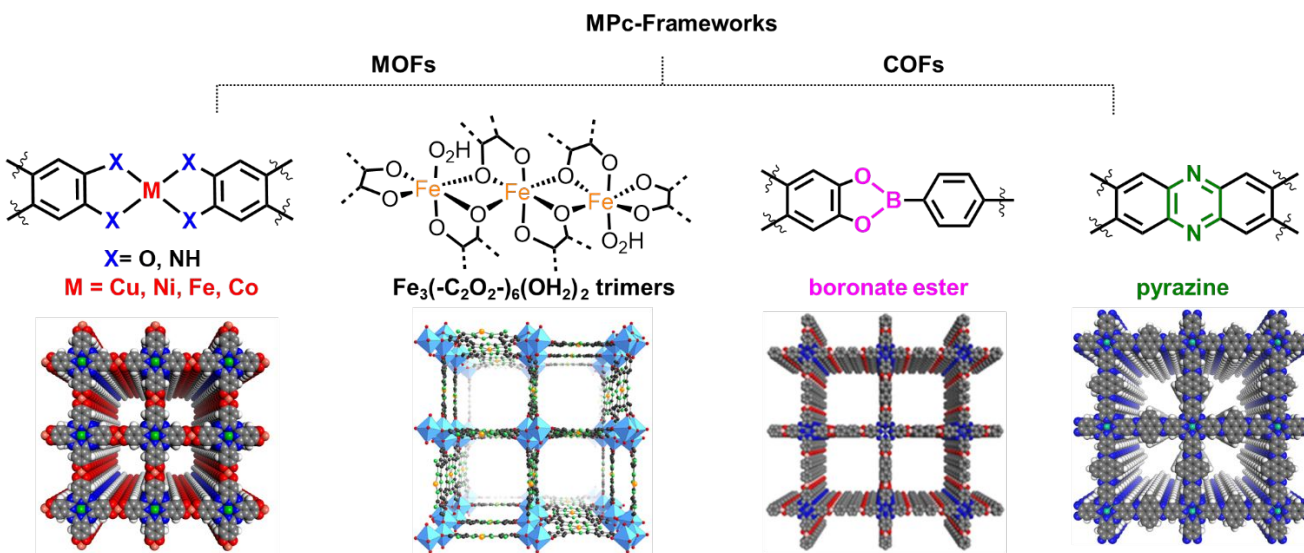
14 Historically, the advancement of multifunctional COFs is  
15 largely associated with the development of suitable  
16 dynamic covalent linkages, which entail reversible bond  
17 formation, regulation of thermodynamic equilibria,<sup>257</sup> and  
18 specific time-length scales for self-correction.<sup>258</sup> The first  
19 successful demonstration of crystalline COF materials  
20 utilized solvothermal self-condensation of boronic acid  
21 linkers, which can similarly combine with catechols to form  
22 boronate ester linkages.<sup>258</sup> Since this discovery, much focus  
23 became devoted to expanding the structural and chemical  
24 diversity using existing synthetic techniques, such as using  
25 borosilicate,<sup>259</sup> imine,<sup>260</sup> triazine and hydrazone linkages.<sup>261</sup>  
26 Not to be trivialized, Schiff base chemistry has constituted  
27 the largest number of COFs to be fabricated using a variety  
28 of complex and functional precursors, and have allowed the  
29 incorporation of useful physio-chemical properties, such as  
30 enhanced chemical stability.<sup>262</sup>

31 The first synthesized COFs — linked with catechol  
32 linkers and 1,4-benzenediboronic acid (BDBA) — were  
33 two dimensional and have provided the foundations on  
34 which to build multifunctional COFs.<sup>263</sup> Following this  
35 strategy, the first MPc-based COFs were built using the  
36 same boronic acid condensation chemistry in 2010, when  
37 Dichtel and coworkers synthesized a NiPc and 1,4-  
38 phenylenebis(boronic acid) linked COF using acetonide-  
39 protected catechol linkers to avoid autoxidation of  
40 precursors.<sup>83</sup> This precedent was the first report of the  
41 organization of MPc monomers within frameworks — as  
42 eclipsed AA stacking — which was attributed to the  
43 tendency of Pcs to aggregate in a cofacial stacking  
44 arrangement. Because of this eclipsed aggregation  
45 arrangement, it became evident that embedding MPcs  
46 within frameworks can either enhance or shift their optical  
47 absorption capability in the visible and near-infrared  
48 regions,<sup>264</sup> and improve their photocurrent generation  
49 capabilities.<sup>84, 264, 265, 266</sup> In fact, from 2010 to 2014, progress  
50

51 on MPc-COFs made using boronate ester linkages has led to  
52 the discovery of interesting new electrical, optical and  
53 photoconductive properties (**Table 3**).<sup>83, 267, 268, 269, 270</sup>

54 While boronate ester linkages have provided the  
55 foundations for deeper insight of structure–property  
56 relationships in MPc frameworks, the materials made using  
57 much of this chemistry exhibited limited chemical stability  
58 and were prone to hydrolysis.<sup>271</sup> Extending COFs to new  
59 linkages in order to enhance chemical stability proved  
60 difficult, as stronger covalent bonds constrain reversibility  
61 and self-correcting behavior during crystallization.<sup>272</sup>  
62 Although attempts of using tetrasubstituted MPcs linked  
63 through imino-linkages were explored,<sup>273, 274</sup> many of the  
64 efforts yielded porous polymers with limited crystallinity.  
65 An inspiration for stable linkages in COFs came in 2013  
66 when Jiang and co-workers revealed a chemically stable and  
67 electronically conjugated organic framework can be  
68 attained using phenazine linkages.<sup>260</sup> This report has  
69 inspired us to pursue a similar synthetic strategy with MPc-  
70 (NH<sub>2</sub>)<sub>8</sub> monomers by condensing them with pyrene  
71 tetraone building blocks. We reported this strategy in 2019,  
72 when our group synthesized pyrazine linked conjugated 2D  
73 MPc COF with the condensation of tetraketone and  
74 octaamino-MPc precursors and reported the presence of  
75 high intrinsic conductivity in COF-DC-8 (*vida infra*)  
76 attributed to the aggregation and co-facial alignment of the  
77 aromatic π-conjugated macrocycles. A few months later, a  
78 2D pyrazine-linked COF was reported by Wang *et al.* in the  
79 same year, where the condensation of 2,3,9,10,16,17,23,24-  
80 octaamino-phthalocyaninato metal [II] (OAPcZn or  
81 OAPcCu) with tert-butylpyrene-tetraone yielded a serrated  
82 AA stacking structure for Zn and Cu-phthalocyanine.<sup>272</sup>

83 The extension of catechol-based precursors to 2D MOFs  
84 began in 2012, where Yaghi and co-workers reported the  
85 first demonstrations of electrical properties due to  
86 favorable d–π orbital overlap in metal-catecholate systems  
87 using 2,3,6,7,10,11-hexahydroxytriphenylene with Co(II)  
88 and Ni(II).<sup>77</sup> This precedent catalyzed the development of a  
89 number of conductive 2D MOFs, extending the use of  
90 catecholate precursors to metal bis(diimine)<sup>76</sup> and  
91 bis(dithiolene)<sup>275</sup> bonding. The use of catechol based MPc  
92 precursors also led to the first reports of 2D MPc-MOFs (M= Ni  
93 and Cu) in 2018 using octaamino- and octahydroxy-  
94 substituted MPc linkers with Ni and Cu metal nodes,  
95 respectively (**Figure 12**). Both 2D MOFs exhibited a wide  
96 range of conductivities that scaled from 10<sup>-6</sup> to 0.2 S cm<sup>-1</sup>.

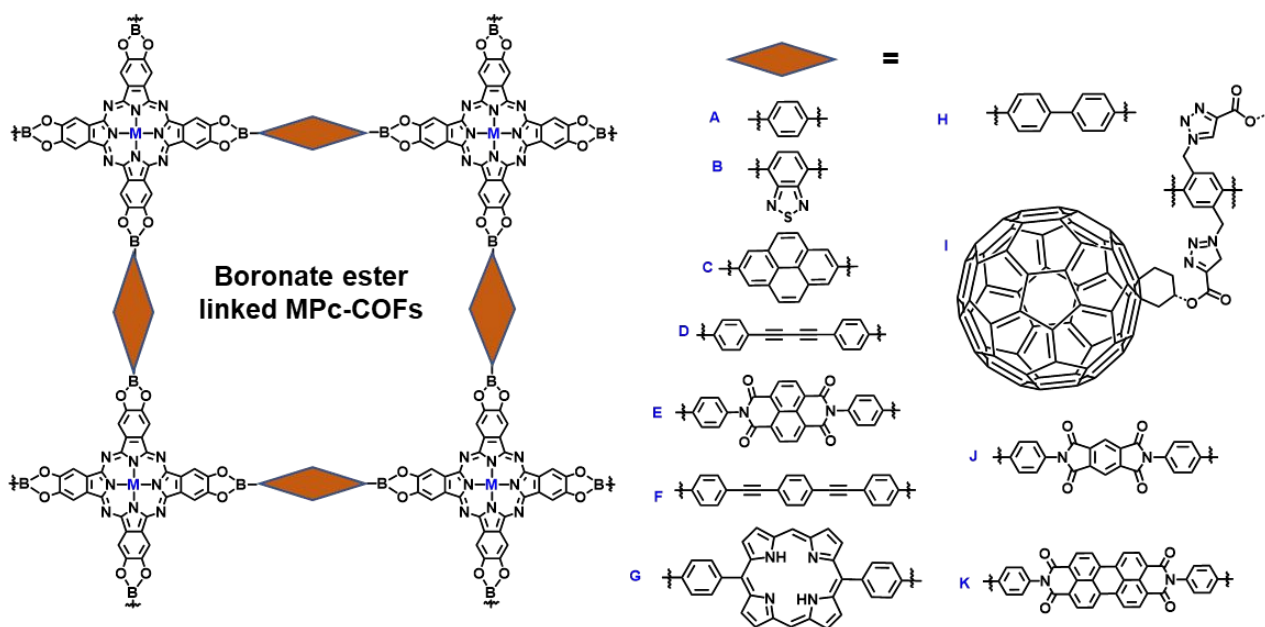


**Figure 12.** Four types of linkages found in recent MPc-MOFs and COFs (left to right) d- $\pi$  linkage, iron cluster trimers, boronate ester and pyrazine. Reprinted with permission from reference <sup>34</sup> Copyright 2019 American Chemical Society. Reprinted with permission from reference <sup>36</sup> Copyright 2019 American Chemical Society. Adapted with permission from reference <sup>83</sup> Copyright 2010 Springer Nature. Adapted with permission from reference <sup>33</sup> Copyright 2019 American Chemical Society.

In 2019, the use of octahydroxy-phthalocyanine linker became more widespread and utilized in the fabrication of 2D and 3D MPc-MOFs and their application towards sensing and catalysis were subsequently explored (**Table 3**). The report of the first 3D MPc-MOF was carried out by Yaghi and coworkers using  $\text{Fe}_3(-\text{C}_2\text{O}_2^-)_6(\text{OH}_2)_2$  trimers and cobalt phthalocyanine-2,3,9,10,16,17,23,24-octaol linkers to generate an extended framework of roc topology.<sup>36</sup> The use of the iron trimer allowed access to electron transport due to favorable orbital overlap between the metal ion and the catecholate, while providing a 3D MOF that gains access to high surface areas with catalytically accessible active sites.

Using new synthetic combinations of MPc-COFs and MOFs to place MPc building blocks with atomic precision

has deepened our understanding of structure–function properties that emerge as a result of governable self-assembly. Approaching the synthesis of new MPc frameworks with this fundamental chemical understanding, in combination with principles of molecular engineering, can enable improvement of MPc-materials and applications toward existing methods strategically and efficiently. For instance, understanding the structure–property relationship that lead to increased electrical properties in MPc-based materials can allow implementation of these relationships in new materials, positioning them as state-of-the-art materials for optoelectronic or solar energy conversion technology.<sup>84, 85, 152, 264, 265, 266, 276, 277</sup>

**Table 2.** MPc-COFs made from boronate ester linkages.

name	linker	BET ( $\text{m}^2\text{g}^{-1}$ )	properties/application	year	ref.
Pc-PBBA	A	506 <sup>a</sup>	absorption: 450–600 nm to near IR organic photovoltaic	2010	83
NiPc-PBBA	A	n/a	optoelectronic devices	2011	267
NiPc-COF	A	624	$\Phi\sum\mu = 3.9 \times 10^{-4} \text{ cm}^2 \text{ V}^{-1} \text{ s}^{-1}$ $I_{\text{dark current}} = 20 \text{ nA}$ , $I_{\text{photocurrent}} = 3 \mu\text{A}$ (under $\lambda > 400\text{nm}$ )	2011	264
NiPc-BTDA	B	877	$\Phi\sum\mu = 5.8 \times 10^{-4} \text{ cm}^2 \text{ V}^{-1} \text{ s}^{-1}$ $I_{\text{dark current}} = 250 \text{ nA}$ , $I_{\text{photocurrent}} = 15 \mu\text{A}$ (under $\lambda > 400\text{nm}$ )	2011	265
ZnPc-Py	C	420		2011	
ZnPc-NDI	D	485			278
ZnPc-DPB	E	490	ordered heterojunctions		
ZnPc-PPE	F	440			
Pc-PBBA	A	506	theoretical hydrogen storage capacity: 45.2 g/L	2012	279
CoPc-COF		517	photocurrent (under $\lambda > 400\text{nm}$ ): CuPc-COF: 110	2012	
CuPc-COF	A	1360	nA		277
ZnPc-COF		985	CoPc-COF: 0.14 nA ZnPc-COF: 0.6 nA		
D <sub>ZnPc</sub> -A <sub>NDI</sub>	E	1410	$\tau_{\text{cs}} = 10 \mu\text{s}$ optoelectronics and photoenergy conversion	2013	276
CoPc-PorDBA	G	1315	H <sub>2</sub> storage capacity: 0.8 wt% CH <sub>4</sub> storage capacity: 0.6 wt%	2013	270
CoPc-BPDA	H	1087	H <sub>2</sub> storage capacity: 1.2 wt% (77 K, 1.0 bar) CH <sub>4</sub> storage capacity: 0.59 wt% (273 K, 1.0 bar)	2013	269
10% N <sub>3</sub> -ZnPc		1051	charge separation lifetime ( $\tau_{\text{cs}}$ )	2014	
25% N <sub>3</sub> -ZnPc	I	1000	$\tau_{\text{cs}} = 2.37 \text{ ms}$ for [C <sub>60</sub> ] <sub>0.3</sub> -ZnPc-COF		84
50% N <sub>3</sub> -ZnPc		886	$\tau_{\text{cs}} = 2.66 \text{ ms}$ for [C <sub>60</sub> ] <sub>0.3</sub> -ZnPc-COF		
[C <sub>60</sub> ] <sub>0.3</sub> -ZnPc		393	$\tau_{\text{cs}} = 2.49 \text{ ms}$ for [C <sub>60</sub> ] <sub>0.5</sub> -ZnPc-COF		

1	[C <sub>60</sub> ] <sub>0.4</sub> -ZnPc	129	photoenergy conversion			
2	[C <sub>60</sub> ] <sub>0.5</sub> -ZnPc	51				
3						
4						
5	ZnPc-PBBA	A	n/a	absorbance: center at 710 nm, shoulder at 610 to 620 nm	2015	268
6						
7	D <sub>CuPc</sub> -A <sub>PyrDI</sub>	J	357			
8	D <sub>CuPc</sub> -A <sub>NDI</sub>	E	1726			
9	D <sub>CuPc</sub> -A <sub>PDI</sub>	K	414	$\tau_{cs}=33 \mu s$ for D <sub>CuPc</sub> -A <sub>DI</sub>	2015	266
10	D <sub>NiPc</sub> -A <sub>PyrDI</sub>	J	1172	photoenergy conversion		
11	D <sub>NiPc</sub> -A <sub>NDI</sub>	E	1432			
12	D <sub>ZnPc</sub> -A <sub>PDI</sub>	K	519			
13						
14	<sup>a</sup> Langmuir surface area. $\sum \mu$ , the sum of carrier mobility. $\Phi$ , the charge carrier generation efficiency. $\tau_{cs}$ , charge separation lifetimes.					
15						

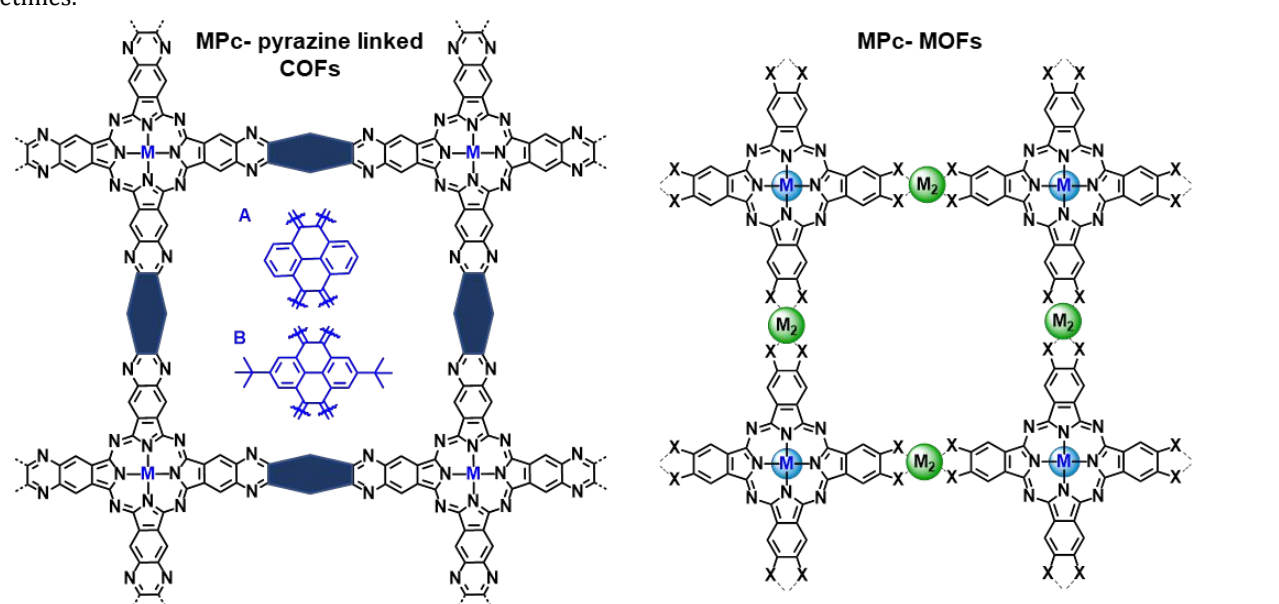


**Table 3.** (Top) Pyrazine linked MPc-COFs and (bottom)MPc-MOFs

name	linker	BET (m <sup>2</sup> g <sup>-1</sup> )	properties/application	year	ref
COF-DC-8	A	360	$\sigma = 2.51 \times 10^{-5} \text{ S/cm}$ (pellet): chemiresistive sensing LODs: 70 ppb for NH <sub>3</sub> , 204 ppb for H <sub>2</sub> S, 5 ppb for NO, and 16 ppb for NO <sub>2</sub>	2019	34
ZnPc-pz	B	487.4	$\sigma \sim 10^{-7} \text{ S/cm}$ (pellet)	2019	272
CuPc-pz		458.9	$\mu_h = \sim 5 \text{ cm}^2/\text{Vs}$		
name	M <sub>2</sub>	BET (m <sup>2</sup> g <sup>-1</sup> )	properties/application	year	ref.
MPC (M=Cr <sup>2+</sup> , Mn <sup>2+</sup> , Fe <sup>2+</sup> , Co <sup>2+</sup> , N <sup>2+</sup> i, Cu <sup>2+</sup> and Zn <sup>2+</sup> )	Ni	n/a	first principle calculations: MnPc-based MOFs exhibits half-metallicity ( $T_c < 170 \text{ K}$ )	2017	280
NiPc-MOF	Ni	593	$\sigma = 0.2 \text{ S/cm}$ (thin film) OER: $V_{onset} < 1.48 \text{ V}$ , over potential < 0.25, mass activity = 883.3 A g <sup>-1</sup> TOF = 2.5 s <sup>-1</sup>	2018	85

1	Cu-CuPc	Cu	358	$\sigma = 9.4 \times 10^{-8}$ to $1.6 \times 10^{-6}$ S cm $^{-1}$ (pellet) LIB cathode charge/discharge capacities: 151 – 128 mAh g $^{-1}$	2018	281
2	NiPc-Ni	Ni and Cu	101	$\sigma = 10^{-4}$ - $10^{-2}$ S/cm (pellet)		
3	NiPc-Cu		284	chemiresistive sensing LODs (1.5 min		
4	NiNPc-Ni		174	exposure): 1.0 – 1.1 ppb for NO, 20-33 ppb for	2019	34
5	NiNPc-Cu		267	H <sub>2</sub> S, 0.31 – 0.33 ppm for NH <sub>3</sub>		
6	PcCu-O <sub>8</sub> -Fe	Fe, Co, Ni, Cu	412 (PcCu-O <sub>8</sub> -Co)	ORR with PcCu-O <sub>8</sub> -Co/CNTs:		
7	PcCu-O <sub>8</sub> -Co			$E_{1/2}=0.83$ V (vs RHE), $j_L=5.3$ mA cm $^{-2}$ ,	2019	282
8	PcCu-O <sub>8</sub> -Ni			discharge current=120 mA cm $^{-2}$ (0.8 V),		
9	PcCu-O <sub>8</sub> -Cu			maximum power density=94 mW cm $^{-2}$		
10	MOF-1992-[Fe] <sub>3</sub>	Fe <sub>3</sub> (-C <sub>2</sub> O <sub>2</sub> -)	1471	CO <sub>2</sub> reduction to CO with MOFs/carbon black:		
11	MOF-1992-[Mg] <sup>3</sup>	<sub>6</sub> (OH <sub>2</sub> ) <sub>2</sub>	1481	$j= -16.5$ mA cm $^{-2}$ (at -0.63 V vs RHE), TOF=0.2 s $^{-1}$ , faradaic efficiency=80±5%	2019	36
12	Fe <sub>2</sub> [PcFe-O <sub>8</sub> ]	Fe	206	$\sigma = 2 \times 10^{-3}$ S/cm (pellet), $\mu=15 \pm 2$ cm $^2$ V $^{-1}$ s $^{-1}$ , superparamagnetic features, magnetic hysteresis up to 350 K	2019	283
13	Fe <sub>2</sub> -O <sub>8</sub> -PcCu	Fe, Zn	n/a	$\sigma = 6.9\text{--}9.7 \times 10^{-3}$ S/cm (I <sub>2</sub> loaded MOFs, pellet)		
14	Zn <sub>2</sub> -O <sub>8</sub> -PcCu			rechargeable Na-I <sub>2</sub> batteries: specific capacity: 204-208 mAh g $^{-1}$ , up to 3200 cycles	2019	282
15	PcCu-O <sub>8</sub> -Zn	Zn	378	Electroreduction of CO <sub>2</sub> to CO $j = 8$ mA cm $^{-2}$ (at -0.7 V vs RHE) faradaic efficiency <sub>CO</sub> (PcCu-O <sub>8</sub> -Zn/CNT) = 88% TOF = 0.39 s $^{-1}$	2020	284

\* $\sigma$ , electrical conductivity.  $\mu_h$ , hole mobility.  $\mu$ , charge carrier mobility.  $E_{1/2}$ , half-wave potential.  $j_L$ , limited current density.  $j$ , current density.

**Controlled growth of MPc-COFs.** The emergent functional properties in MPc frameworks lend themselves to several unique applications. In order to develop these multifunctional properties to their full potential, it is first critical to understand the fundamental intrinsic and physical parameters of material behavior. The examination of these properties in their pristine form can be difficult to achieve as framework materials generally precipitate in an insoluble microcrystalline bulk powder, too small to fully characterize using single crystal diffraction techniques and difficult to process within devices. Using other existing procedures, such as electron microdiffraction and grazing incidence x-ray diffraction (GIXRD), can enable us a closer look at the relative orientations, crystallinity, and defects within a material that form as a result of dynamic equilibria. For COFs, polymerization can undergo either kinetic control or thermodynamic control, in which structural organization and bond formation can occur subsequently or simultaneously, respectively.<sup>263</sup> Depending on the type of equilibrium, these dynamics can influence many of the structural characteristics seen in the final morphology of the material, such as crystallinity, presence of defects, composition of edge sites, etc., which can then influence other fundamental properties.

Although it is important to mention here that there exists extensive precedent concerning the advancement of

controlled MOF growth using techniques such as anchoring to surfaces with functionalized self-assembled monolayers, electrospray ionization, seeding methods,<sup>285</sup> or electrochemical approaches,<sup>286</sup> these can be difficult to implement for controlled COF growth. Much of the research concerning the templated growth of MPc-based COFs to date represent template growth on single layered graphene (SLG) (*vida infra*). As of now, other reported methods of MPc-framework synthesis rely on solvothermal approaches, which have yielded the report of a single crystal structure of an MPc-based MOF.<sup>36</sup> In general, MOF growth is controlled by judiciously selecting the solvents and modulators to allow for dynamic bond formation and to prevent the precipitation of non-crystalline material, such as with the synthesis of Zr-MOF, UiO-67.<sup>287</sup> In addition, electrochemical, mechanochemical, and sonochemical means of control are available along with layer-by-layer deposition, liquid phase epitaxial growth and seeded growth to form thin films.<sup>287</sup> An interesting approach by Ameloot *et al.* demonstrated that electrochemical control allowed for spatial control of MOFs on a substrate.<sup>286</sup> Yet control over MPc-based COFs is difficult due to their nature to precipitate from solution before a large single crystal can grow. In order to improve MPc-based MOF and COF growth, solvothermal methods need to be tuned to optimize the specific molecular building blocks in each specific case or

external methods of control like those used for general MOFs and COFs need to be implemented.

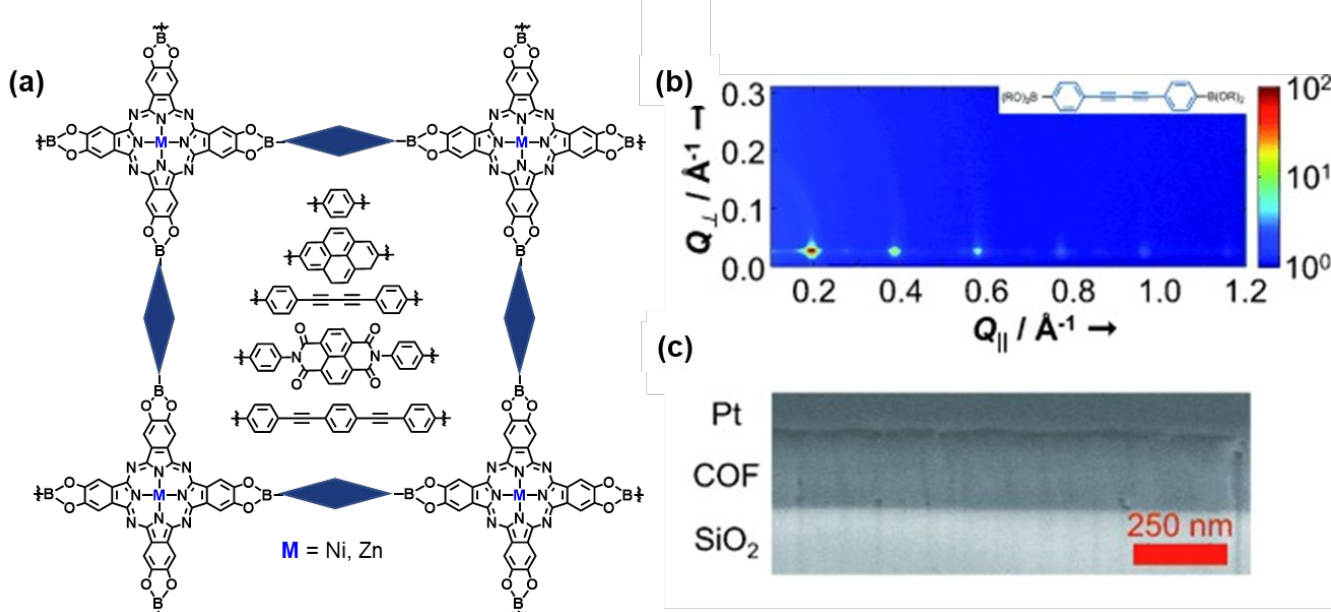
As COFs generally precipitate in the form of an insoluble powder, they are difficult to process and interface with substrates, which limit their applications. Fabricating uniform thin films of COFs templated on the surface of substrates as nanosheets can limit the presence of grain boundaries, improve electrical properties, and alleviate some of such limitations.<sup>288</sup> In this context, the physical properties of COF films (grain boundaries, edge sites, thickness etc.) may profoundly influence device performance, so achieving new levels of control over framework growth is key to optimize framework materials for effective interfacing. Thus, understanding the kinetics of COF growth is crucial because it can enable morphological control, improve structural fidelity, and harness desired properties. Towards this end, studies of templating 2D framework films on various substrate surfaces have been reported using techniques to achieve monolayer and multilayer growth such as solvothermal,<sup>267</sup> interfacial synthesis,<sup>289, 290</sup> and drop casting.<sup>263, 291</sup>

The controlled orientation and layer-by-layer growth of 2D materials through the solvothermal bottom-up approach was pioneered by Dichtel and co-workers in 2011.<sup>267</sup> This work utilized single layered graphene (SLG) to template NiPc-PBBA COF films to enhance their crystallinity and control the alignment of thin films. The authors took advantage of GIXRD technique, which measures the periodicity and orientation of COF films relative the surfaces and found ordered parallel stacking with respect to the surface of the substrate (Figure 13b). Using this characterization method established new routes for direct observation of the thin film organization onto the surface of graphene to enable long range ordered  $\pi$ -systems for enhanced interfacial alignment with optoelectronic devices.

Towards the rational design and manipulation of ordered framework materials with tunable physical

properties, Dichtel's group also systematically expanded the lattice of ZnPc COFs using four linear diboronic acid linkers to accommodate specific domains on the surface of semiconductors.<sup>278</sup> Using a technique previously demonstrated using NiPc-PBBA, the ZnPc COF films were grown on single layer graphene/silica substrates to improve the interface with electrodes or incorporate into devices. Superior crystallinity and alignment were observed in ZnPc-DPB (diphenylbutadiene) COF (Figure 13b), which was credited to its diphenylbutadiene linker, due to its ease of attaining a coplanar conformation needed during COF formation. This work demonstrated the opportunity to position extended  $\pi$ -systems in a predictable fashion while exhibiting precise control over pore sizes that may accommodate other functional groups, such as fullerenes.

The ability to organize functional  $\pi$ -electron systems on substrates provides reliable and optimized interfacing with electrodes while permitting the capability to both quantify and optimize COF properties. Due to their insoluble, polycrystalline nature, there exists challenges related to characterization of COF structures and the ability to control their morphology. Understanding their nucleation and growth dynamics using innovative techniques such as *in-situ* electron microscopy<sup>292</sup> is the first step in gaining new levels of control over crystallinity and framework morphology. In terms of characterization, applying existing techniques such as microcrystal electron diffraction (MicroED),<sup>293</sup> can provide new insight to edge site functionality, domain size and defects. Additionally, work by Dichtel and co-workers are pioneering new ways to understand and control COF growth mechanisms using colloidal COF nanoparticles and observing their structure formation using *in situ* X-Ray diffraction.<sup>294</sup> Building on these fundamental insights allows for research to apply principles of molecule engineering to access new levels of control over COF properties.<sup>83, 263, 267, 268, 278, 295</sup>



1  
2  
3  
4  
5  
6  
7  
8  
9  
10  
11  
12  
13  
14  
15  
16  
17  
18  
19  
20  
21  
22  
23  
24  
25  
26  
27  
28  
29  
30  
31  
32  
33  
34  
35  
36  
37  
38  
39  
40  
41  
42  
43  
44  
45  
46  
47  
48  
49  
50  
51  
52  
53  
54  
55  
56  
57  
58  
59  
60

**Figure 13.** MPc-based COFs based on Ni and Zn phthalocyanines joined by (top to bottom) benzene, pyrene, diphenylbutadiyne, naphthalenediimide, and phenylbis(phenylethynyl) units. (b) characterization using grazing incidence diffraction (top) and (c) SEM image (bottom) of ZnPc- DPB (diphenylbutadiyne) analog. Reprinted with permission from reference <sup>278</sup> Copyright 2012 Wiley-VCH Verlag. (<https://creativecommons.org/licenses/by/3.0/>)

## MULTI-FUNCTIONAL PROPERTIES IN MPc-BASED FRAMEWORKS

Engineering metal- and covalent organic frameworks to serve target function requires the consideration of at least three features: desired properties, chemical building blocks, and how their structural self-organization can achieve those properties.<sup>25, 251, 253</sup> Implementing these features through the lens of reticular chemistry has yielded frameworks with commercially available carboxylate based organic linkers and inorganic secondary building units,<sup>253</sup> resulting in rigid structures with new topologies, high surface areas, and functional internal surface chemistries, largely been applied towards gas storage and separation. Using reticular chemistry in combination with the strategic synthesis of novel precursors (rather than commercially available starting materials) has enabled the discovery of new properties in frameworks and led to a deeper understanding of their structure-function relationships. Utilizing MPc building blocks in the context of reticular principles enables access to unique multifunctional properties because of their diverse array of functional chemical and physical properties that can be harnessed, enhanced, and manipulated when integrated into frameworks. Thus, through the introduction of peripheral substituents, generally synthesized through tetramerization of substituted phthalonitriles to generate planar 2,3,9,10,16,17,23,24-octa-substituted phthalocyanines, the incorporation of MPcs into frameworks can be realized.

**Electronic properties.** The design and tailoring of intrinsic electronic properties in MOFs and COFs are essential for unlocking their full potential as functional semiconductors in areas such as fuel cells, supercapacitors, and chemiresistive sensing<sup>22</sup>, where surfaces and interfaces are central in operation and device performance.<sup>296</sup> Conductivity( $\sigma$ ) is proportional to the product of mobility ( $\mu$ ) and the concentration of electrons (n) and the concentration of holes (p):

$$\sigma = e(n \mu_e + p \mu_h) \quad (1)$$

where  $\mu_e$  is electron mobility and  $\mu_h$  is hole mobility, defined in units of S/cm. Charge mobility depends on the efficiency of charge transport, and is dictated by the effective mass ( $m^*$ ) of charge carries and the frequency of scattering events ( $\tau$ ), where e is elemental charge:

$$\mu = \frac{e\tau}{m^*} \quad (2)$$

and is almost always defined in units of  $\text{cm}^2 \text{V}^{-1}\text{s}^{-1}$ . A semiconducting material can follow two mechanisms, band or hopping transport.<sup>22, 296</sup> In both systems, to achieve high mobility, a material needs good spatial and orbital overlap and symmetry.<sup>22</sup> In MOF and COF materials, two strategies to achieve conductivity based on these principles involve  $\pi$ -conjugation in COFs and d- $\pi$  conjugation in MOFs.<sup>22</sup>

The extensive precedent concerning the electrical behavior of MPc monomers has established an excellent foundation for utilizing this information in frameworks for significantly improved charge transport properties. MPc monomers in the pristine form usually exhibit insulating electrical behavior ( $10^{-12} \text{ S/cm}$ ).<sup>46, 297</sup> Embedding MPcs into frameworks systems has been shown to provide collectively improved bulk conductivities by nine orders of magnitude (up to  $2.51 \times 10^{-5} \text{ S/cm}$ ).<sup>34</sup> In MPc-COFs, this improvement has largely been attributed to the optimized orbital overlap of  $\pi$ -orbitals to generate conduction bands through the crystallographic axis. Interpretation of this charge transport dynamics, with the insight of density functional theory in MPc-COFs,<sup>34, 272, 298</sup> has led to their initial demonstrations toward donor-acceptor type structures for photoelectronics and chemiresistive sensing.

### Photoelectronic properties in MPc-frameworks.

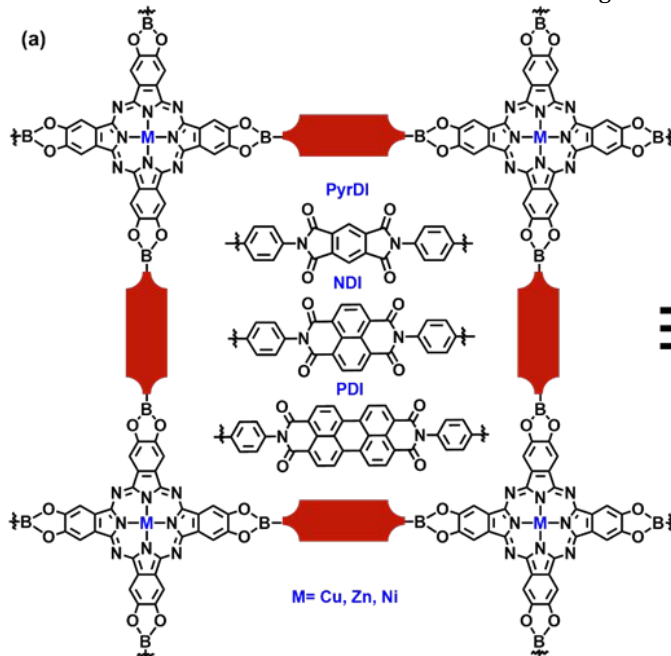
Photo-induced electron transfer and separation are important concepts in developing artificial photosynthesis and systems for photoenergy conversion and storage.<sup>276</sup> Phthalocyanines are natural electron donor candidates for these systems because they absorb a wide range of wavelengths in the visible and near-IR spectrum and have tunable redox potentials.<sup>243</sup> Accordingly, there is extensive precedent of covalently or noncovalently linking phthalocyanines to electron acceptor moieties in reported D-A complexes.<sup>299</sup> Within these systems, it has been demonstrated that molecular orientation of both constituents is crucial for optimized conversion efficiency.<sup>246</sup> A limitation of current D-A systems using MPcs is the lack of control over their organization and assembly to create long-lived charge-separated states for optimizing energy conversion technology. To create photoinduced electron transfer to investigate the charge dynamics and lifetimes of the donor-acceptor COFs, time-resolved electron spin resonance (TR-ESR) is usually employed and constitutes an exponential function defined by:

$$\Phi = \alpha \exp [-t/\tau_{CS}] \quad (3)$$

where  $\alpha$ ,  $t$ , and  $\tau_{CS}$  are the proportional factor, time, and lifetime, respectively.<sup>84, 266, 276</sup>

Conductive frameworks are valuable materials in this regard because they allow control over position of donor/acceptor moieties and consequently, tuning of charge carrier dynamics.<sup>266, 300</sup> An electron donor-acceptor type framework can be realized through either direct incorporation of electron rich/deficient monomers into the skeleton of the framework or post-synthetic functionalization of the open channels. Careful consideration of placement and orientation of D-A moieties can provide several advantages over monomer based systems, including increased charge separation lifetimes.<sup>84</sup> To this effect, Jiang and coworkers expanded their design of electron donor-acceptor COFs and surveyed the structure-property relationship of various electron donating

1 phthalocyanines and electron accepting pyromellitic, 2 naphthalene and perylene diimide (PyrDI, NDI, and PDI, 3 respectively) derivatives (**Figure 14**).<sup>266</sup> In this strategy, 4 MPcs act as electron donors while diimides, including 5 pyromellitic diimide, naphthalene diimide, and perylene 6 diimide, act as electron acceptors. The study found that the 7 heterojunctions in the COFs enable fast charge separation, 8 and the aligned donor-acceptor  $\pi$ -columns enable long- 9 distance charge delocalization and long-lived charge 10 separation, up to  $\tau_{cs} = 33 \mu\text{s}$  for  $\text{D}_{\text{CuPc}}\text{-A}_{\text{DI}}\text{-COF}$ .<sup>266, 276</sup> This 11 charge separation lifetime was several orders of magnitude 12 higher than those reported for similar systems using 13 donor-acceptor-donor triads featuring ZnPc as and 14 perylenediimide (PDI).<sup>244</sup> The investigation of optimum 15 structures using density-functional tight-binding (DFTB) 16 methods of each  $\text{D}_{\text{MPc}}\text{-A}_{\text{DI}}\text{-COFs}$  were carried out to reveal 17 the significant influences of the central metal and diimide 18 acceptor on total crystal stacking energy. The charge 19 separation lifetimes were observed to be relatively longer 20 in the  $\text{D}_{\text{CuPc}}\text{-A}_{\text{DI}}\text{-COF}$ , which may be influenced by stacking 21 behavior among the different metal MPcs, which affect 22 charge hopping. The ordered one-dimensional square 23 channels in MPc-COFs can also be used for immobilizing 24 channels in MPc-COFs can also be used for immobilizing 25



electron acceptors to realize effective charge separation. In 2014, Jiang and coworkers used click chemistry to immobilize fullerene-based electron acceptors into the channels of ZnPc-BDBA (with X% N<sub>3</sub>-ZnPc) for photoinduced charge generation of ZnPc<sup>•+</sup> and C<sub>60</sub><sup>•-</sup> radical species that were delocalized in the  $\pi$ -system.<sup>84</sup> Indeed radical cation species in porphyrins and phthalocyanines have been shown to be stable compounds due to their electronic flexibility.<sup>301</sup> The authors use TR-ESR to examine the charge dynamics, where they observed a narrow spectral width indicating weak dipolar interactions between the two spatially separated species.<sup>84</sup>

Pioneered by the work of Jiang and coworkers, using MPc-COFs in D-A systems has shown exceptional potential for charge separation and solar energy conversion. Control over the structural order and orientation in D-A systems provides the advantage to create long-lived charge separation lifetimes and allows investigation of structure-property relationships, including compositional effects of the acceptor, stacking mode, lattice expansion, and metal cavity in MPc.

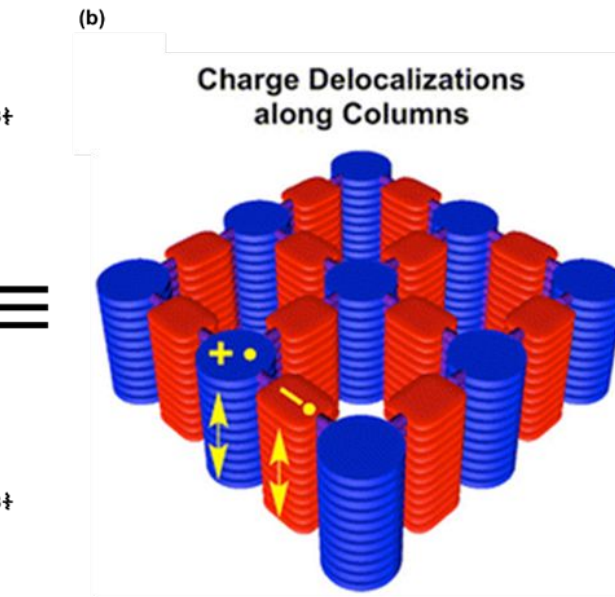


**Figure 14.** (a) Donor-acceptor COFs ( $\text{D}_{\text{MPc}}\text{-A}_{\text{DI}}\text{-COFs}$ ) with covalently linked phthalocyanine-diimide (MPc-DI) structures (b) motion of charges in the  $\pi$ -columns leads to two different lifetimes. Reprinted with permission from reference<sup>266</sup> Copyright 2015 American Chemical Society.

**Electrical conductivity in MPc-frameworks.** In 2011, Ding *et al.* showed that high carrier mobility can be achieved through preorganized conduction paths along vertically aligned NiPc  $\pi$ -systems within NiPc-BDBA (1,4-benzenediboronic acid) COF. The same group used principles of molecular design to manipulate the nature of charge carriers in MPc-COFs through the incorporation of an electron-deficient benzothiadiazole (BTDA) group to manipulate the charge mobilities of reported NiPc-COF.<sup>265</sup> The n-channel conducting COF was reported to have high mobility ( $0.6 \text{ cm}^2 \text{ V}^{-1} \text{ s}^{-1}$ ) and absorb over a wide range of the

visible spectrum (up to 1000 nm) with high sensitivity in the near-infrared region. These properties were attributed to the AA stacking arrangement of the 2D MPc-polymer sheets.

The transition from linking MPc-COFs using boronate ester linkages to the implementation of pyrazine linkages was first demonstrated by our group in 2019.<sup>34</sup> Using previously developed condensation chemistry between diamines and diketones,<sup>302</sup> and after significant optimization, we reported the annulation of 2,3,9,10,16,17,23,24-octa- aminophthalocyanine Ni(II) and

1 pyrene-4,5,9,10-tetraone (**Figure 15a**), to generate a fully  
 2 conjugated framework with square pores. This new  
 3 framework material, termed COF-DC-8, displayed the  
 4 highest intrinsic conductivity reported of COFs at the time  
 5 ( $2.51 \times 10^{-5}$  S/cm), credited to favorable spatial and  
 6 energetic orbital overlap. During the same year, Feng and  
 7 coworkers investigated the electrical, electrochemical and  
 8 optical properties in two isorecticular pyrazine-based MPC-  
 9 pz COF (M= Zn and Cu) with tetra-butylpyrene-tetraone  
 10 linkers.<sup>272</sup> The group reported conductivity ( $\sim 5 \times 10^{-7}$  S/cm),  
 11 charge density ( $\sim 10^{12}$  cm $^{-3}$ ), charge carrier scattering rate  
 12 ( $\sim 3 \times 10^{13}$  s $^{-1}$ ), and effective mass ( $\sim 2.3$  m $_0$ ) values of the  
 13 majority carriers (holes) with mobilities up to  $\sim 5$  cm $^2$  V $^{-1}$ S $^{-1}$ .<sup>272</sup> DFT was used to reveal anisotropic charge transport,  
 14 where in-plane transport was null due to an extremely large  
 15 effective mass for charge carriers and localization of

16 electron density causing flat bands, with negligible influence  
 17 from different metal species.<sup>272</sup>

18 The reports of conductive MPC-based MOFs have  
 19 largely relied on octahydroxy- and octaamino-MPCs linked  
 20 with redox active transition metals to increase  
 21 concentrations and mobilities of charge carriers.<sup>22, 69</sup> In  
 22 plane 2D  $\pi$ -conjugation through  $\pi$ -d orbitals (**Figure 12**)  
 23 has been a widely applied strategy to create long-range  $\pi$ -  
 24 electron delocalization in MPC-based MOFs.<sup>34, 76, 85, 281, 303</sup> All  
 25 reported MPC-based MOFs exhibit conductivity values that  
 26 range from 0.2 S/cm (2,3,9,10,16,17,23,24-octa-amino-  
 27 phthalocyaninato nickel(II) ligand connected with Ni MOF  
 28 measured on thin film on quartz) to a range of  $9.4 \times 10^{-6}$   
 29 S/cm -  $1.6 \times 10^{-6}$  S/cm (CuPc(OH) $_8$  linked with Cu(II) ions  
 30 and measured on powder pellet).<sup>281</sup> The former attributes  
 31 the low conductivity values to the presence of a negatively  
 32 charged framework skeleton, suggested by the presence of  
 33

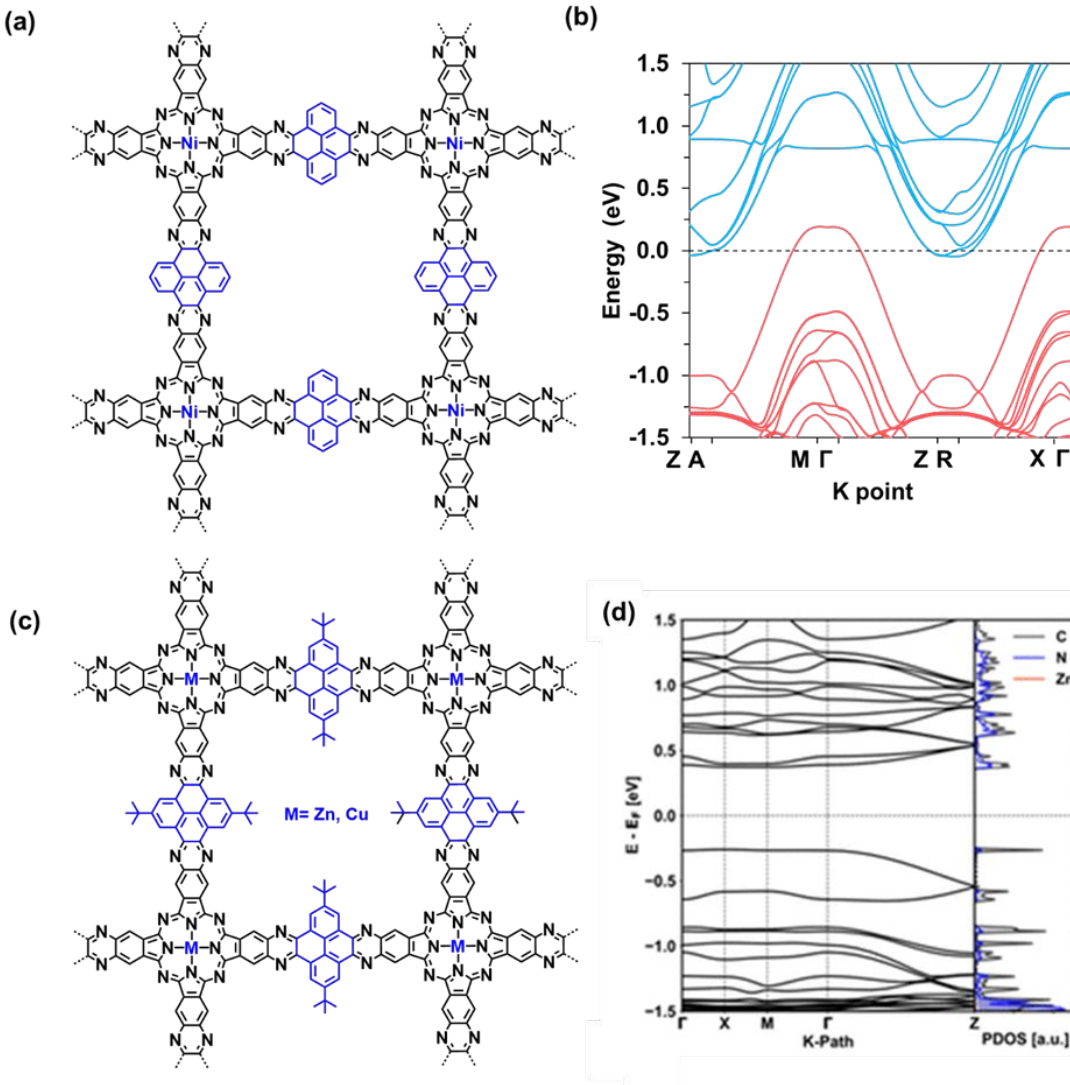


**Figure 15.** (a) Chemical structure of COF-DC-8 and (b) electronic band structure of COF-DC-8 (c) Chemical structure of MPc-pz COF and (d) serrated AA stacked multilayers of ZnPc-pz. Reprinted with permission from reference <sup>33</sup> Copyright 2019 American Chemical Society. Reprinted with permission from reference <sup>272</sup>. Copyright 2019 American Chemical Society.

ammonium cations,<sup>281</sup> which may be optimized using improved  $d\pi-p\pi$  interactions and control over redox state. In catechol type linkers, changing the metal node can have a dramatic effect on the neutrality or residual charge on a MOF skeleton, as the nature of redox state (catechol, quinone or semiquinone) can vary from metal to metal.<sup>34</sup> Other than perturbations arising from the frameworks itself, much of the physical factors, including the measurement technique, can affect the quantitative value of conductivity. For instance, parameters such as temperature, light,<sup>304</sup> work function, grain boundaries, or lattice strain can perturb electrical measurements.

Integrating electrical properties into MPc frameworks opens the door to a whole new chapter of multifunctional properties for applications that range from chemical sensing to energy conversion.<sup>32, 69</sup> Despite the excellent progress in understanding the structure–property relationships of MPc-frameworks with electrical properties, some limitations remain. Once the understanding of how these properties are influenced through the implementation of morphological control (nanorods vs. sheets), single crystal studies of transport, and pure ordered monolayer is improved, the finding can be implemented into optimized materials for use in state-of-the-art devices.

**Magnetic Properties in Frameworks.** Embedding magnetic properties within conductive frameworks is attractive feature for use in spintronics, where conductive and magnetic properties must exist simultaneously. Designing functional materials that display both semiconducting and magnetic behavior is challenging but can be realized effectively through MPc-based frameworks, where a richly conjugated framework skeleton and the presence of two metal centers can lead to a larger

compositional variety of materials with strategically selected multifunctional properties. Providing initial insight toward achieving this goal, Li *et al.* used first principle calculations to predict high temperature ferromagnetism in a series of charge neutral metal octaiminophthalocyanine (MOIPc) MOFs with  $M = Cr^{2+}, Mn^{2+}, Fe^{2+}, Co^{2+}, Ni^{2+}, Cu^{2+}, Zn^{2+}$  interconnected with  $Ni^{2+}$  linkers.<sup>280</sup> All materials examined exhibited low band gaps (0.28 – 0.35 eV) and a trend in magnetic moment that was strongly influenced by the nature of the metal center  $Cr(4.11\mu_B) > Mn(3\mu_B) > Fe(2\mu_B) > Co$  and  $Cu(1\mu_B) > Ni$  and  $Zn(0\mu_B)$ . Intriguingly, the Mn containing analog exhibited strong ferromagnetic ordering with high  $T_c$  at 170 K. Remarkable, this property persisted for several heteroatomic crosslinker analogs with 230 K for  $NiO_4$  linkers and 150 K for  $NS_4$  linkers. The authors attribute this ferromagnetic property to strong hybridization between the d orbitals of Mn constituent and  $\pi$ -orbitals of the Pc ligand within the monomer unit, which was absent in other structural MPc analogs. This study critically illustrates how the favorable properties of  $d-\pi$  conjugation in MPc monomer can be further amplified within a semiconductive framework to cause strong ferromagnetic coupling through strong interlayer coupling.

In 2019, Yang *et al.* synthesized and reported the first FePc-based 2D MOF with both semiconductive and magnetic properties (**Figure 16 a and b**), with charge mobilities that reached  $5 \pm 2 \text{ cm}^2 \text{ V}^{-1} \text{ s}^{-1}$ .<sup>283</sup> The group observed the presence of long range magnetic coupling between the iron centers in  $K_3Fe_2[PcFe-O_8]$  where the spin density is localized on the Fe atoms in phthalocyanine, while the square planar  $Fe-O_4$  nodes are slightly polarized by the delocalized  $\pi$ -orbitals among Fe(d), C(p), O(p) and N(p), as demonstrated previously.

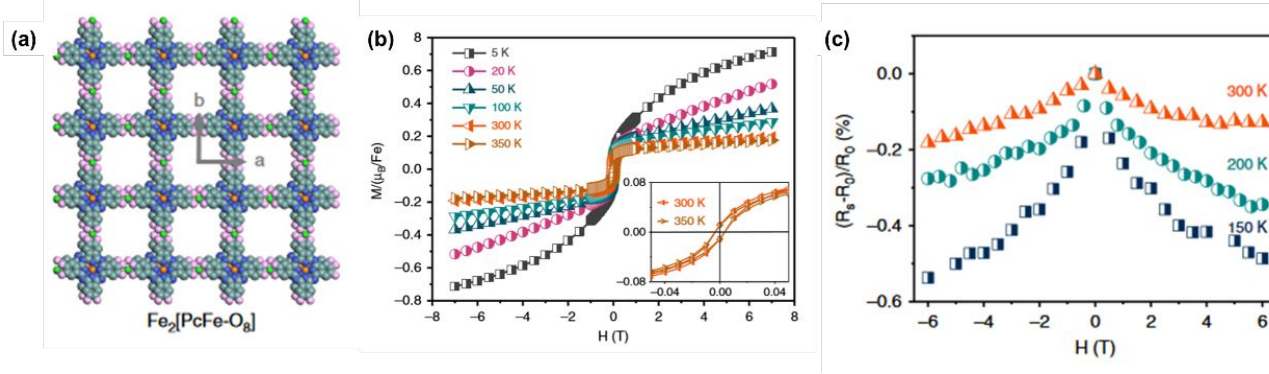


**Figure 16.** (a)  $K_3Fe_2[PcFe-O_8]$  MOF (b) Magnetic hysteresis loops obtained at different temperatures for  $K_3Fe_2[PcFe-O_8]$  with AA-serrated stacking mode (c) Magnetic field dependence of the magnetoresistance by measuring the changes of the electrical resistance in an applied field (-6–6 T) at different temperatures. Reprinted with permission from ref <sup>283</sup> Copyright 2019 Springer Nature. (<http://creativecommons.org/licenses/by/4.0/>)

As also shown with MPc molecular units, the magnetic properties of MPc frameworks are strongly correlated with the electronic ground state of the central metal atom hybridized with the ligand states.<sup>280</sup> Not to be trivialized, parameters such as crystallinity can also affect the

ferromagnetic behavior of the bimetallic MOFs.<sup>283</sup> Although in its infancy, this field as can provide new materials for information storage technology and data processing, yet challenges with miniaturization of such materials still remain.<sup>87</sup>

**Electrochemically active frameworks.** MPC-containing framework materials that contain redox active organic and inorganic components can permit a synergistic combination of functional properties and electroactive sites, which can be capitalized as stimuli-responsive sensors, porous conductors, energy storage systems, and electrocatalysts.<sup>305,306</sup> The unique structural features of MPC monomers have enabled their practical use as electroactive components, such as well-defined redox active sites for selective sensors,<sup>307</sup> redox capacitance for energy systems,<sup>308</sup> and high density of active sites for catalysis.<sup>53</sup> Some of the limiting aspects of their potential in such fields remain low conductivities, high operating temperatures, high driving voltages in devices, and post synthetic requirements for enhanced performances. Embedding MPCs within frameworks offer a new platform to harness the full potential of their electroactive abilities. In this context, MPC-frameworks can offer extended conjugation, high porosity, large surface to volume ratios, redox active surface chemistry, and improved accessibility to active sites. These properties can be designed and anticipated using computational approaches, where chemical principles can be exploited to select organic and inorganic building blocks that can access low band energies, influence charge state and promote redox activity.<sup>305</sup> In addition to these advantages, MPC-frameworks can help reveal the underlying mechanisms of host-guest interactions, such as ligand binding and charge-transfer, which are needed for rational design principles and has already demonstrated using MPC-based MOFs.<sup>36,282</sup>

**Sensing.** As demonstrated above, MPc-based monomers act as excellent sensing components in a collection of device architectures, yet there are several fundamental limitations of their physicochemical properties in the context of chemical sensing that may be overcome through their integration into frameworks. *First*, the low-intrinsic conductivity of MPc's may be vastly improved when integrated into a framework as a result of cofacial alignment, facilitating their interface with devices.

*Second*, the fabrication of MPc thin films with long range order, high crystallinity and control over alignment on various substrates may be enabled, increasing the number of active sites for analyte docking and improving the sensitivity of chemiresistive sensors. *Third*, embedding MPcs into frameworks enables further understanding the fundamental mechanisms of sensing may be investigated through the variation in framework chemical composition and probing interactions with oxidative or reducing gases. *Fourth*, MPc's modular and tunable scaffolds can enable the design of interactive framework systems with high binding affinities toward specific gas probes, augmenting sensitivity and selectivity in sensing systems.

The recent development of conductive MOFs has enabled their utility as chemiresistive sensors.<sup>22</sup> Despite the relative novelty of this feature in both MPC-based MOFs and COFs, several demonstrations using other framework materials have already showcased the advantages of using hybrid framework materials for gas sensing compared to other polymer or inorganic based sensors, including tunable surface chemistry for modular binding sites.<sup>32,309</sup> In 2019, our group demonstrated the exceptional performance of bimetallic MPC-MOFs and pyrazine linked MPC-COFs towards low-power chemiresistive sensing. Our group capitalized on molecular engineering principles to access synergistic properties in MPC-based frameworks regarding chemical sensing. As anticipated, the bimetallic NiPc-Cu and Ni linked MOFs demonstrated higher conductivity values by 5-7 orders of magnitude compared to NiPc analogs. The NiPc and pyrene-4,5,9,10-tetraone linked COF demonstrated conductivity ( $2.51 \times 10^{-5}$  S/cm) which, at the time, was the highest bulk conductivity achieved within an intrinsically conductive COF. The devices made from bimetallic MOFs achieved exceptional sensitivity at sub-part-per-million (ppm) to part-per-billion (ppb) detection limits toward NH<sub>3</sub> (0.31–0.33 ppm), H<sub>2</sub>S (19–32 ppb), and NO (1.0–1.1 ppb) at low driving voltages (0.01–1.0 V) within 1.5 min of exposure (**Figure 17**).

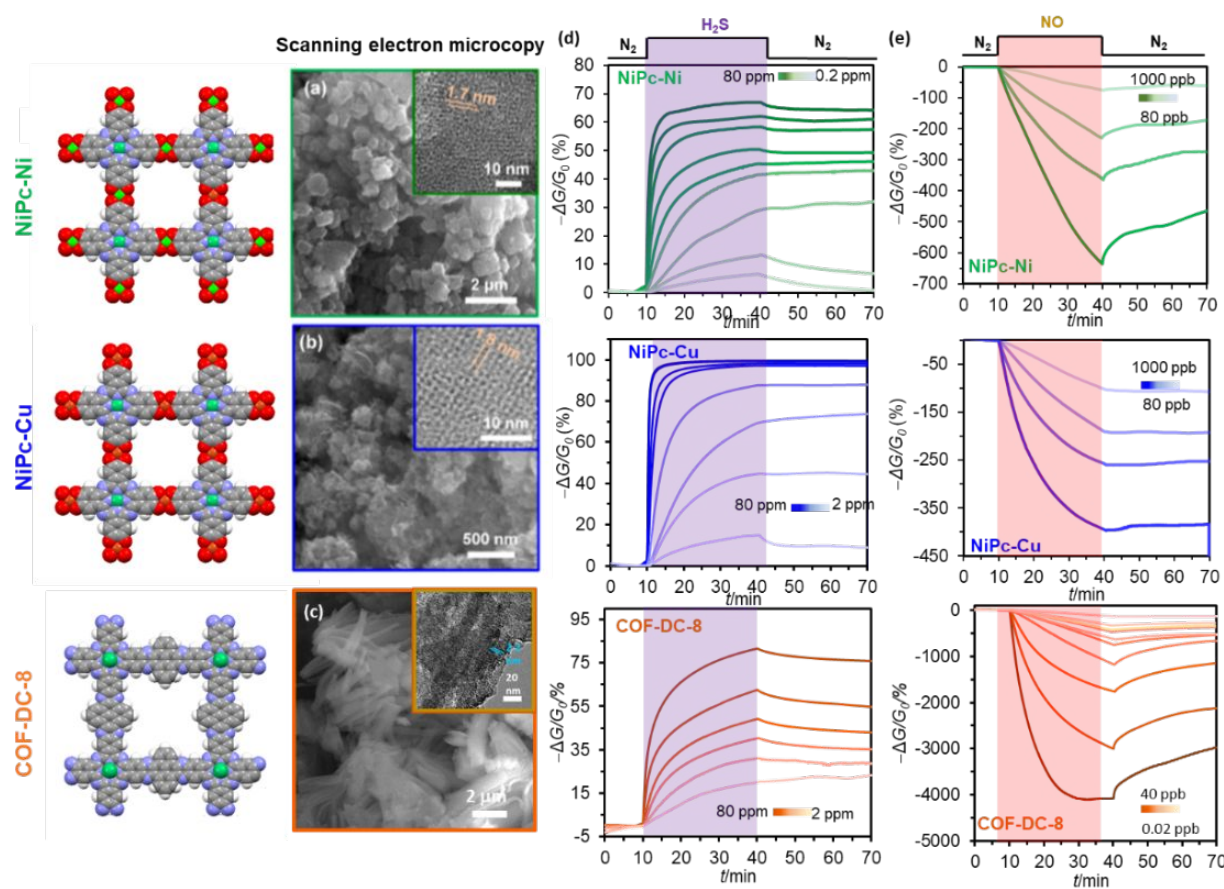


**Figure 17.** (a-c) Scanning electron images of NiPc-Ni, NiPc-Cu and COF-DC-8, respectively. (d) Chemiresistive responses ( $-\Delta G/G_0$ ) to  $\text{H}_2\text{S}$  (from top to bottom) NiPc-Ni, NiPc-Cu and COF-DC-8, respectively. (e) Chemiresistive responses to NO of (from top to bottom) NiPc-Ni, NiPc-Cu and COF-DC-8, respectively. Adapted with permission from reference (34) Copyright 2019 American Chemical Society.

To gain insight into the sensing mechanism of MPC-frameworks, X-ray photoelectron spectroscopy (XPS) and electron paramagnetic resonance (EPR) analysis studies (Figure 18) were performed to provide information regarding changes in chemical composition and associated redox events. EPR studies demonstrated that exposing NiPc-M MOFs to  $\text{H}_2\text{S}$ , a typical electron donor, decreased the content of C=O bonds, indicating potential reduction of the organic portion of the MPC ligands (Figure 18 c and e). Conversely, exposure to NO, a potential electron acceptor, the NiPc in NiPc-Ni was oxidized, as evident from the increased content of C=O bonds. XPS also confirmed the oxidation of the metal centers from  $\text{Cu}^+$  to  $\text{Cu}^{2+}$  in NiPc-Cu after exposure to NO, while the intensity of the EPR signal ( $g = 2.021$ ) from the Cu-centered radical increased (Figure 18f). These spectral techniques are a valuable tool in understanding the sites of surface interactions and mechanisms of sensing, which are crucial for optimization of the parameters of sensing in MPC-frameworks.<sup>309</sup>

Assimilating MPC units within frameworks for chemiresistive sensing have provided access to low dimensional materials with excellent conductivities to facilitate the fabrication of low-power devices and exceptional sensitivities to gas probes. However, several challenges remain in order to optimize these materials to

their full potential and improve device performance. While the materials have shown exceptional sensitivity, selectivity remains unoptimized and ability to detect and differentiate complex mixtures of gases has not yet been developed. There are also related technical challenges, such as device stability, cross-reactivity, and material scale-up strategies, that must be addressed. Thus far, the reported MPC-MOFs and COFs have provided an excellent platform for the future design and development of chemical sensors and other electronically associated device applications. Interesting future directions to optimize device performance and signal transduction mechanisms can capitalize on templated growth of framework thin films to improve device interfaces and examine structure-function properties of thin films on sensing performance.

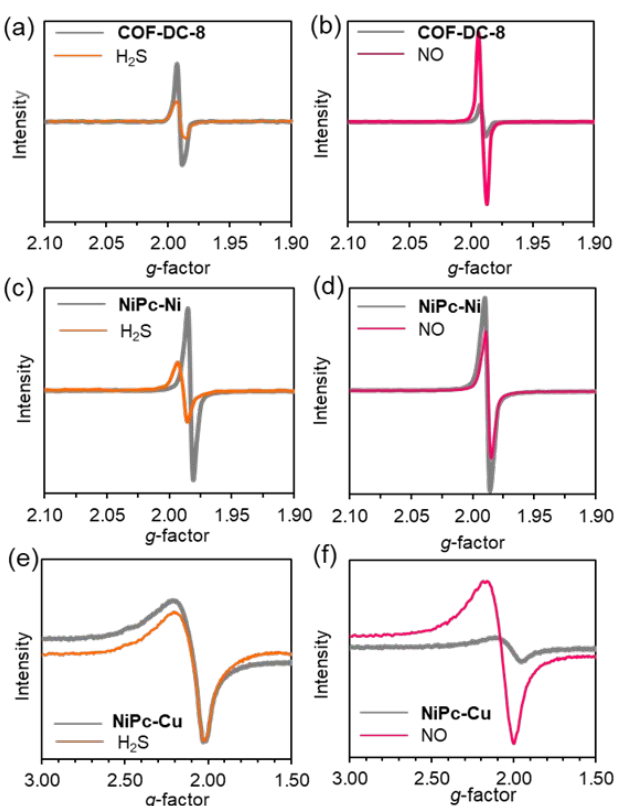


**Figure 18.** (a-b) EPR spectra (77 K) of COF-DC-8 (grey) and COF-DC-8 after  $\text{H}_2\text{S}$  exposure (orange) and NO exposure (pink). (c-d) EPR spectra (77 K) of NiPc-Ni (grey) and after  $\text{H}_2\text{S}$  exposure (orange) and NO exposure (pink). (e-f) EPR spectra (77 K) of NiPc-Cu (grey) and after  $\text{H}_2\text{S}$  exposure (orange) and NO exposure (pink). Reprinted with permission from reference (34) Copyright 2019 American Chemical Society.

**Catalysis.** Catalysis is implicated in the processing of over 80% of all manufactured products,<sup>310</sup> and the design of new catalysts is immensely important in helping to address some of the vital challenges facing our society today. Phthalocyanines have had extensive use as the active species in both heterogeneous and homogenous catalytic reactions, where their accessibility, stability, and tunability have provided advantageous over other materials.<sup>53</sup> However, for heterogeneous catalysis, MPcs are generally immobilized on the surfaces of substrates using covalent and non-covalent interactions which usually entails synthetic modifications, can obscure active sites and in some cases, can be involved in the catalytic process, which obscure mechanistic insights.<sup>53</sup> Assimilating MPc monomers into frameworks for catalysis provides several advantages over substrate deposition, including higher availability of accessible sites for higher turnover numbers.

As previously mentioned, MPc monomers have been used in a variety of catalytic oxidations, such as OERs, either in combination with inorganic complexes<sup>203</sup> or supported by CNTs.<sup>204</sup> Early work by Parmon and coworkers demonstrated that adding MPc catalysts to trisbipyridyl complexes of ruthenium (III) is necessary to catalyze the water oxidation reaction, which requires a four-electron

oxidation of  $\text{H}_2\text{O}$  to  $\text{O}_2$ .<sup>203</sup> Much focus has also been devoted to combining MPcs with conductive carbon supports to prevent their aggregation and improve their interface to carbon electrodes, leading to enhanced OER performances.<sup>203, 204, 311, 312</sup> Water oxidation catalysis has also been performed with MOFs, where Zheng *et al.* used an optimized FeNi-DOBDC-3 to report exceptional current densities of 50 and 100  $\text{mA}/\text{cm}^2$  at overpotentials of only 270 and 287 mV, respectively.<sup>313</sup>

Integrating MPcs into frameworks for heterogeneous catalysis provides the exceptional advantages of high surface area, large pores for product/reactant transport, stabilization effects of intermediates, and high density of catalytic active sites. Du and co-workers demonstrated this using octa-amino-phthalocyaninato Ni(II)-based MOF coordinated with nickel(II) salt.<sup>85</sup> The NiPc moiety was examined as an electrocatalytically active site towards water oxidation catalysis and shown to have outstanding performance with high mass activity ( $883.3 \text{ A g}^{-1}$ ), TOF (2.5  $\text{s}^{-1}$ ) at a low onset potential (1.48 V). The authors attributed this performance towards its 2D structure and good conductivity.

There is extensive precedent concerning the use of MPc monomers for the reduction of oxygen, where remarkably, activity can be modulated through alteration of the metal center.<sup>188</sup> For example, Fe and Mn MPcs promote the four-electron reduction with rupture of the O–O bond at low overpotentials,<sup>314 205</sup> without the formation of hydrogen peroxide, while Co, Ni and Cu MPcs promote the reduction of  $\text{O}_2$  only via two-electron to give hydrogen peroxide.<sup>188, 205</sup> Additionally, ORR dynamics on nanostructured iron(II) phthalocyanine/multi-walled carbon nanotubes composites have shown enhanced ORR activity (low onset potential, 5 mV, and catalytic current response of  $2 \text{ mA cm}^2$ ) due to the large surface area leading to higher density of active sites for the adsorption of molecular oxygen.<sup>312</sup> Oxygen reduction catalysis was first carried out with a well-defined and intrinsically conductive MOF ( $\text{Ni}_3(\text{HITP})_2$ ) by Dincă and coworkers in 2016, where the material performed ( $j = -50 \text{ mA cm}^2$ ) with an onset potential of 0.82 V in a 0.10 M aqueous solution of KOH (pH=13.0) comparable to values obtained by most active non-platinum group metal electrocatalysts to date.<sup>315</sup> In 2019, Feng and co-workers also capitalized on the well-defined and readily accessible active sites of  $\text{PcCu-O}_8\text{-Co}$  MOF to improve electron transfer capacity for oxygen reduction catalysis.<sup>282</sup> The well-defined structure and active sites provided an ideal platform for mechanistic investigations, which is critical for optimizing performance. The  $\text{PcCu-O}_8\text{-Co}$  MOFs were combined with carbon nanotubes (CNTs) to improve effective electron transfer between the  $\text{PcCu-O}_8\text{-Co}$  and the ORR electrode.  $\text{PcCu-O}_8\text{-Co}/\text{CNT}$  material exhibited a record value among the reported intrinsic MOF electrocatalysts for ORR activity ( $E_{1/2} = 0.83 \text{ V}$  vs. RHE,  $n=3.93$ , and  $j_L=5.3 \text{ mA cm}^2$ ) in alkaline media. To compare, CuPc monomers have previously shown low electrocatalytic activity for  $\text{O}_2$  reduction<sup>316</sup> or must be heated to very high temperatures<sup>317</sup> to achieve such performances.

The catalytic reduction of  $\text{CO}_2$  has been carried out using MPcs since 1974, when Meshitsuka *et al.* first observed Co or Ni MPcs deposited graphite electrodes exhibited catalytic activity in the presence of  $\text{CO}_2$ .<sup>318</sup> Since then, extensive research has been carried out using CoPc monomers either independently,<sup>319, 79</sup> blended with CNTs<sup>79, 320, 321</sup> or polymers.<sup>322</sup> Han *et al.* recently demonstrated that *in situ* polymerization of cobalt phthalocyanine on CNTs yields a thin uniform coating that suppresses aggregation and enlarges their electrochemically active surface area while also enhancing stability.<sup>320</sup> Their hybrid electrocatalyst selectively reduced  $\text{CO}_2$  to CO with a large faradic efficiency of ~90%, a turnover frequency (TOF) of 4,900  $\text{hr}^{-1}$  at  $\eta = 0.5$  V. In 2015, Lin *et al.* demonstrated a 26-fold improvement over molecular cobalt complexes when using a cobalt based porphyrin COF for the conversion of  $\text{CO}_2$  to CO (90% faradaic efficiency and turnover numbers up to 290,000 with initial turnover frequency of 9400 hour<sup>-1</sup>).<sup>323</sup> Yaghi and coworkers used a structurally similar cobalt phthalocyanine-2,3,9,10,16,17,23,24-octaol to construct the first three-dimensional MPc-based MOF-1992 with accessible one-dimensional channels to use as cathodes in  $\text{CO}_2$  reduction (Figure 19a).<sup>36</sup> Embedding accessible electroactive sites within three dimensional conductive MOFs enables high catalyst loading (electrode coverage 270 nmol/cm<sup>2</sup>), and current densities (~16.5 mA cm<sup>-2</sup> at a potential of ~0.63 V). MOF-1992 is conductive and measurements indicate that the charge transport pathways pass both the iron trimers and CoPc linkers. In 2020 Zhong *et al.* used CuPc and zinc-bis(dihydroxy) complex ( $\text{ZnO}_4$ ) for  $\text{CO}_2$  reduction and found high CO selectivity (88%), turnover frequency 0.39 s<sup>-1</sup> and long-term durability (>10 h).<sup>284</sup> This group found that the molar ratio of catalytically generated CO/H<sub>2</sub> can be tuned from 1:7 to 4:1 by increasing the applied potential from -0.4 to -1.2 V vs. RHE.

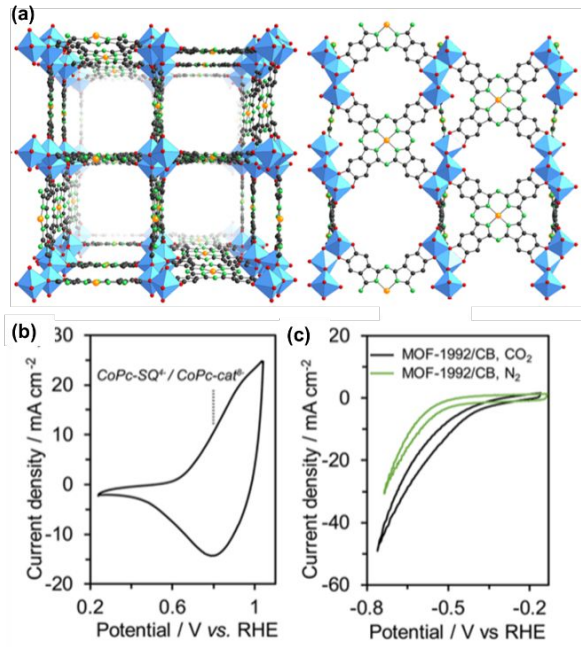


**Figure 19.** (a) Single crystal X-ray structure of MOF-1992 (b) Cyclic voltammetry (CV) for MOF-1992/CB (CB,

carbon black). The vertical line shows the potential of the CoPc-semiquinolinate ( $\text{CoPc-SQ}^4-$ /CoPc-catecholate ( $\text{CoPc-cat}^8-$ ) redox couple. (c) CV for MOF-1992/CB in a  $\text{CO}_2$ -saturated (black, pH 6.8) and  $\text{N}_2$  saturated (green, pH 7.2)  $\text{KHCO}_3$  solution. Reprinted with permission from reference (36) Copyright 2019 American Chemical Society.

**Energy Storage using MPc-Frameworks.** Society and the global economy highly depend on technology that enables the capture and storage of chemical energy.<sup>215, 218</sup> Electrochemical energy storage is of particular importance, where the prolific use of Li-ion batteries in portable electronics and smart technology has increased demand for more efficient, environmentally friendly, and cost-effective energy storage systems. Although in its infancy, the investigation of MPc-based frameworks for energy storage has yielded extremely promising preliminary data.<sup>282</sup> The advantages of using such materials in the context of batteries and supercapacitors include high porosity, tendency to stack in layers like graphene, well dispersed active sites, and high conductivity.<sup>282</sup> Thus, several research groups have begun to explore the electron transfer abilities of MPc-frameworks as potential replacements for porous materials traditionally used in Li ion or  $\text{Na}-\text{I}_2$  batteries, such as graphene.

Feng, Dong and coworkers recently investigated the catalytic ability of CuPc linked with square planar cobalt-bisdihydroxy complexes ( $\text{Co-O}_4$ ) ( $\text{CuPc-O}_8\text{-Co}$ ) and combined with CNTs as an ORR electrocatalyst for zinc-air batteries.<sup>282</sup> Combining the MPc-MOFs with CNTs to improve the conductivity of the ORR electrode.<sup>282</sup> This material exhibited excellent catalytic activity with a half potential of 0.83 V vs. RH and a limiting current density of 5.3 mA cm<sup>-2</sup>, which exceeds other MOF electrocatalysts. After mechanistic studies, the authors concluded that the reduction occurred at the  $\text{Co-O}_x$  sites in which the M-OH bond or  $\text{O}_2^{2-}/\text{OH}^-$  exchange was promoted via the single occupied  $e_g$  orbital.  $\text{CuPc-O}_8\text{-Co}$  was implemented as an electrocatalysts in zinc-air batteries and exhibited a circuit voltage of 1.37 V, a discharge current density of 120 mA cm<sup>-2</sup> @ 0.8 V, and a maximum power density of 94 mW cm<sup>-2</sup>, which surpasses the current state-of-the-art Pt/C electrocatalyst.<sup>282</sup> The exceptional ORR capabilities indicated that the electrocatalysts could additionally perform well in fuel cells and metal-air batteries.

In the same year, Feng, Zhang, and coworkers investigated the ability of CuPc-MOFs in  $\text{Na}-\text{I}_2$  batteries.<sup>282</sup> The current use of Li batteries is unsustainable and a switch to the more economical and greener NaI batteries would be beneficial since both Na and I can be extracted relatively cheaply from large supplies in the ocean. One major problem with current NaI batteries is their poor cycle stability due to the dissolution of polyiodide into the electrolyte. The MOF in question ( $\text{Fe}_2\text{-O}_8\text{-CuPc}$ ) exhibited a specific capacity of 150 mAh g<sup>-1</sup> after 3200 cycles with a coulombic efficiency of 99.3% which surpasses the best literature precedent (stable for <2000 cycles).<sup>282</sup> The improved battery was enabled by the dense population of metal centers, which are more polar than carbon, the  $\pi$ -system that enables electron transfer and the porous nature of the MOF that allows for

retention of  $I_2$ . The ability to prevent polyiodide dissolution enables longer energy storage capability. Both catalysts outperformed or performed well compared to the current

state-of-the-art electrocatalysts, proving their capacity to open a new and more efficient means of energy storage.

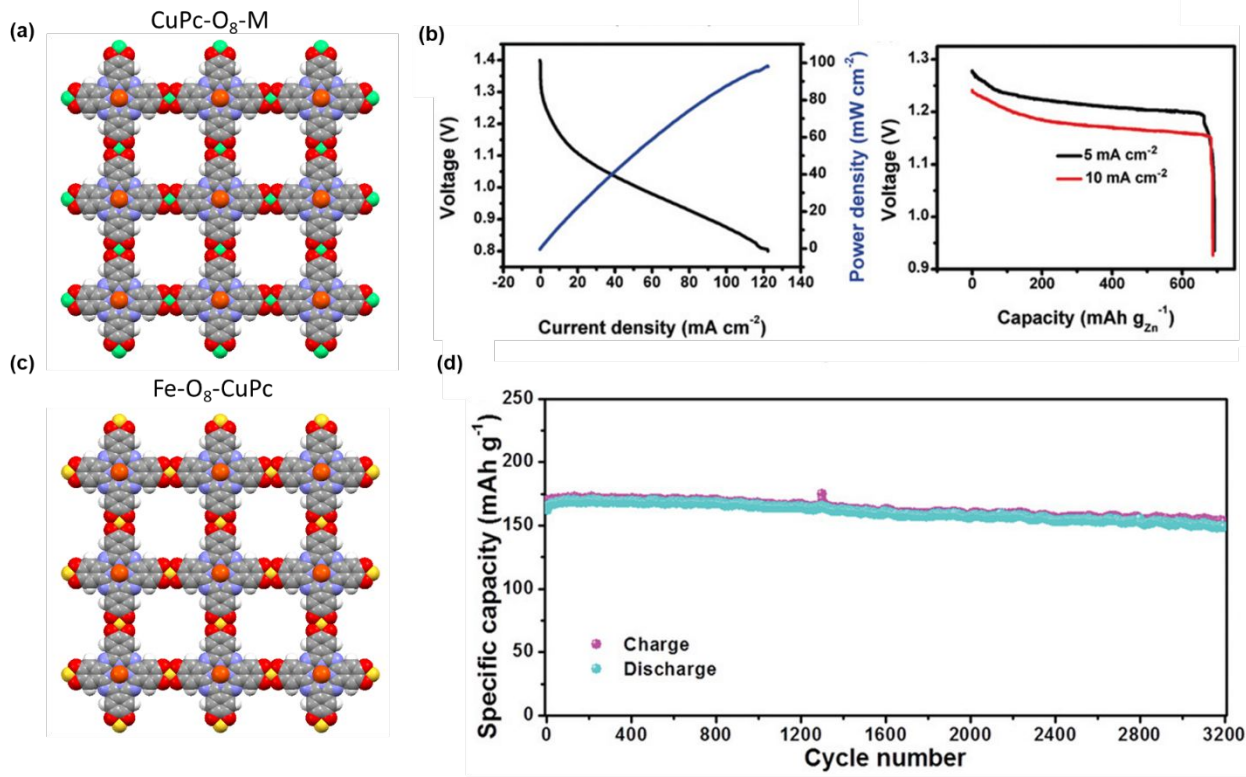


**Figure 20.** (a) Structure of CuPc-O<sub>8</sub>-M with discharge curve and (b) power density of zinc-air battery with CuPc-O<sub>8</sub>-Co/CNT as the electrocatalysts and the specific capacity of the zinc-air battery (c) schematic modeling of Fe-O<sub>8</sub>-CuPc with (d) a plot of long time cycles of Fe-O<sub>8</sub>-CuPc/I<sub>2</sub> electrodes at 1.5 A g<sup>-1</sup>. (a) Adapted and (b) reproduced with permission from reference <sup>282</sup> Copyright 2019 Wiley-VCH Verlag. (<https://creativecommons.org/licenses/by/4.0/>) (c) Adapted and (d) reproduced with permission from reference <sup>288</sup> Copyright 2019 Wiley-VCH Verlag. (<https://creativecommons.org/licenses/by/4.0/>)

Given the novelty of MPc-based framework materials in the energy storage field, the fact that batteries using these materials as electrocatalysts achieve such exceptional metrics bodes well for future research. With the optimization of these devices to incorporate the most efficient frameworks with the optimal linkers and metals, performance is bound to improve. The next steps for research may lead from metal-air and NaI batteries to other electrochemical energy storage systems like capacitors, supercapacitors, and fuel cells.

## CONCLUSIONS AND OUTLOOK

From the intentional fracture across the crystalline plane of flint to directing the electrical properties of silicon to develop the first commercially produced integrated circuit,<sup>324</sup> the properties of materials have helped address vital challenges to our survival and propelled the technology of our society. Understanding and harnessing the functional structure–property relationships has laid the groundwork for generating materials with new and valuable properties. However, addressing unprecedented

challenges in growing technological complexity using the principles of molecular engineering, where performance toward functional materials can be rationally designed and constructed from molecular building blocks, has the potential to address new challenges with complex, emergent, and multifaceted function in materials. MPc-based frameworks are one example of multifunctional materials where emergent function can be rationally derived from their molecular building blocks.

Complex and emergent systems are inherently difficult to predict and are sensitive to parameters to which a designer may be unaware. The first step towards systematizing the control over complex chemical systems and the generation of emergent properties is to establish the fundamental chemical principles that determine the properties and the interactions of chosen components. A few general concepts to consider utilizing in material design to target functional properties include principles of reticular chemistry, computational strategies, controlled or templated growth, and comprehensive characterization strategies such as GIXRD.

Ongoing computational and experimental investigation of the fundamental properties of matter can assist in the understanding of molecular systems.<sup>325</sup> Prior to synthesis, computational assessment of a library of promising materials can provide a great opportunity to identify the best candidate for a target property and to gain basic molecular-level insights into the structure–property relationships.<sup>326</sup> Some of these computational strategies include various DFT methods,<sup>312</sup> Monte Carlo and microkinetic modeling.<sup>313</sup> Framework systems are an excellent platform to use these computational strategies to compare the electronic structure of the frameworks to that of the constituent building blocks, which can lead us to understand the nature of the emergent property. These strategies have been developed for treating both organic and organic-inorganic hybrid systems to assist in understanding their intrinsic conductivity,<sup>291</sup> charge transport properties,<sup>272</sup> the origin of magnetism,<sup>280, 283</sup> identification of the catalytic and molecular binding sites,<sup>313</sup> description of the host–guest interactions,<sup>282</sup> the analysis of structural defects,<sup>327</sup> and others.<sup>314</sup> For instance, electronic structure calculations using a finite portion of the infinite crystal can give insight into the energetic state, electronic band edges (frontier orbitals) and spatial location of the valence and conduction bands in organometallic polymers, which can aide in the prediction of their electronic properties.<sup>291</sup> Li and co-workers used these first principle calculations to locate the source of the emergent strong ferromagnetic coupling in MnPc-based 2D MOFs, which they concluded likely results from the hybridization of  $\pi$  symmetry orbitals between the metal and phthalocyanine scaffold.<sup>280</sup> Furthermore, simulation strategies can be used to observe the influences of electronic structure or optical properties using strategies such as metal substitution, ligand engineering, host-guest inclusion and lattice strain.<sup>291</sup>

Once these fundamental principles are established, an assembly process that steers the system towards higher complexity—typically through a controlled growth in size in at least one dimension—can lead to the acquisition of specific emergent properties. Frameworks constitute an ideal platform for investigating the principles of complexity and emergence because they involve governable systems where modular building blocks permit the investigation of specific modifications to the overall properties. This controlled growth requires the development of robust and reliable synthetic strategies for achieving bottom-up assembly. Reticular chemistry is one such tool towards achieving a high level of structural and morphological control beyond the molecule.

It is essential to first build a systematic platform for understanding the underlying parameters affecting certain properties in MPc-frameworks. For example, a common and variable emergent property among morphologically distinct conductive materials is charge transport, which appears to be critically influenced by both fundamental material properties and through contact measurement techniques. For instance, grain boundaries in pressed pellets introduce large bulk resistances<sup>304</sup> when compared

to their thin film equivalents grown on quartz substrates,<sup>85</sup> which can lead to very different conductivity values of isoreticular materials. Comparing these quantitative metrics across various MPc-framework materials in the context of structure–property relationships, measurement techniques must be standardized. It is also important to address other fundamental factors influencing electrical properties in MPc-frameworks that arise from the molecular constituents, such as oxidation states and the presence of counterions within a charged framework.<sup>281</sup> Recognition of how redox states influence the electrical properties in framework materials is the first step towards control over the interactions that produce them.

As we build the platform through which we compare across existing and novel MPc-frameworks, normalization of characterization through existing techniques such as X-ray photoelectron spectroscopy (XPS) and electrochemical characterization will permit a broader understanding of charge states and its influence on conductivity. It is important to emphasize that these measurements should be performed after activation of the framework pores through various solvent extracting procedures, which should be kept consistent and clearly described in reports of framework materials. Furthermore, systematically examining batch-to-batch-reproducibility of obtained conductivity, charge mobility, or photocurrent values should be included in future work.

Much of the recent progress towards functional MOFs and COFs has followed general synthetic procedures of well-known chemistry. Some challenges associated with the use of MPc as linkers in frameworks is that commercial access to functionalized MPcs is relatively limited or nonexistent. Additionally, when compared to other symmetric and conjugated linkers, the synthesis, purification and solubility of functionalized MPcs is challenging and substantially longer, requiring considerable synthetic expertise for each individual MPc monomer. Although, recent progress in this area has permitted access to a broader range of several new MPcs that will likely continue to allow access to novel MPc-frameworks. This progress has laid the foundation on which to build optimized nanomaterials in fields such as optoelectronics, photovoltaics, catalysis, energy storage and sensing, still the expansion of synthetic reticular linking strategies for connecting the monomer building blocks is poised to enable access to novel structures with novel properties in the future. Efforts in computational molecular design, guided by quantum mechanical and molecular dynamics simulations, are particularly important in identifying how novel linker chemistry may influence the emergent structure–property relationships in framework materials. While the synthetic toolkit of reticular chemistry has significantly expanded, the synthetic access to functionalized MPc-based building blocks with peripheral functionalization amenable to being assembled into frameworks remains extremely limited. Limited access to modular and reliable synthetic strategies for monomer synthesis, lack of commercial access to building blocks, and limited understanding of chemical properties and stability

of these molecular entities are existing hurdles that need to be overcome to enable more rapid and diverse access to MPc-based framework structures.

Current synthetic efforts have established initial access to MPc-based framework materials as microcrystalline powders. While the porosity and hierarchical features of several members of this class of materials have been characterized, much remains unknown about the mechanistic aspects of polymerization strategies that lead to the assembly of these materials. Fundamental investigation of in-situ growth using methods of colloidal chemistry, and capitalizing on recent advances in in-situ electron microscopy<sup>285, 292</sup> and atomic force microscopy<sup>294, 328</sup> may provide unique insight into the nucleation and growth of this class of framework materials, which will enhance the ability to tailor their function. Such morphological control can also offer a new platform for identifying the intrinsic and multifunctional structure-property relationships, such as charge transport, which are sensitive to factors such as defects and device architecture.

It is also important to point out that no knowledge currently exists about crystalline domain sizes, the termination of edge sites, and the distribution of defects within this class of materials. These structural considerations, while relatively well-studied for other framework systems,<sup>329</sup> will greatly influence the function of the material and should be carefully considered and reported. While improved understanding of growth mechanisms mentioned above may ultimately enable access to single crystal entities that can be rigorously characterized by electron diffraction and scanning tunneling microscopy, development of new tools for the high throughput analysis of micro and nano crystals with atomic resolution are needed. Micro electron diffraction<sup>293, 330</sup> offers one such tool for microcrystal analysis. Atomic force microscopy, microindentation studies, and strategic surface modification may provide additional insight into the termination of the surface of these materials. These techniques can provide detailed observations and direct visualizations of framework lattice/structure mismatching, crystal orientations, nucleation and growth sites, mechanical properties and film thicknesses.<sup>331</sup>

We anticipate that recent developments in operando techniques that permit in-situ analysis of specific structure-property relationships will enable unprecedented insight into understanding and characterizing host-guest interactions, electrochemically active sites, and reaction intermediates. Given that reticular synthesis enables bottom-up and top-down (e.g., metal or ligand exchange) control over the chemical composition of framework materials, these techniques will be extremely useful in understanding how distinct structural features of framework materials govern their function.

This perspective has documented the integration and performance of MPcs across multiple fields, which has very recently resulted in their natural assimilation into framework materials. We have highlighted the disciplines where MPc-based frameworks have initially demonstrated great potential, although building on these studies through

development of novel synthetic techniques and compositional progression will allow expansion of the field towards state-of-the-art MPc-based materials in areas such as sensing, energy conversion and storage, magnetoelectronics, optoelectronics and catalysis. It is equally as important to elucidate and assign the source of the emergent functional properties across each discipline, which can permit their optimization with emphasis on tunability and control.

Utilizing the principles of molecular engineering along with the diverse structural and functional properties inherent to MPcs to achieve desired structure–property relationships has the potential to propel technological fields within materials chemistry to the forefront of state-of-the-art designs and applications. Harnessing these principles is expected to generate new opportunities to discover emergent properties that result from rigidly defining the chemistry and function of MPcs within materials towards applications. The dramatic advancement of MPc-based framework materials that has been achieved over the past decade, along with recent resurgence over the past two years, indicates rapid growth that is poised for transformative applications enabled by the molecular design, synthetic access, and multifunctional properties of MPc-based framework materials.

## AUTHOR INFORMATION

### Corresponding Author

\*E-mail: katherine.a.mirica@dartmouth.edu.

### Author Contributions

The manuscript was written through contributions of all authors. All authors have given approval to the final version of the manuscript.

### Notes

The authors declare no competing financial interest.

## Biographies

**Katherine Mirica** earned her B.S. in Chemistry from Boston College and her Ph.D. in Chemistry from Harvard University. After completing her postdoctoral training at the Massachusetts Institute of Technology, she began her independent scientific career at Dartmouth College in 2015. Her research interests span the topics of self-assembly, as well as design and synthesis of multifunctional materials for applications in chemical sensing, catalysis, energy conversion and storage, and in adhesion science.

**Aylin Aykanat** obtained a B.S in Chemistry and Biology from State University of New York at New Paltz in 2012. She received her M.Sc. in Organic Chemistry from Boğaziçi University in Istanbul under the supervision of Prof. Ersin Acar in 2015. She became a graduate student with Prof. Mirica at Dartmouth College in 2015, where

she focuses on the synthesis and applications of conductive coordination polymers and two-dimensional phthalocyanine-based MOFs.

Zheng Meng obtained his B.S. at the University of Science and Technology Beijing in 2011. He received his Ph.D. at the Institute of Chemistry, Chinese Academy of Sciences under the supervision of Prof. Chuan-Feng Chen in 2016. He then moved to Dartmouth College to work as a postdoctoral researcher with Prof. Mirica. His current interests focus on the development of new two-dimensional conductive frameworks materials and their applications in sensing, catalysis, and electronics.

Georganna Benedetto is a chemistry graduate student at Dartmouth College. She received her B.A. dual degree in Chemistry and Spanish at Colby College in Maine. In fall 2019, she began her graduate studies with Professor Mirica at Dartmouth, focusing on the synthesis of metal and covalent organic frameworks for CO<sub>2</sub> reduction and gas sensation applications.

## ACKNOWLEDGMENT

The authors acknowledge support from start-up funds provided by Dartmouth College, from Walter and Constance Burke Research Initiation Award, the Arthur L. Irving Institute for Energy & Society, the Army Research Office Young Investigator Program Grant No. W911NF-17-1-0398, National Science Foundation EPSCoR award (#1757371), Sloan Research Fellowship (FG-2018-10561), Cottrell Scholars Award (#26019) from the Research Corporation for the Advancement of Science, US Army Cold Regions Research & Engineering Lab (award number W913E519C0008), 3M Non-Tenured Faculty Award, and NSF CAREER award (#1945218).

## ABBREVIATIONS

BDBA	benzene diboronic acid
bpy	bipyridine
BTDA	benzothiadiazole
CNT	Carbon nanotube
COF	Covalent organic framework
CPA	Constant potential amperometry
D-A	Donor-acceptor
DFTB	Density-functional tight-binding
dib	diisocyanobenzene
D <sub>MPC</sub> -A <sub>DI</sub> -	Donor-acceptor-COF
DPB	diphenylbutadiyne
DPV	Differential pulse voltammetry
E <sub>bO<sub>2</sub></sub>	Oxygen binding energy
EPS	Electron paramagnetic resonance
GIXRD	Grazing incidence x-ray diffraction
h	holes
HR-STM	High-resolution scanning tunneling microscopy
IP	Ionization potential
j	Current densities
L-B	Langmuir-Blodgett
LDA	Linear discriminant analysis
LIB	Lithium ion battery
LOD	Limit of detection
m*	Effective mass
MicroED	Microcrystal electron diffraction

MOF	Metal-organic framework
MPC	Metallophthalocyanine
MPC-DI	Phthalocyanine-diimide
MPy	Metalloporphyrin
MWCNT	Multi-walled carbon nanotube
n	density
OER	Oxygen evolution reaction
OFET	Organic field effect transistor
ORR	Oxygen reduction reaction
Pc	Phthalocyanine
PDI	perylene diimide
PDMS	polydimethylsiloxane
ppb	Part-per-billion
ppm	Part-per-million
RHE	Reversible hydrogen electrode
SLG	Single layered graphene
T <sub>c</sub>	Critical temperature
TiOPc	Titanyl phthalocyanine
TOF	Turnover frequency
TON	Turnover number
TR-ESR	Time-resolved electron spin resonance
XPS	X-ray photoelectron spectroscopy

σ	conductivity
Σ	Sum of carrier mobilities
τ	Scattering events

Charge carrier generation efficiency

## REFERENCES

- (1) National Research Council. *Materials Science and Engineering for the 1990s: Maintaining Competitiveness in the Age of Materials*. The National Academies Press: Washington, DC, 1989; p 320.
- (2) National Research Council. *Materials Science and Engineering: The History, Scope, and Nature of Materials Science and Engineering*. The National Academies Press: Washington, DC, 1975; p 288.
- (3) Michael F. Ashby, P. J. F., Daniel L. Schodek, *Nanomaterials, Nanotechnologies and Design*. Butterworth-Heinemann: 2009; p 560.
- (4) Independent Group of Scientists Appointed by the Secretary General. *The Future Is Now: Science for Achieving Sustainable Development*; United Nations, New York: 2019.
- (5) Whitesides, G. M.; Ismagilov, R. F., Complexity in chemistry. *Science*. **1999**, 284, 89-92.
- (6) Yu, H. D.; Regulacio, M. D.; Ye, E.; Han, M. Y., Chemical routes to top-down nanofabrication. *Chem Soc Rev*. **2013**, 42, 6006-6018.
- (7) Hobbs, R. G.; Petkov, N.; Holmes, J. D., Semiconductor Nanowire Fabrication by Bottom-Up and Top-Down Paradigms. *Chem. Mater.* **2012**, 24, 1975-1991.
- (8) Zhang, X.-S., Micro/Nano Integrated Fabrication Technology and Its Applications in Microenergy Harvesting. *Springer-Verlag Berlin Heidelberg*. **2016**.
- (9) Lehn, J.-M., Towards Complex Matter: Supramolecular Chemistry and Self-organization. *Eur. Rev.* **2009**, 17, 263-280.

(10) Yoshinari, M., ; Wolfgang Kaisser; B H Rabin; Akira Kawasaki; Renée G Ford, *Functionally graded materials : design, processing, and applications*. New York : Springer Science and Business Media, LLC, : 1999.

(11) Sanchez, C.; Boissiere, C.; Cassaignon, S.; Chaneac, C.; Durupthy, O.; Faustini, M.; Grosso, D.; Laberty-Robert, C.; Nicole, L.; Portehault, D.; Ribot, F.; Rozes, L.; Sassoye, C., Molecular Engineering of Functional Inorganic and Hybrid Materials. *Chem. Mater.* **2013**, 26, 221-238.

(12) Roncali, J., Molecular Engineering of the Band Gap of  $\pi$ -Conjugated Systems: Facing Technological Applications. *Macromol. Rapid Commun.* **2007**, 28, 1761-1775.

(13) Yuan, Y. Z., G., Porous Aromatic Frameworks as a Platform for Multifunctional Applications. *ACS Cent Sci.* **2019**, 5, 409-418.

(14) Ashkenasy, G.; Cahen, D.; Cohen, R.; Shanzer, A.; Vilan, A., Molecular Engineering of Semiconductor Surfaces and Devices. *Accounts of Chemical Research.* **2002**, 35, 121-128.

(15) Han, M. Y.; Ozyilmaz, B.; Zhang, Y.; Kim, P., Energy band-gap engineering of graphene nanoribbons. *Phys Rev Lett.* **2007**, 98, 206805.

(16) van Mullekom, H., Developments in the chemistry and band gap engineering of donor-acceptor substituted conjugated polymers. *Mater. Sci.* **2001**, 32, 1-40.

(17) Mathew, S.; Yella, A.; Gao, P.; Humphry-Baker, R.; Curchod, B. F. E.; Ashari-Astani, N.; Tavernelli, I.; Rothlisberger, U.; Nazeeruddin, M. K.; Grätzel, M., Dye-sensitized solar cells with 13% efficiency achieved through the molecular engineering of porphyrin sensitizers. *Nat. Chem.* **2014**, 6, 242.

(18) Millar, D. I. A.; Maynard-Casely, H. E.; Allan, D. R.; Cumming, A. S.; Lennie, A. R.; Mackay, A. J.; Oswald, I. D. H.; Tang, C. C.; Pulham, C. R., Crystal engineering of energetic materials: Co-crystals of CL-20. *CrystEngComm.* **2012**, 14, 3742.

(19) Sato, K.; Katayama-Yoshida, H., First principles materials design for semiconductor spintronics. *Semiconductor Science and Technology.* **2002**, 17, 367-376.

(20) Zhai, Q.-G.; Bu, X.; Mao, C.; Zhao, X.; Daemen, L.; Cheng, Y.; Ramirez-Cuesta, A. J.; Feng, P., An ultra-tunable platform for molecular engineering of high-performance crystalline porous materials. *Nat. Commun.* **2016**, 7, 13645.

(21) Seh, Z. W.; Kibsgaard, J.; Dickens, C. F.; Chorkendorff, I.; Norskov, J. K.; Jaramillo, T. F., Combining theory and experiment in electrocatalysis: Insights into materials design. *Science.* **2017**, 355.

(22) Sun, L.; Campbell, M. G.; Dinca, M., Electrically Conductive Porous Metal-Organic Frameworks. *Angew Chem Int Ed Engl.* **2016**, 55, 3566-3579.

(23) Whitesides, G. M.; Grzybowski, B., Self-assembly at all scales. *Science.* **2002**, 295, 2418-2421.

(24) Seoane, B.; Castellanos, S.; Dikhtierenko, A.; Kapteijn, F.; Gascon, J., Multi-scale crystal engineering of metal organic frameworks. *Coord. Chem. Rev.* **2016**, 307, 147-187.

(25) Yaghi, O. M.; O'Keeffe, M.; Ockwig, N. W.; Chae, H. K.; Eddaoudi, M.; Kim, J., Reticular synthesis and the design of new materials. *Nature.* **2003**, 423, 705-714.

(26) Jiang, J., Functional Phthalocyanine Molecular Materials. *Springer* **Feb 2, 2010**.

(27) Imahori, H.; Umeyama, T.; Kurotobi, K.; Takano, Y., Self-assembling porphyrins and phthalocyanines for photoinduced charge separation and charge transport. *Chem Commun (Camb).* **2012**, 48, 4032-4045.

(28) Van Nostrum, C. F.; Nolte, R. J. M., Functional supramolecular materials: self-assembly of phthalocyanines and porphyrazines. *Chem Commun.* **1996**.

(29) Claessens, C. G.; Martínez-Díaz, M. V.; Torres, T., Supramolecular Phthalocyanine-Based Systems. In *Supramolecular Chemistry*, 2012.

(30) Martínez-Díaz, M. V.; de la Torre, G.; Torres, T., Lighting porphyrins and phthalocyanines for molecular photovoltaics. *Chem Commun (Camb).* **2010**, 46, 7090-7108.

(31) Allendorf, M. D.; Stavila, V., Crystal engineering, structure-function relationships, and the future of metal-organic frameworks. *CrystEngComm.* **2015**, 17, 229-246.

(32) Campbell, M. G.; Dinca, M., Metal-Organic Frameworks as Active Materials in Electronic Sensor Devices. *Sensors (Basel).* **2017**, 17.

(33) Meng, Z.; Stoltz, R. M.; Mirica, K. A., Two-Dimensional Chemiresistive Covalent Organic Framework with High Intrinsic Conductivity. *J Am Chem Soc.* **2019**, 141, 11929-11937.

(34) Meng, Z.; Aykanat, A.; Mirica, K. A., Welding Metallophthalocyanines into Bimetallic Molecular Meshes for Ultrasensitive, Low-Power Chemiresistive Detection of Gases. *J Am Chem Soc.* **2019**, 141, 2046-2053.

(35) Yang, D.; Gates, B. C., Catalysis by Metal Organic Frameworks: Perspective and Suggestions for Future Research. *ACS Catal.* **2019**, 9, 1779-1798.

(36) Matheu, R.; Gutierrez-Puebla, E.; Monge, M. A.; Diercks, C. S.; Kang, J.; Prevot, M. S.; Pei, X.; Hanikel, N.; Zhang, B.; Yang, P.; Yaghi, O. M., Three-Dimensional Phthalocyanine Metal-Catecholates for High Electrochemical Carbon Dioxide Reduction. *J Am Chem Soc.* **2019**, 141, 17081-17085.

(37) Zhou, J.; Wang, B., Emerging crystalline porous materials as a multifunctional platform for electrochemical energy storage. *Chem. Soc. Rev.* **2017**, 46, 6927-6945.

(38) Zou, Q.; Liu, K.; Abbas, M.; Yan, X., Peptide-Modulated Self-Assembly of Chromophores toward

Biomimetic Light-Harvesting Nanoarchitectonics. *Adv Mater.* **2016**, *28*, 1031-1043.

(39) Ishihara, S.; Labuta, J.; Van Rossum, W.; Ishikawa, D.; Minami, K.; Hill, J. P.; Ariga, K., Porphyrin-based sensor nanoarchitectonics in diverse physical detection modes. *Phys Chem* **2014**, *16*, 9713-9746.

(40) Barona-Castano, J. C.; Carmona-Vargas, C. C.; Brocksom, T. J.; de Oliveira, K. T., Porphyrins as Catalysts in Scalable Organic Reactions. *Molecules*. **2016**, *21*, 310.

(41) Liang, Q.; Zhang, M.; Zhang, Z.; Liu, C.; Xu, S.; Li, Z., Zinc phthalocyanine coupled with UIO-66 (NH<sub>2</sub>) via a facile condensation process for enhanced visible-light-driven photocatalysis. *J. Alloys Compd.* **2017**, *690*, 123-130.

(42) McKeown, N. B., Phthalocyanine Materials: Synthesis, Structure and Function. *Cambridge University Press*. **Jul 13, 1998**, 6.

(43) de la Torre, G.; Nicolau, M.; Torres, T., Phthalocyanines: Synthesis, Supramolecular Organization, and Physical Properties. **2001**, 1-111.

(44) Sakamoto, K.; Ohno-Okumura, E., Syntheses and Functional Properties of Phthalocyanines. *Materials*. **2009**, *2*, 1127-1179.

(45) Claessens, C. G.; Blau, W. J.; Cook, M.; Hanack, M.; Nolte, R. J. M.; Torres, T.; Wohrle, D., Phthalocyanines and phthalocyanine analogues: The quest for applicable optical properties. *Monatsh Chem.* **2001**, *132*, 3-11.

(46) Claessens, C. G.; Hahn, U.; Torres, T., Phthalocyanines: from outstanding electronic properties to emerging applications. *Chem Rec.* **2008**, *8*, 75-97.

(47) de la Torre, G.; Claessens, C. G.; Torres, T., Phthalocyanines: old dyes, new materials. Putting color in nanotechnology. *Chem. Commun.* **2007**, 2000-2015.

(48) Melville, O. A.; Lessard, B. H.; Bender, T. P., Phthalocyanine-Based Organic Thin-Film Transistors: A Review of Recent Advances. *ACS Appl Mater Interfaces*. **2015**, *7*, 13105-13118.

(49) Wöhrle, D.; Schnurpfeil, G.; Makarov, S. G.; Kazarin, A.; Suvorova, O. N., Practical Applications of Phthalocyanines – from Dyes and Pigments to Materials for Optical, Electronic and Photo-electronic Devices. *Macroheterocycles*. **2012**, *5*, 191-202.

(50) Sekkat, N.; van den Bergh, H.; Nyokong, T.; Lange, N., Like a bolt from the blue: phthalocyanines in biomedical optics. *Molecules*. **2011**, *17*, 98-144.

(51) McConnell, I.; Li, G.; Brudvig, G. W., Energy conversion in natural and artificial photosynthesis. *Chem Biol.* **2010**, *17*, 434-447.

(52) Karkas, M. D.; Verho, O.; Johnston, E. V.; Akermark, B., Artificial photosynthesis: molecular systems for catalytic water oxidation. *Chem Rev.* **2014**, *114*, 11863-12001.

(53) Sorokin, A. B., Phthalocyanine metal complexes in catalysis. *Chem Rev.* **2013**, *113*, 8152-8191.

(54) Ramos, A. A.; Nascimento, F. B.; de Souza, T. F.; Omori, A. T.; Manieri, T. M.; Cerchiaro, G.; Ribeiro, A. O., Photochemical and Photophysical Properties of Phthalocyanines Modified with Optically Active Alcohols. *Molecules*. **2015**, *20*, 13575-13590.

(55) Grobosch, M.; Schmidt, C.; Kraus, R.; Knupfer, M., Electronic properties of transition metal phthalocyanines: The impact of the central metal atom (d<sub>5</sub>-d<sub>10</sub>). *Org. Electron.* **2010**, *11*, 1483-1488.

(56) Wang, J.; Shi, Y.; Cao, J.; Wu, R., Magnetization and magnetic anisotropy of metallophthalocyanine molecules from the first principles calculations. *Appl. Phys. Lett.* **2009**, *94*, 122502.

(57) Zhou, J.; Sun, Q., Magnetism of phthalocyanine-based organometallic single porous sheet. *J Am Chem Soc.* **2011**, *133*, 15113-15119.

(58) Colson, J. W.; Dichtel, W. R., Rationally synthesized two-dimensional polymers. *Nat Chem.* **2013**, *5*, 453-465.

(59) Diercks, C. S.; Yaghi, O. M., The atom, the molecule, and the covalent organic framework. *Science*. **2017**, 355.

(60) Boileau, N. T.; Cranston, R.; Mirka, B.; Melville, O. A.; Lessard, B. H., Metal phthalocyanine organic thin-film transistors: changes in electrical performance and stability in response to temperature and environment. *RSC Advances*. **2019**, *9*, 21478-21485.

(61) Marsh, D.; Mink, L., Microscale Synthesis and Electronic Absorption Spectroscopy of Tetraphenylporphyrin H<sub>2</sub>(TPP) and Metalloporphyrins ZnII(TPP) and NiII(TPP). *J. Chem. Educ.* **1996**, 73.

(62) Lan, M.; Zhao, H.; Yuan, H.; Jiang, C.; Zuo, S.; Jiang, Y., Absorption and EPR spectra of some porphyrins and metalloporphyrins. *Dyes Pigm.* **2007**, *74*, 357-362.

(63) Kerp, H. R.; Donker, H.; Koehorst, R. B. M.; Schaafsma, T. J.; van Faassen, E. E., Exciton transport in organic dye layers for photovoltaic applications. *Chem. Phys. Lett.* **1998**, *298*, 302-308.

(64) Keller, N.; Calik, M.; Sharapa, D.; Soni, H. R.; Zehetmaier, P. M.; Rager, S.; Auras, F.; Jakowetz, A. C.; Gorling, A.; Clark, T.; Bein, T., Enforcing Extended Porphyrin J-Aggregate Stacking in Covalent Organic Frameworks. *J Am Chem Soc.* **2018**, *140*, 16544-16552.

(65) Gao, Y.; Zhang, X.; Ma, C.; Li, X.; Jiang, J., Morphology-controlled self-assembled nanostructures of 5,15-di[4-(5-acetylsulfanylpenoxy)phenyl]porphyrin derivatives. Effect of metal-ligand coordination bonding on tuning the intermolecular interaction. *J Am Chem Soc.* **2008**, *130*, 17044-17052.

(66) Hendon, C. H.; Rieth, A. J.; Korzynski, M. D.; Dinca, M., Grand Challenges and Future Opportunities for Metal-Organic Frameworks. *ACS Cent Sci.* **2017**, *3*, 554-563.

(67) Jiang, J.; Zhao, Y.; Yaghi, O. M., Covalent

Chemistry beyond Molecules. *J Am Chem Soc.* **2016**, *138*, 3255-3265.

(68) Li, B.; Wen, H. M.; Zhou, W.; Chen, B., Porous Metal-Organic Frameworks for Gas Storage and Separation: What, How, and Why? *J Phys Chem Lett.* **2014**, *5*, 3468-3479.

(69) Ko, M.; Mendecki, L.; Mirica, K. A., Conductive two-dimensional metal-organic frameworks as multifunctional materials. *Chem Commun (Camb).* **2018**, *54*, 7873-7891.

(70) Aziz, A.; Ruiz-Salvador, A. R.; Hernández, N. C.; Calero, S.; Hamad, S.; Grau-Crespo, R., Porphyrin-based metal-organic frameworks for solar fuel synthesis photocatalysis: band gap tuning via iron substitutions. *J Mater. Chem. A.* **2017**, *5*, 11894-11904.

(71) Lee, C. Y.; Farha, O. K.; Hong, B. J.; Sarjeant, A. A.; Nguyen, S. T.; Hupp, J. T., Light-harvesting metal-organic frameworks (MOFs): efficient strut-to-strut energy transfer in bipy and porphyrin-based MOFs. *J Am Chem Soc.* **2011**, *133*, 15858-15861.

(72) Liu, Y.; Yang, Y.; Sun, Q.; Wang, Z.; Huang, B.; Dai, Y.; Qin, X.; Zhang, X., Chemical adsorption enhanced CO<sub>2</sub> capture and photoreduction over a copper porphyrin based metal organic framework. *ACS Appl Mater Interfaces.* **2013**, *5*, 7654-7658.

(73) Markovitsi, D.; Germain, A.; Millie, P.; Lecuyer, P.; Gallos, L.; Argyrakis, P.; Bengs, H.; Ringsdorf, H., Triphenylene Columnar Liquid Crystals: Excited States and Energy Transfer. *The Journal of Physical Chemistry.* **1995**, *99*, 1005-1017.

(74) van de Craats, A. M.; Siebbeles, L. D. A.; Bleyl, I.; Haarer, D.; Berlin, Y. A.; Zharikov, A. A.; Warman, J. M., Mechanism of Charge Transport along Columnar Stacks of a Triphenylene Dimer. *J. Phys. Chem. B.* **1998**, *102*, 9625-9634.

(75) Rose, A.; Lugmair, C. G.; Swager, T. M., Excited-State Lifetime Modulation in Triphenylene-Based Conjugated Polymers. *J Am Chem Soc.* **2001**, *123*, 11298-11299.

(76) Sheberla, D.; Sun, L.; Blood-Forsythe, M. A.; Er, S.; Wade, C. R.; Brozek, C. K.; Aspuru-Guzik, A.; Dinca, M., High electrical conductivity in Ni(3)(2,3,6,7,10,11-hexamino triphenylene)(2), a semiconducting metal-organic graphene analogue. *J Am Chem Soc.* **2014**, *136*, 8859-8862.

(77) Hmadeh, M.; Lu, Z.; Liu, Z.; Gándara, F.; Furukawa, H.; Wan, S.; Augustyn, V.; Chang, R.; Liao, L.; Zhou, F.; Perre, E.; Ozolins, V.; Suenaga, K.; Duan, X.; Dunn, B.; Yamamoto, Y.; Terasaki, O.; Yaghi, O. M., New Porous Crystals of Extended Metal-Catecholates. *Chem. Mater.* **2012**, *24*, 3511-3513.

(78) Tan, Y. W.; Zhang, Y.; Bolotin, K.; Zhao, Y.; Adam, S.; Hwang, E. H.; Das Sarma, S.; Stormer, H. L.; Kim, P., Measurement of scattering rate and minimum conductivity in graphene. *Phys Rev Lett.* **2007**, *99*, 246803.

(79) Manbeck, G. F.; Fujita, E., A review of iron and cobalt porphyrins, phthalocyanines and related complexes for electrochemical and photochemical reduction of carbon dioxide. *J. Porphyr. Phthalocyanines.* **2015**, *19*, 45-64.

(80) Liao, M. S.; Watts, J. D.; Huang, M. J.; Gorun, S. M.; Kar, T.; Scheiner, S., Effects of Peripheral Substituents on the Electronic Structure and Properties of Unligated and Ligated Metal Phthalocyanines, Metal = Fe, Co, Zn. *J Chem Theory Comput.* **2005**, *1*, 1201-1210.

(81) Pedrosa, J. M.; Dooling, C. M.; Richardson, T. H.; Hyde, R. K.; Hunter, C. A.; Martín, M. T.; Camacho, L., Influence of Molecular Organization of Asymmetrically Substituted Porphyrins on Their Response to NO<sub>2</sub> Gas. *Langmuir.* **2002**, *18*, 7594-7601.

(82) Functional Phthalocyanine Molecular Materials. *2010*, *135*.

(83) Spitzer, E. L.; Dichtel, W. R., Lewis acid-catalysed formation of two-dimensional phthalocyanine covalent organic frameworks. *Nat. Chem.* **2010**, *2*, 672-677.

(84) Chen, L.; Furukawa, K.; Gao, J.; Nagai, A.; Nakamura, T.; Dong, Y.; Jiang, D., Photoelectric covalent organic frameworks: converting open lattices into ordered donor-acceptor heterojunctions. *J Am Chem Soc.* **2014**, *136*, 9806-9809.

(85) Jia, H.; Yao, Y.; Zhao, J.; Gao, Y.; Luo, Z.; Du, P., A novel two-dimensional nickel phthalocyanine-based metal-organic framework for highly efficient water oxidation catalysis. *J. Mater. Chem. A.* **2018**, *6*, 1188-1195.

(86) Mukherjee, D.; Manjunatha, R.; Sampath, S.; Ray, A. K., Phthalocyanines as Sensitive Materials for Chemical Sensors. In *Materials for Chemical Sensing*, 2017; pp 165-226.

(87) Bartolomé, J.; Monton, C.; Schuller, I. K., Magnetism of Metal Phthalocyanines. In *Molecular Magnets*, 2014; pp 221-245.

(88) Williams, G.; Sutty, S.; Klenkler, R.; Aziz, H., Renewed interest in metal phthalocyanine donors for small molecule organic solar cells. *Sol. Energy Mater. Sol. Cells.* **2014**, *124*, 217-226.

(89) Miller, J. D.; Baron, E. D.; Scull, H.; Hsia, A.; Berlin, J. C.; McCormick, T.; Colussi, V.; Kenney, M. E.; Cooper, K. D.; Oleinick, N. L., Photodynamic therapy with the phthalocyanine photosensitizer Pc 4: the case experience with preclinical mechanistic and early clinical-translational studies. *Toxicol Appl Pharmacol.* **2007**, *224*, 290-299.

(90) Doyle, J. J.; Wang, J.; O'Flaherty, S. M.; Chen, Y.; Slodek, A.; Hegarty, T.; Carpenter II, L. E.; Wöhrle, D.; Hanack, M.; Blau, W. J., Nonlinear optical performance of chemically tailored phthalocyanine-polymer films as solid-state optical limiting devices. *J. Opt. A. Pure Appl Op.* **2008**, *10*.

(91) Lim, C. K.; Shin, J.; Lee, Y. D.; Kim, J.; Oh, K. S.; Yuk, S. H.; Jeong, S. Y.; Kwon, I. C.; Kim, S., Phthalocyanine-aggregated polymeric nanoparticles as

1 tumor-homing near-infrared absorbers for  
2 photothermal therapy of cancer. *Theranostics*. **2012**, *2*,  
3 871-879.

4 (92) Stillman, M. J. N., T. , In Phthalocyanines:  
5 Properties and Applications. C. C. Leznoff, A. B. P. L., Ed.  
6 Eds. VCH Publishers: New York, 1989; Vol. 1, p p. 133.

7 (93) Rawling, T.; McDonagh, A., Ruthenium  
8 phthalocyanine and naphthalocyanine complexes:  
9 Synthesis, properties and applications. *Coord. Chem.  
Rev.* **2007**, *251*, 1128-1157.

10 (94) Leznoff, C. C.; Black, L. S.; Hiebert, A.; Causey, P.  
11 W.; Christendat, D.; Lever, A. B. P., Red manganese  
12 phthalocyanines from highly hindered  
13 hexadecaalkoxyphthalocyanines. *Inorganica Chimica  
Acta*. **2006**, *359*, 2690-2699.

14 (95) Kobayashi, N.; Nakajima, S.; Ogata, H.; Fukuda,  
15 T., Synthesis, spectroscopy, and electrochemistry of  
16 tetra-tert-butylated tetraazaporphyrins,  
17 phthalocyanines, naphthalocyanines, and  
18 anthracocyanines, together with molecular orbital  
19 calculations. *Chemistry*. **2004**, *10*, 6294-6312.

20 (96) Cook, M. J., Properties of some alkyl substituted  
21 phthalocyanines and related macrocycles. *Chem Rec.*  
22 **2002**, *2*, 225-236.

23 (97) Kment, S.; Kluson, P.; Drobek, M.; Kuzel, R.;  
24 Gregora, I.; Kohout, M.; Hubicka, Z., Preparation of thin  
25 phthalocyanine layers and their structural and  
26 absorption properties. *Thin Solid Films*. **2009**, *517*,  
27 5274-5279.

28 (98) Erk, P.; Hengelsberg, H., Phthalocyanine Dyes  
29 and Pigments. In *The Porphyrin Handbook*, 2003; pp  
30 105-149.

31 (99) Minari, T.; Seto, M.; Nemoto, T.; Isoda, S.;  
32 Tsukagoshi, K.; Aoyagi, Y., Molecular-packing-enhanced  
33 charge transport in organic field-effect transistors  
34 based on semiconducting porphyrin crystals. *Appl. Phys.  
35 Lett.* **2007**, *91*, 123501.

36 (100) Thompson, J. A.; Murata, K.; Miller, D. C.;  
37 Stanton, J. L.; Broderick, W. E.; Hoffman, B. M.; Ibers, J.  
38 A., Synthesis of high-purity phthalocyanines (pc): high  
39 intrinsic conductivities in the molecular conductors  
40 H<sub>2</sub>(pc)I and Ni(pc)I. *Inorg. Chem.* **1993**, *32*, 3546-3553.

41 (101) Eley, D. D., Phthalocyanines as semiconductors.  
42 *Nature*. **1948**, *162*, 819.

43 (102) Özer, L. M.; Özer, M.; Altindal, A.; Özkaray, A. R.;  
44 Salih, B.; Bekaroğlu, Ö., Synthesis, characterization,  
45 OFET and electrochemical properties of novel dimeric  
46 metallophthalocyanines. *Dalton Trans.* **2013**, *42*, 6633-  
47 6644.

48 (103) Nazeeruddin, M. K.; Humphry-Baker, R.; Officer,  
49 D. L.; Campbell, W. M.; Burrell, A. K.; Gratzel, M.,  
50 Application of metalloporphyrins in nanocrystalline  
51 dye-sensitized solar cells for conversion of sunlight into  
52 electricity. *Langmuir*. **2004**, *20*, 6514-6517.

53 (104) Che, C.-M.; Hou, Y.-J.; Chan, M. C. W.; Guo, J.; Liu,  
54 Y.; Wang, Y., [meso-  
55 Tetrakis(pentafluorophenyl)porphyrinato]platinum(ii)  
56

57 as an efficient, oxidation-resistant red phosphor:  
58 spectroscopic properties and applications in organic  
59 light-emitting diodes. *J. Mater. Chem.* **2003**, *13*, 1362-  
60 1366.

(105) Henari, F. Z., Optical switching in  
organometallic phthalocyanine. *J Opt a-Pure Appl Op.*  
**2001**, *3*, 188-190.

(106) Gould, R. D., Structure and electrical conduction  
properties of phthalocyanine thin films. *Coord. Chem.  
Rev.* **1996**, *156*, 237-274.

(107) Turek, P.; André, J.-J.; Giraudieu, A.; Simon, J., Preparation and study of a lithium phthalocyanine radical: optical and magnetic properties. *Chem. Phys. Lett.* **1987**, *134*, 471-476.

(108) Brinkmann, M.; Chaumont, C.; André, J. J., Dark conductivity in the x and alpha polymorphs of lithium phthalocyanine. *Thin Solid Films*. **1998**, *324*, 68-77.

(109) Advanced Functional MaterialsInabe, T.; Tajima, H., Phthalocyanines-versatile components of molecular conductors. *Chem Rev.* **2004**, *104*, 5503-5534.

(110) Martinsen, J.; Greene, R. L.; Palmer, S. M.; Hoffman, B. M., Low-temperature metallic conductivity in a metallocyclic crystal: nickel phthalocyanine iodide. *J. Am. Chem. Soc.* **1983**, *105*, 677-678.

(111) Passard, M.; Blanc, J. P.; Maleysson, C., Gaseous oxidation and compensating reduction of lutetium bis-phthalocyanine and lutetium phthalo-naphthalocyanine films. *Thin Solid Films*. **1995**, *271*, 8-14.

(112) Matumoto, A.; Hoshino, N.; Akutagawa, T.; Matsuda, M., N-Type Semiconducting Behavior of Copper Octafluorophthalocyanine in an Organic Field-Effect Transistor. *Appl. Sci.* **2017**, *7*, 1111.

(113) Guldin, D. M.; Zilberman, I.; Gouloumis, A.; Vázquez, P.; Torres, T., Metallophthalocyanines: Versatile Electron-Donating Building Blocks for Fullerene Dyads. *J. Chem. Phys. B*. **2004**, *108*, 18485-18494.

(114) Engelkamp, H.; Middelbeek, S.; Nolte, R. J., Self-assembly of disk-shaped molecules to coiled-coil aggregates with tunable helicity. *Science*. **1999**, *284*, 785-788.

(115) Schouten, P. G.; Warman, J. M.; de Haas, M. P.; van Nostrum, C. F.; Gelinck, G. H.; Nolte, R. J. M.; Copyn, M. J.; Zwikker, J. W.; Engel, M. K., The Effect of Structural Modifications on Charge Migration in Mesomorphic Phthalocyanines. *J Am Chem Soc.* **1994**, *116*, 6880-6894.

(116) Di Natale, C.; Macagnano, A.; Repole, G.; Saggio, G.; D'Amico, A.; Paolesse, R.; Boschi, T., The exploitation of metalloporphyrins as chemically interactive material in chemical sensors. *Mater. Sci. Eng. C*. **1998**, *5*, 209-215.

(117) Torrens, F.; Ortí, E.; Sánchez-Marin, J., Electrically Conductive Phthalocyanine Assemblies. Structural and Non-Integer Oxidation Number Considerations. In *Lower-Dimensional Systems and Molecular Electronics*, 1990; pp 461-466.

(118) Stock, T. J. Z.; Nogami, J., Copper phthalocyanine thin films on Cu(111): Sub-monolayer to multi-layer. *Surface Science*. **2015**, 637-638, 132-139.

(119) Li, L.; Tang, Q.; Li, H.; Hu, W.; Yang, X.; Shuai, Z.; Liu, Y.; Zhu, D., Organic thin-film transistors of phthalocyanines. *Pure Appl. Chem.* **2008**, 80, 2231-2240.

(120) Madhuri, K. P.; John, N. S.; Angappane, S.; Santra, P. K.; Bertram, F., Influence of Iodine Doping on the Structure, Morphology, and Physical Properties of Manganese Phthalocyanine Thin Films. *J. Chem. Phys. C* **2018**, 122, 28075-28084.

(121) Heutz, S.; Mitra, C.; Wu, W.; Fisher, A. J.; Kerridge, A.; Stoneham, M.; Harker, A. H.; Gardener, J.; Tseng, H. H.; Jones, T. S.; Renner, C.; Aeppli, G., Molecular Thin Films: A New Type of Magnetic Switch. *Adv. Mater.* **2007**, 19, 3618-3622.

(122) Arillo-Flores, O. I.; Fadlallah, M. M.; Schuster, C.; Eckern, U.; Romero, A. H., Magnetic, electronic, and vibrational properties of metal and fluorinated metal phthalocyanines. *Phys. Rev. B* **2013**, 87.

(123) Liu, L.; Yang, K.; Jiang, Y.; Song, B.; Xiao, W.; Song, S.; Du, S.; Ouyang, M.; Hofer, W. A.; Castro Neto, A. H.; Gao, H. J., Revealing the atomic site-dependent g factor within a single magnetic molecule via the extended Kondo effect. *Phys Rev Lett.* **2015**, 114, 126601.

(124) Lee, S.; Yudkowsky, M.; Halperin, W. P.; Ogawa, M. Y.; Hoffman, B. M., One-dimensional magnetism in copper phthalocyanine. *Phys Rev B Condens Matter*. **1987**, 35, 5003-5007.

(125) Assour, J. M.; Kahn, W. K., Electron Spin Resonance of  $\alpha$ - and  $\beta$ -Cobalt Phthalocyanine1a. *J Am Chem Soc.* **1965**, 87, 207-212.

(126) Srivastava, T. S.; Przybylinski, J. L.; Nath, A., Moessbauer study of the intermolecular interactions in the  $\gamma$  and  $\delta$  polymorphs of iron and cobalt phthalocyanin. *Inorg. Chem.* **2002**, 13, 1562-1564.

(127) Barraclough, C. G.; Gregson, A. K.; Mitra, S., Interpretation of the magnetic properties of manganese (II) phthalocyanine. *J. Chem. Phys.* **1974**, 60, 962-968.

(128) Kataoka, T.; Sakamoto, Y.; Yamazaki, Y.; Singh, V. R.; Fujimori, A.; Takeda, Y.; Ohkochi, T.; Fujimori, S. I.; Okane, T.; Saitoh, Y.; Yamagami, H.; Tanaka, A., Electronic configuration of Mn ions in the - molecular ferromagnet -Mn phthalocyanine studied by soft X-ray magnetic circular dichroism. *Solid State Commun.* **2012**, 152, 806-809.

(129) Evangelisti, M.; Bartolomé, J.; de Jongh, L. J.; Filoti, G., Magnetic properties of  $\gamma$ -iron(II) phthalocyanin. *Phys. Rev. B* **2002**, 66.

(130) Filoti, G.; Kuz'min, M. D.; Bartolomé, J., Mössbauer study of the hyperfine interactions and spin dynamics in  $\gamma$ -iron(II) phthalocyanin. *Phys. Rev. B* **2006**, 74.

(131) Otero, R.; Gallego, J. M.; de Parga, A. L.; Martin, N.; Miranda, R., Molecular self-assembly at solid surfaces. *Adv Mater.* **2011**, 23, 5148-5176.

(132) Kondo, J., Resistance Minimum in Dilute Magnetic Alloys. *Prog. Theor. Phys.* **1964**, 32, 37-49.

(133) Zhao, A.; Hu, Z.; Wang, B.; Xiao, X.; Yang, J.; Hou, J. G., Kondo effect in single cobalt phthalocyanine molecules adsorbed on Au(111) monoatomic steps. *J. Chem. Phys.* **2008**, 128, 234705.

(134) Sun, X.; Li, Z. Y.; Jibran, M.; Pratt, A.; Yamauchi, Y.; Wang, B., Reversible switching of the spin state in a manganese phthalocyanine molecule by atomic nitrogen. *Phys. Chem. Chem. Phys.* **2017**, 19, 32655-32662.

(135) Kügel, J.; Karolak, M.; Krönlein, A.; Serrate, D.; Bode, M.; Sangiovanni, G., Reversible magnetic switching of high-spin molecules on a giant Rashba surface. *Quantum Materials*. **2018**, 3.

(136) Wang, Y.; Li, X.; Zheng, X.; Yang, J., Spin switch in iron phthalocyanine on Au(111) surface by hydrogen adsorption. *J. Chem. Phys.* **2017**, 147, 134701.

(137) Strozecka, A.; Soriano, M.; Pascual, J. I.; Palacios, J. J., Reversible change of the spin state in a manganese phthalocyanine by coordination of CO molecule. *Phys. Rev. Lett.* **2012**, 109, 147-202.

(138) Wackerlin, C.; Chylarecka, D.; Kleibert, A.; Muller, K.; Iacovita, C.; Nolting, F.; Jung, T. A.; Ballav, N., Controlling spins in adsorbed molecules by a chemical switch. *Nat. Commun.* **2010**, 1, 61.

(139) Zhou, R.; Josse, F.; Gopel, W.; Ozturk, Z. Z.; Bekaroglu, O., Phthalocyanines as sensitive materials for chemical sensors. *Appl. Organomet. Chem.* **1996**, 10, 557-577.

(140) D'Amico, A.; Di Natale, C.; Paolesse, R.; Macagnano, A.; Mantini, A., Metalloporphyrins as basic material for volatile sensitive sensors. *Sens. Actuators B Chem.* **2000**, 65, 209-215.

(141) Andringa, A.-M.; Spijkman, M.-J.; Smits, E. C. P.; Mathijssen, S. G. J.; Hal, P. A. v.; Setayesh, S.; Willard, N. P.; Borshchev, O. V.; Ponomarenko, S. A.; Blom, P. W. M.; de Leeuw, D. M., Gas sensing with self-assembled monolayer field-effect transistors. *Org. Electron.* **2010**, 11, 895-898.

(142) Ho, K.-C.; Tsou, Y.-H., Chemiresistor-type NO gas sensor based on nickel phthalocyanine thin films. *Sens. Actuators B Chem.* **2001**, 77, 253-259.

(143) Nyokong, T., Phthalocyanines and related complexes as electrocatalysts for the detection of nitric oxide. *Talanta*. **2003**, 61, 27-35.

(144) Kumar, A.; Brunet, J.; Varenne, C.; Ndiaye, A.; Pauly, A.; Penza, M.; Alvisi, M., Tetra-tert-butyl copper phthalocyanine-based QCM sensor for toluene detection in air at room temperature. *Sens. Actuators B Chem.* **2015**, 210, 398-407.

(145) Kumar, A.; Brunet, J.; Varenne, C.; Ndiaye, A.; Pauly, A., Phthalocyanines based QCM sensors for aromatic hydrocarbons monitoring: Role of metal atoms

and substituents on response to toluene. *Sens. Actuators B Chem.* **2016**, *230*, 320-329.

(146) Jakubik, W. P.; Urbańczyk, M. W.; Kochowski, S.; Bodzenta, J., Palladium and phthalocyanine bilayer films for hydrogen detection in a surface acoustic wave sensor system. *Sens. Actuators B Chem.* **2003**, *96*, 321-328.

(147) Kubo, Y.; Yamamoto, M.; Ikeda, M.; Takeuchi, M.; Shinkai, S.; Yamaguchi, S.; Tamao, K., A colorimetric and ratiometric fluorescent chemosensor with three emission changes: fluoride ion sensing by a triarylborane- porphyrin conjugate. *Angew Chem Int Ed Engl.* **2003**, *42*, 2036-2040.

(148) Lee, C.; Lee, D. H.; Hong, J.-I., Colorimetric anion sensing by porphyrin-based anion receptors. *Tetrahedron Lett.* **2001**, *42*, 8665-8668.

(149) Rakow, N. A.; Suslick, K. S., A colorimetric sensor array for odour visualization. *Nature* **2000**, *406*, 710-713.

(150) Brown, M. D.; Schoenfisch, M. H., Catalytic selectivity of metallophthalocyanines for electrochemical nitric oxide sensing. *Electrochim Acta* **2018**, *273*, 98-104.

(151) Park, C.; Hyun Yun, D.; Kim, S.-T.; Woo Park, Y., Enhancement of the NO<sub>2</sub>-sensing capability of copper phthalocyanine by measuring the relative resistance change. *Sens. Actuators B Chem.* **1996**, *30*, 23-27.

(152) Jiang, D. P.; Lu, A. D.; Li, Y. J.; Pang, X. M.; Hua, Y. L., Interaction between copper tetra-(2,4-ditert-amylphenoxy) phthalocyanine Langmuir-Blodgett films as a gas-sensitive sensor and NH<sub>3</sub>. *Thin Solid Films* **1991**, *199*, 173-179.

(153) Parr, A. T. J.; Krier, A.; Collins, R. A., Adsorption and bulk diffusion of chlorine in monoclinic lead phthalocyanine thin film gas sensors. *Thin Solid Films* **1993**, *230*, 225-228.

(154) Kanefusa, S.; Nitta, M., The detection of H<sub>2</sub> gas by metal phthalocyanine-based gas sensors. *Sens. Actuators B Chem.* **1992**, *9*, 85-90.

(155) Mockert, H.; Schmeisser, S.; Göpel, W., Lead phthalocyanine (PbPc) as a prototype organic material for gas sensors: comparative electrical and spectroscopic studies to optimize O<sub>2</sub> and NO<sub>2</sub> sensing. *Sens. Actuators* **1989**, *19*, 159-176.

(156) Wright, J., Gas adsorption on phthalocyanines and its effects on electrical properties. *Prog. Surf. Sci.* **1989**, *31*, 1-60.

(157) Bohrer, F. I.; Colesniuc, C. N.; Park, J.; Schuller, I. K.; Kummel, A. C.; Trogler, W. C., Selective detection of vapor phase hydrogen peroxide with phthalocyanine chemiresistors. *J Am Chem Soc.* **2008**, *130*, 3712-3713.

(158) Bora, M.; Schut, D.; Baldo, M. A., Combinatorial detection of volatile organic compounds using metal-phthalocyanine field effect transistors. *Anal Chem.* **2007**, *79*, 3298-3303.

(159) Tsai, A. L.; Berka, V.; Martin, E.; Olson, J. S., A "sliding scale rule" for selectivity among NO, CO, and O<sub>2</sub> by heme protein sensors. *Biochem.* **2012**, *51*, 172-186.

(160) Liu, J.; Masuda, Y.; Sekido, E.; Wakida, S.-I.; Hiiro, K., Phosphate ion-sensitive coated-wire/field-effect transistor electrode based on cobalt phthalocyanine with poly(vinyl chloride) as the membrane matrix. *Analytica Chimica Acta* **1989**, *224*, 145-151.

(161) Someya, T.; Dodabalapur, A.; Gelperin, A.; Katz, H. E.; Bao, Z., Integration and Response of Organic Electronics with Aqueous Microfluidics. *Langmuir* **2002**, *18*, 5299-5302.

(162) Han, J.; Xu, X.; Rao, X.; Wei, M.; Evans, D. G.; Duan, X., Layer-by-layer assembly of layered double hydroxide/cobalt phthalocyanine ultrathin film and its application for sensors. *J. Mater. Chem.* **2011**, *21*, 2126-2130.

(163) Siqueira, J. R., Jr.; Gasparotto, L. H.; Crespilho, F. N.; Carvalho, A. J.; Zucolotto, V.; Oliveira, O. N., Jr., Physicochemical properties and sensing ability of metallophthalocyanines/chitosan nanocomposites. *J Phys Chem B* **2006**, *110*, 22690-22694.

(164) Shi, M.; Chen, Z.; Guo, L.; Liang, X.; Zhang, J.; He, C.; Wang, B.; Wu, Y., A multiwalled carbon nanotube/tetra- $\beta$ -isoheptyloxyphthalocyanine cobalt(ii) composite with high dispersibility for electrochemical detection of ascorbic acid. *J. Mater. Chem. B* **2014**, *2*.

(165) Pakapongpan, S.; Mensing, J. P.; Phokharatkul, D.; Lomas, T.; Tuantranont, A., Highly selective electrochemical sensor for ascorbic acid based on a novel hybrid graphene-copper phthalocyanine-polyaniline nanocomposites. *Electrochimica Acta* **2014**, *133*, 294-301.

(166) Shaymurat, T.; Tang, Q.; Tong, Y.; Dong, L.; Liu, Y., Gas dielectric transistor of CuPc single crystalline nanowire for SO(2) detection down to sub-ppm levels at room temperature. *Adv Mater.* **2013**, *25*, 2269-2273, 2376.

(167) Xu, H.; Xiao, J.; Yan, L.; Zhu, L.; Liu, B., An electrochemical sensor for selective detection of dopamine based on nickel tetrasulfonated phthalocyanine functionalized nitrogen-doped graphene nanocomposites. *J. Electroanal. Chem.* **2016**, *779*, 92-98.

(168) Bohrer, F. I.; Sharoni, A.; Colesniuc, C.; Park, J.; Schuller, I. K.; Kummel, A. C.; Trogler, W. C., Gas sensing mechanism in chemiresistive cobalt and metal-free phthalocyanine thin films. *J Am Chem Soc.* **2007**, *129*, 5640-5646.

(169) Zhou, R.; Josse, F.; Gpel, W.; ztrk, Z. Z.; Bekaro?lu, Phthalocyanines as Sensitive Materials for Chemical Sensors. *Appl. Organomet. Chem.* **1996**, *10*, 557-577.

(170) Rana, M. K.; Sinha, M.; Panda, S., Gas sensing

behavior of metal-phthalocyanines: Effects of electronic structure on sensitivity. *Chem. Phys.* **2018**, 513, 23-34.

(171) Schöllhorn, B.; Germain, J. P.; Pauly, A.; Maleysson, C.; Blanc, J. P., Influence of peripheral electron-withdrawing substituents on the conductivity of zinc phthalocyanine in the presence of gases. Part 1: reducing gases. *Thin Solid Films.* **1998**, 326, 245-250.

(172) Guillaud, G.; Simon, J.; Germain, J. P., Metallophthalocyanines: Gas sensors, resistors and field effect transistors. *Coord. Chem. Rev.* **1998**, 178-180, 1433-1484.

(173) Oprea, A.; Weimar, U.; Simon, E.; Fleischer, M.; Frerichs, H. P.; Wilbertz, C.; Lehmann, M., Copper phthalocyanine suspended gate field effect transistors for NO<sub>2</sub> detection. *Sens. Actuators B Chem.* **2006**, 118, 249-254.

(174) Ho, K.-C.; Chen, C.-M.; Liao, J.-Y., Enhancing chemiresistor-type NO gas-sensing properties using ethanol-treated lead phthalocyanine thin films. *Sens. Actuators B Chem.* **2005**, 108, 418-426.

(175) Klyamer, D. D.; Sukhikh, A. S.; Krasnov, P. O.; Gromilov, S. A.; Morozova, N. B.; Basova, T. V., Thin films of tetrafluorosubstituted cobalt phthalocyanine: Structure and sensor properties. *Appl. Surf. Sci.* **2016**, 372, 79-86.

(176) Kaya, E. N.; Tuncel, S.; Basova, T. V.; Banimuslem, H.; Hassan, A.; Gürek, A. G.; Ahsen, V.; Durmuş, M., Effect of pyrene substitution on the formation and sensor properties of phthalocyanine-single walled carbon nanotube hybrids. *Sens. Actuators B Chem.* **2014**, 199, 277-283.

(177) Bohrer, F. I.; Colesniuc, C. N.; Park, J.; Ruidiaz, M. E.; Schuller, I. K.; Kummel, A. C.; Troglar, W. C., Comparative gas sensing in cobalt, nickel, copper, zinc, and metal-free phthalocyanine chemiresistors. *J Am Chem Soc.* **2009**, 131, 478-485.

(178) Ridhi, R.; Saini, G. S. S.; Tripathi, S. K., Sensing of volatile organic compounds by copper phthalocyanine thin films. *Mater Res Express.* **2017**, 4.

(179) Li, X.; Jiang, Y.; Xie, G.; Tai, H.; Sun, P.; Zhang, B., Copper phthalocyanine thin film transistors for hydrogen sulfide detection. *Sens. Actuators B Chem.* **2013**, 176, 1191-1196.

(180) Wang, Y.; Hu, N.; Zhou, Z.; Xu, D.; Wang, Z.; Yang, Z.; Wei, H.; Kong, E. S.-W.; Zhang, Y., Single-walled carbon nanotube/cobalt phthalocyanine derivative hybrid material: preparation, characterization and its gas sensing properties. *J. Mater. Chem.* **2011**, 21.

(181) Wang, B.; Wu, Y.; Wang, X.; Chen, Z.; He, C., Copper phthalocyanine noncovalent functionalized single-walled carbon nanotube with enhanced NH3 sensing performance. *Sens. Actuators B Chem.* **2014**, 190, 157-164.

(182) Wang, B.; Zhou, X.; Wu, Y.; Chen, Z.; He, C., Lead phthalocyanine modified carbon nanotubes with enhanced NH3 sensing performance. *Sens. Actuators B Chem.* **2012**, 171-172, 398-404.

(183) Radhakrishnan, S.; Deshpande, S. D., Conducting polymers functionalized with phthalocyanine as nitrogen dioxide sensors. *Sensors.* **2002**, 2, 185-194.

(184) Kumar, S.; Kaur, N.; Sharma, A. K.; Mahajan, A.; Bedi, R. K., Improved Cl<sub>2</sub> sensing characteristics of reduced graphene oxide when decorated with copper phthalocyanine nanoflowers. *RSC Advances.* **2017**, 7, 25229-25236.

(185) Hatchett, D. W.; Josowicz, M., Composites of intrinsically conducting polymers as sensing nanomaterials. *Chem Rev.* **2008**, 108, 746-769.

(186) Obirai, J. C.; Nyokong, T., Thiol oxidation at 2-mercaptopurimidine-appended cobalt phthalocyanine modified glassy carbon electrodes. *J. Electroanal. Chem.* **2007**, 600, 251-256.

(187) Pereira-Rodrigues, N.; Cofre, R.; Zagal, J. H.; Bedioui, F., Electrocatalytic activity of cobalt phthalocyanine CoPc adsorbed on a graphite electrode for the oxidation of reduced L-glutathione (GSH) and the reduction of its disulfide (GSSG) at physiological pH. *Bioelectrochemistry.* **2007**, 70, 147-154.

(188) Zagal, J. H.; Griveau, S.; Silva, J. F.; Nyokong, T.; Bedioui, F., Metallophthalocyanine-based molecular materials as catalysts for electrochemical reactions. *Coord. Chem. Rev.* **2010**, 254, 2755-2791.

(189) Xu, H.; Xiao, J.; Liu, B.; Griveau, S.; Bedioui, F., Enhanced electrochemical sensing of thiols based on cobalt phthalocyanine immobilized on nitrogen-doped graphene. *Biosens Bioelectron.* **2015**, 66, 438-444.

(190) Perez, E. F.; Neto, G. d. O.; Tanaka, A. A.; Kubota, L. T., Electrochemical Sensor for Hydrazine Based on Silica Modified with Nickel Tetrasulfonated Phthalocyanine. *Electroanalysis.* **1998**, 10, 111-115.

(191) Araujo, I. M.; Zampa, M. F.; Moura, J. B.; dos Santos, J. R., Jr.; Eaton, P.; Zucolotto, V.; Veras, L. M.; de Paula, R. C.; Feitosa, J. P.; Leite, J. R.; Eiras, C., Contribution of the cashew gum (*Anacardium occidentale* L.) for development of layer-by-layer films with potential application in nanobiomedical devices. *Mater Sci Eng C Mater Biol Appl.* **2012**, 32, 1588-1593.

(192) Chernyshov, D. V.; Shvedene, N. V.; Antipova, E. R.; Pletnev, I. V., Ionic liquid-based miniature electrochemical sensors for the voltammetric determination of catecholamines. *Anal Chim Acta.* **2008**, 621, 178-184.

(193) Maree, S.; Nyokong, T., Electrocatalytic behavior of substituted cobalt phthalocyanines towards the oxidation of cysteine. *J. Electroanal. Chem.* **2000**, 492, 120-127.

(194) Koyun, O.; Gorduk, S.; Gencten, M.; Sahin, Y., A novel copper(II) phthalocyanine-modified multiwalled carbon nanotube-based electrode for sensitive electrochemical detection of bisphenol A. *New J Chem.* **2019**, 43, 85-92.

(195) Agboola, B. O.; Vilakazi, S. L.; Ozoemena, K. I., Electrochemistry at cobalt(II)tetrasulfophthalocyanine-

1 multi-walled carbon nanotubes modified glassy carbon  
2 electrode: a sensing platform for efficient suppression  
3 of ascorbic acid in the presence of epinephrine. *J Solid*  
4 *State Electrochem.* **2008**, *13*, 1367-1379.

5 (196) Mount, G. H.; Rumburg, B.; Havig, J.; Lamb, B.;  
6 Westberg, H.; Yonge, D.; Johnson, K.; Kincaid, R.,  
7 Measurement of atmospheric ammonia at a dairy using  
8 differential optical absorption spectroscopy in the mid-  
ultraviolet. *Atmos. Environ.* **2002**, *36*, 1799-1810.

9 (197) Rath, H. J.; Wimmer, J., Gas chromatographic  
10 analysis of traces of hydrogen sulfide in hydrogen.  
11 *Chromatographia.* **1980**, *13*, 513-514.

12 (198) Hayat, H.; Griffiths, T.; Brennan, D.; Lewis, R. P.;  
13 Barclay, M.; Weirman, C.; Philip, B.; Searle, J. R., The  
14 State-of-the-Art of Sensors and Environmental  
15 Monitoring Technologies in Buildings. *Sensors (Basel).*  
16 **2019**, *19*.

17 (199) Basu, B.; Satapathy, S.; Bhatnagar, A. K., Merox  
18 and Related Metal Phthalocyanine Catalyzed Oxidation  
19 Processes. *Catal Rev Sci Eng.* **1993**, *35*, 571-609.

20 (200) Nyokong, T., Effects of substituents on the  
21 photochemical and photophysical properties of main  
22 group metal phthalocyanines. *Coord. Chem. Rev.* **2007**,  
23 *251*, 1707-1722.

24 (201) Parton, R. F.; Vankelecom, I. F.; Casselman, M. J.;  
25 Bezoukhanova, C. P.; Uytterhoeven, J. B.; Jacobs, P. A., An  
26 efficient mimic of cytochrome P-450 from a zeolite-  
27 encaged iron complex in a polymer membrane. *Nature.*  
28 **1994**, *370*, 541-544.

29 (202) Li, P. S.; Wang, M. Y.; Duan, X. X.; Zheng, L. R.;  
30 Cheng, X. P.; Zhang, Y. F.; Kuang, Y.; Li, Y. P.; Ma, Q.; Feng,  
31 Z. X.; Liu, W.; Sun, X. M., Boosting oxygen evolution of  
32 single-atomic ruthenium through electronic coupling  
33 with cobalt-iron layered double hydroxides. *Nat. Commun.* **2019**, *10*.

34 (203) Elizarova, G. L.; Matvienko, L. G.; Lozhkina, N. V.;  
35 Maizlish, V. E.; Parmon, V. N., Homogeneous Catalysts  
36 for Dioxygen Evolution from Water - Oxidation of Water  
37 by Trisbipyridylruthenium(III) in the Presence of  
38 Metallophthalocyanines. *React Kinet Catal L.* **1981**, *16*,  
39 285-288.

40 (204) Abbaspour, A.; Mirahmadi, E., Electrocatalytic  
41 activity of iron and nickel phthalocyanines supported  
42 on multi-walled carbon nanotubes towards oxygen  
43 evolution reaction. *Electrochimica Acta.* **2013**, *105*, 92-  
44 98.

45 (205) Zagal, J.; Páez, M.; Tanaka, A. A.; dos Santos, J. R.;  
46 Linkous, C. A., Electrocatalytic activity of metal  
47 phthalocyanines for oxygen reduction. *J. Electroanal. Chem.* **1992**, *339*, 13-30.

48 (206) Shi, Z.; Zhang, J. J., Density functional theory  
49 study of transitional metal macrocyclic complexes'  
50 dioxygen-binding abilities and their catalytic activities  
51 toward oxygen reduction reaction. *J Phys Chem C.* **2007**,  
52 *111*, 7084-7090.

53 (207) Vasudevan, P.; Santosh; Mann, N.; Tyagi, S.,  
54 Transition-Metal Complexes of Porphyrins and  
55 Phthalocyanines as Electrocatalysts for Dioxygen  
56 Reduction. *Transit Metal Chem.* **1990**, *15*, 81-90.

57 (208) Hebie, S.; Bayo-Bangoura, M.; Bayo, K.; Servat,  
58 K.; Morais, C.; Napporn, T. W.; Kokoh, K. B.,  
59 Electrocatalytic activity of carbon-supported  
60 metallophthalocyanine catalysts toward oxygen  
reduction reaction in alkaline solution. *J Solid State  
Electrochem.* **2016**, *20*, 931-942.

61 (209) Zhang, X.; Wu, Z.; Zhang, X.; Li, L.; Li, Y.; Xu, H.;  
62 Li, X.; Yu, X.; Zhang, Z.; Liang, Y.; Wang, H., Highly  
63 selective and active CO<sub>2</sub> reduction electrocatalysts  
64 based on cobalt phthalocyanine/carbon nanotube  
65 hybrid structures. *Nat Commun.* **2017**, *8*, 14675.

66 (210) Manbeck, G. F.; Fujita, E., A review of iron and  
67 cobalt porphyrins, phthalocyanines and related  
68 complexes for electrochemical and photochemical  
69 reduction of carbon dioxide. *Journal of Porphyrins and  
70 Phthalocyanines.* **2015**, *19*, 45-64.

71 (211) Grodkowski, J.; Dhanasekaran, T.; Neta, P.;  
72 Hambright, P.; Brunschwig, B. S.; Shinozaki, K.; Fujita, E.,  
73 Reduction of cobalt and iron phthalocyanines and the  
74 role of the reduced species in catalyzed photoreduction  
75 of CO<sub>2</sub>. *J Phys Chem A.* **2000**, *104*, 11332-11339.

76 (212) Kazuya Hiratsuka, K. T., Hideo Sasaki and  
77 Shinobu Toshima, Electrocatalytic behavior of  
78 tetrasulfonated metallophthalocyanines in the reduction  
79 of carbon dioxide  
80 *Chem. Soc. Jpn.* pp. 1137-1140, 1977..

81 (213) Christensen, P. A.; Hamnett, A.; Muir, A. V. G., An  
82 in-situ ftir study of the electroreduction of CO<sub>2</sub> by copc-  
83 coated edge graphite electrodes. *J. Electroanal. Chem.  
Interf. Electrochem.* **1988**, *241*, 361-371.

84 (214) Shibata, M.; Furuya, N., Simultaneous reduction  
85 of carbon dioxide and nitrate ions at gas-diffusion  
86 electrodes with various metallophthalocyanine  
87 catalysts. *Electrochimica Acta.* **2003**, *48*, 3953-3958.

88 (215) Chen, L.; Shaw, L. L., Recent advances in  
89 lithium-sulfur batteries. *Journal of Power Sources.*  
90 **2014**, *267*, 770-783.

91 (216) Scrosati, B., Recent advances in lithium ion  
92 battery materials. *Electrochimica Acta.* **2000**, *45*, 2461-  
93 2466.

94 (217) Oni, J.; Ozoemena, K. I., Phthalocyanines in  
95 batteries and supercapacitors. *J. Porphyr.  
Phthalocyanines.* **2012**, *16*, 754-760.

96 (218) Wang, C.; Xie, Z.; Zhou, Z., Lithium-air batteries:  
97 Challenges coexist with opportunities. *APL Materials.*  
98 **2019**, *7*, 040701.

99 (219) Li, W.; Yu, A.; Higgins, D. C.; Llanos, B. G.; Chen,  
100 Z., Biologically Inspired Highly Durable Iron  
101 Phthalocyanine Catalysts for Oxygen Reduction  
102 Reaction in Polymer Electrolyte Membrane Fuel Cells. *J  
Am Chem Soc.* **2010**, *132*, 17056-17058.

103 (220) Crowther, O.; Du, L.-S.; Moureau, D. M.; Bicaku,  
104 I.; Salomon, M.; Lawson, J. W.; Lucente, L. R.; Mock, K.;  
105 Fellner, J. P.; Scanlon, L. G., Effect of conductive carbon

on capacity of iron phthalocyanine cathodes in primary lithium batteries. *Journal of Power Sources*. **2012**, 217, 92-97.

(221) Yang, W.; Zhang, R.; Luo, K.; Zhang, W.; Zhao, J., Electrocatalytic performances of multi-walled carbon nanotubes chemically modified by metal phthalocyanines in Li/SOCl<sub>2</sub>batteries. *RSC Advances*. **2016**, 6, 75632-75639.

(222) Xu, Z.; Zhao, J.; Li, H.; Li, K.; Cao, Z.; Lu, J., Influence of the electronic configuration of the central metal ions on catalytic activity of metal phthalocyanines to Li/SOCl<sub>2</sub> battery. *Journal of Power Sources*. **2009**, 194, 1081-1084.

(223) Bernstein, P. A.; Lever, A. B. P., Two-electron oxidation of cobalt phthalocyanines by thionyl chloride. Implications for lithium/thionyl chloride batteries. *Inorg. Chem.* **1990**, 29, 608-616.

(224) Xu, Z.; Zhang, G.; Cao, Z.; Zhao, J.; Li, H., Effect of N atoms in the backbone of metal phthalocyanine derivatives on their catalytic activity to lithium battery. *Journal of Molecular Catalysis A: Chemical*. **2010**, 318, 101-105.

(225) Chidembo, A. T.; Ozoemena, K. I.; Agboola, B. O.; Gupta, V.; Wildgoose, G. G.; Compton, R. G., Nickel(ii) tetra-aminophthalocyanine modified MWCNTs as potential nanocomposite materials for the development of supercapacitors. *Energy & Environmental Science*. **2010**, 3, 228-236.

(226) Trahan, M. J.; Jia, Q.; Mukerjee, S.; Plichta, E. J.; Hendrickson, M. A.; Abraham, K. M., Cobalt Phthalocyanine Catalyzed Lithium-Air Batteries. *Journal of The Electrochemical Society*. **2013**, 160, A1577-A1586.

(227) Zhang, R.; Wang, J.; Xu, B.; Huang, X.; Xu, Z.; Zhao, J., Catalytic Activity of Binuclear Transition Metal Phthalocyanines in Electrolyte Operation of Lithium/Thionyl Chloride Battery. *Journal of The Electrochemical Society*. **2012**, 159, H704-H710.

(228) Wang, Y.; Wu, K.; Kröger, J.; Berndt, R., Review Article: Structures of phthalocyanine molecules on surfaces studied by STM. *AIP Advances*. **2012**, 2, 041402.

(229) Sk, R.; Deshpande, A., Unveiling the emergence of functional materials with STM: metal phthalocyanine on surface architectures. *Mol. Syst. Des. Eng.* **2019**, 4, 471-483.

(230) Yudasaka, M.; Kikuchi, R.; Ohki, Y.; Yoshimura, S., Nitrogen-containing carbon nanotube growth from Ni phthalocyanine by chemical vapor deposition. *Carbon*. **1997**, 35, 195-201.

(231) Rubira, R. J. G.; Aoki, P. H. B.; Constantino, C. J. L.; Alessio, P., Supramolecular architectures of iron phthalocyanine Langmuir-Blodgett films: The role played by the solution solvents. *Appl. Surf. Sci.* **2017**, 416, 482-491.

(232) Chan, K.-Y.; Tou, T.-Y.; Teo, B.-S., Effects of substrate temperature on electrical and structural properties of copper thin films. *Microelectronics J.* **2006**, 37, 930-937.

(233) Kang, S. J.; Joung, Y. H., Influence of substrate temperature on the optical and piezoelectric properties of ZnO thin films deposited by rf magnetron sputtering. *Appl. Surf. Sci.* **2007**, 253, 7330-7335.

(234) Wei, Y.; Robey, S. W.; Reutt-Robey, J. E., Flux-Selected Titanyl Phthalocyanine Monolayer Architecture on Ag (111). *J. Chem. Phys. C*. **2008**, 112, 18537-18542.

(235) Sun, K.; Tao, M. L.; Tu, Y. B.; Wang, J. Z., Off-Center Rotation of CuPc Molecular Rotor on a Bi(111) Surface and the Chiral Feature. *Molecules*. **2017**, 22.

(236) Dou, W.; Huang, S.; Zhang, R. Q.; Lee, C. S., Molecule-substrate interaction channels of metal-phthalocyanines on graphene on Ni(111) surface. *J. Chem. Phys.* **2011**, 134, 094705.

(237) Zhang, J. L.; Zhong, J. Q.; Lin, J. D.; Hu, W. P.; Wu, K.; Xu, G. Q.; Wee, A. T. S.; Chen, W., Towards single molecule switches. *Chem. Soc. Rev.* **2015**, 44, 2998-3022.

(238) Zhang, J. L.; Xu, J. L.; Niu, T. C.; Lu, Y. H.; Liu, L.; Chen, W., Reversible Switching of a Single-Dipole Molecule Imbedded in Two-Dimensional Hydrogen-Bonded Binary Molecular Networks. *J. Chem. Phys. C*. **2014**, 118, 1712-1718.

(239) Hanack, M.; Deger, S.; Lange, A., Bisaxially coordinated macrocyclic transition metal complexes. *Coord. Chem. Rev.* **1988**, 83, 115-136.

(240) Ishikawa, N.; Sugita, M.; Ishikawa, T.; Koshihara, S. Y.; Kaizu, Y., Lanthanide double-decker complexes functioning as magnets at the single-molecular level. *J. Am. Chem. Soc.* **2003**, 125, 8694-8695.

(241) Elemans, J. A. A. W.; Rowan, A. E.; Nolte, R. J. M., Mastering molecular matter. Supramolecular architectures by hierarchical self-assembly. *J. Mater. Chem.* **2003**, 13, 2661-2670.

(242) Lin, C. F.; Zhang, M.; Liu, S. W.; Chiu, T. L.; Lee, J. H., High photoelectric conversion efficiency of metal phthalocyanine/fullerene heterojunction photovoltaic device. *Int J Mol Sci.* **2011**, 12, 476-505.

(243) D'Souza, F.; Ito, O., Supramolecular donor-acceptor hybrids of porphyrins/phthalocyanines with fullerenes/carbon nanotubes: electron transfer, sensing, switching, and catalytic applications. *Chem Commun (Camb)*. **2009**, 4913-4928.

(244) Zink-Lorre, N.; Font-Sanchis, E.; Seetharaman, S.; Karr, P. A.; Sastre-Santos, A.; D'Souza, F.; Fernandez-Lazaro, F., Directly Linked Zinc Phthalocyanine-Perylenediimide Dyads and a Triad for Ultrafast Charge Separation. *Chemistry*. **2019**, 25, 10123-10132.

(245) Gouloumis, A.; Gonzalez-Rodriguez, D.; Vazquez, P.; Torres, T.; Liu, S.; Echegoyen, L.; Ramey, J.; Hug, G. L.; Guldi, D. M., Control over charge separation in phthalocyanine-anthraquinone conjugates as a function of the aggregation status. *J Am Chem Soc.* **2006**, 128, 12674-12684.

(246) Rand, B. P.; Cheyns, D.; Vasseur, K.; Giebink, N. C.; Mothy, S.; Yi, Y.; Coropceanu, V.; Beljonne, D.; Cornil, J.; Brédas, J.-L.; Genoe, J., The Impact of Molecular Orientation on the Photovoltaic Properties of a Phthalocyanine/Fullerene Heterojunction. *Adv. Funct. Mater.* **2012**, 22, 2987-2995.

(247) Guldi, D. M.; Gouloumis, A.; Vázquez, P.; Torres, T.; Georgakilas, V.; Prato, M., Nanoscale Organization of a Phthalocyanine–Fullerene System: Remarkable Stabilization of Charges in Photoactive 1-D Nanotubules. *J Am Chem Soc.* **2005**, 127, 5811-5813.

(248) Zhang, F.; Ma, Y.; Chi, Y.; Yu, H.; Li, Y.; Jiang, T.; Wei, X.; Shi, J., Self-assembly, optical and electrical properties of perylene diimide dyes bearing unsymmetrical substituents at bay position. *Sci. Rep.* **2018**, 8, 8208.

(249) El-Khously, M. E.; Ito, O.; Smith, P. M.; D'Souza, F., Intermolecular and supramolecular photoinduced electron transfer processes of fullerene–porphyrin/phthalocyanine systems. *J. Photochem.* **2004**, 5, 79-104.

(250) Yaghi, O. M., Reticular Chemistry–Construction, Properties, and Precision Reactions of Frameworks. *J Am Chem Soc.* **2016**, 138, 15507-15509.

(251) Yaghi, O. M.; Kalmutzki, M. J.; Diercks, C. S., Introduction to Reticular Chemistry: Metal-Organic Frameworks and Covalent Organic Frameworks. **2019**.

(252) Paz, F. A.; Klinowski, J.; Vilela, S. M.; Tome, J. P.; Cavaleiro, J. A.; Rocha, J., Ligand design for functional metal-organic frameworks. *Chem Soc Rev.* **2012**, 41, 1088-1110.

(253) Stock, N.; Biswas, S., Synthesis of metal-organic frameworks (MOFs): routes to various MOF topologies, morphologies, and composites. *Chem Rev.* **2012**, 112, 933-969.

(254) Gao, W. Y.; Chrzanowski, M.; Ma, S., Metal-metallocporphyrin frameworks: a resurging class of functional materials. *Chem Soc Rev.* **2014**, 43, 5841-5866.

(255) Yaghi, O. M.; Li, H., Hydrothermal Synthesis of a Metal-Organic Framework Containing Large Rectangular Channels. *J Am Chem Soc.* **1995**, 117, 10401-10402.

(256) Yaghi, O. M., Reticular Chemistry: Molecular Precision in Infinite 2D and 3D. *Mol. Front. J.* **2019**, 03, 66-83.

(257) Sharma, R. K.; Yadav, P.; Yadav, M.; Gupta, R.; Rana, P.; Srivastava, A.; Zbořil, R.; Varma, R. S.; Antonietti, M.; Gawande, M. B., Recent development of covalent organic frameworks (COFs): synthesis and catalytic (organic-electro-photo) applications. *Mater. Horiz.* **2019**.

(258) Waller, P. J.; Gandara, F.; Yaghi, O. M., Chemistry of Covalent Organic Frameworks. *Acc Chem Res.* **2015**, 48, 3053-3063.

(259) Hunt, J. R.; Doonan, C. J.; LeVangie, J. D.; Cote, A. P.; Yaghi, O. M., Reticular synthesis of covalent organic borosilicate frameworks. *J Am Chem Soc.* **2008**, 130, 11872-11873.

(260) Guo, J.; Xu, Y.; Jin, S.; Chen, L.; Kaji, T.; Honsho, Y.; Addicoat, M. A.; Kim, J.; Saeki, A.; Ihee, H.; Seki, S.; Irle, S.; Hiramatsu, M.; Gao, J.; Jiang, D., Conjugated organic framework with three-dimensionally ordered stable structure and delocalized  $\pi$  clouds. *Nat. Commun.* **2013**, 4, 2736.

(261) Uribe-Romo, F. J.; Doonan, C. J.; Furukawa, H.; Oisaki, K.; Yaghi, O. M., Crystalline covalent organic frameworks with hydrazone linkages. *J Am Chem Soc.* **2011**, 133, 11478-11481.

(262) Segura, J. L.; Mancheno, M. J.; Zamora, F., Covalent organic frameworks based on Schiff-base chemistry: synthesis, properties and potential applications. *Chem Soc Rev.* **2016**, 45, 5635-5671.

(263) Colson, J. W.; Dichtel, W. R., Rationally synthesized two-dimensional polymers. *Nature Chemistry.* **2013**, 5, 453-465.

(264) Ding, X.; Guo, J.; Feng, X.; Honsho, Y.; Guo, J.; Seki, S.; Maitarad, P.; Saeki, A.; Nagase, S.; Jiang, D., Synthesis of metallophthalocyanine covalent organic frameworks that exhibit high carrier mobility and photoconductivity. *Angew Chem Int Ed Engl.* **2011**, 50, 1289-1293.

(265) Ding, X.; Chen, L.; Honsho, Y.; Feng, X.; Saengsawang, O.; Guo, J.; Saeki, A.; Seki, S.; Irle, S.; Nagase, S.; Parasuk, V.; Jiang, D., An n-channel two-dimensional covalent organic framework. *J Am Chem Soc.* **2011**, 133, 14510-14513.

(266) Jin, S.; Supur, M.; Addicoat, M.; Furukawa, K.; Chen, L.; Nakamura, T.; Fukuzumi, S.; Irle, S.; Jiang, D., Creation of Superheterojunction Polymers via Direct Polycondensation: Segregated and Bicontinuous Donor-Acceptor pi-Columnar Arrays in Covalent Organic Frameworks for Long-Lived Charge Separation. *J Am Chem Soc.* **2015**, 137, 7817-7827.

(267) Colson, J. W.; Woll, A. R.; Mukherjee, A.; Levendorf, M. P.; Spitler, E. L.; Shields, V. B.; Spencer, M. G.; Park, J.; Dichtel, W. R., Oriented 2D Covalent Organic Framework Thin Films on Single-Layer Graphene. *Science.* **2011**, 332, 228-231.

(268) Colson, J. W.; Mann, J. A.; DeBlase, C. R.; Dichtel, W. R., Patterned growth of oriented 2D covalent organic framework thin films on single-layer graphene. *J. Polym. Sci.* **2015**, 53, 378-384.

(269) Neti, V. S. P. K.; Wu, X.; Hosseini, M.; Bernal, R. A.; Deng, S.; Echegoyen, L., Synthesis of a phthalocyanine 2D covalent organic framework. *CrystEngComm.* **2013**, 15, 7157.

(270) Neti, V. S. P. K.; Wu, X.; Deng, S.; Echegoyen, L., Synthesis of a phthalocyanine and porphyrin 2D covalent organic framework. *CrystEngComm.* **2013**, 15, 6892.

(271) Zhao, F.; Liu, H.; Mathe, S. D. R.; Dong, A.; Zhang, J., Covalent Organic Frameworks: From Materials

Design to Biomedical Application. *Nanomaterials (Basel)*. **2017**, 8.

(272) Wang, M.; Ballabio, M.; Wang, M.; Lin, H. H.; Biswal, B. P.; Han, X.; Paasch, S.; Brunner, E.; Liu, P.; Chen, M.; Bonn, M.; Heine, T.; Zhou, S.; Canovas, E.; Dong, R.; Feng, X., Unveiling Electronic Properties in Metal-Phthalocyanine-Based Pyrazine-Linked Conjugated Two-Dimensional Covalent Organic Frameworks. *J Am Chem Soc*. **2019**, 141, 16810-16816.

(273) Li, H.; Ding, X.; Han, B. H., Porous Azo-Bridged Porphyrin-Phthalocyanine Network with High Iodine Capture Capability. *Chemistry*. **2016**, 22, 11863-11868.

(274) Ding, X.; Han, B. H., Metallophthalocyanine-based conjugated microporous polymers as highly efficient photosensitizers for singlet oxygen generation. *Angew Chem Int Ed Engl*. **2015**, 54, 6536-6539.

(275) Clough, A. J.; Yoo, J. W.; Mecklenburg, M. H.; Marinescu, S. C., Two-dimensional metal-organic surfaces for efficient hydrogen evolution from water. *J Am Chem Soc*. **2015**, 137, 118-121.

(276) Jin, S.; Ding, X.; Feng, X.; Supur, M.; Furukawa, K.; Takahashi, S.; Addicoat, M.; El-Khoushy, M. E.; Nakamura, T.; Irle, S.; Fukuzumi, S.; Nagai, A.; Jiang, D., Charge dynamics in a donor-acceptor covalent organic framework with periodically ordered bicontinuous heterojunctions. *Angew Chem Int Ed Engl*. **2013**, 52, 2017-2021.

(277) Ding, X.; Feng, X.; Saeki, A.; Seki, S.; Nagai, A.; Jiang, D., Conducting metallophthalocyanine 2D covalent organic frameworks: the role of central metals in controlling  $\pi$ -electronic functions. *Chem Commun*. **2012**, 48, 8952.

(278) Spitzer, E. L.; Colson, J. W.; Uribe-Romo, F. J.; Woll, A. R.; Giovino, M. R.; Saldivar, A.; Dichtel, W. R., Lattice expansion of highly oriented 2D phthalocyanine covalent organic framework films. *Angew Chem Int Ed Engl*. **2012**, 51, 2623-2627.

(279) Guo, J.-H.; Zhang, H.; Liu, Z.-P.; Cheng, X.-L., Multiscale Study of Hydrogen Adsorption, Diffusion, and Desorption on Li-Doped Phthalocyanine Covalent Organic Frameworks. *J. Chem. Phys. C*. **2012**, 116, 15908-15917.

(280) Li, W.; Sun, L.; Qi, J.; Jarillo-Herrero, P.; Dinca, M.; Li, J., High temperature ferromagnetism in  $\pi$ -conjugated two-dimensional metal-organic frameworks. *Chem Sci*. **2017**, 8, 2859-2867.

(281) Nagatomi, H.; Yanai, N.; Yamada, T.; Shiraishi, K.; Kimizuka, N., Synthesis and Electric Properties of a Two-Dimensional Metal-Organic Framework Based on Phthalocyanine. *Chemistry*. **2018**, 24, 1806-1810.

(282) Zhong, H.; Ly, K. H.; Wang, M.; Krupskaya, Y.; Han, X.; Zhang, J.; Zhang, J.; Kataev, V.; Buchner, B.; Weidinger, I. M.; Kaskel, S.; Liu, P.; Chen, M.; Dong, R.; Feng, X., A Phthalocyanine-Based Layered Two-Dimensional Conjugated Metal-Organic Framework as a Highly Efficient Electrocatalyst for the Oxygen Reduction Reaction. *Angew Chem Int Ed Engl*. **2019**, 58, 10677-10682.

(283) Yang, C.; Dong, R.; Wang, M.; Petkov, P. S.; Zhang, Z.; Wang, M.; Han, P.; Ballabio, M.; Brauninger, S. A.; Liao, Z.; Zhang, J.; Schwotzer, F.; Zschech, E.; Klauss, H. H.; Canovas, E.; Kaskel, S.; Bonn, M.; Zhou, S.; Heine, T.; Feng, X., A semiconducting layered metal-organic framework magnet. *Nat Commun*. **2019**, 10, 3260.

(284) Zhong, H.; Ghorbani-Asl, M.; Ly, K. H.; Zhang, J.; Ge, J.; Wang, M.; Liao, Z.; Makarov, D.; Zschech, E.; Brunner, E.; Weidinger, I. M.; Zhang, J.; Krasheninnikov, A. V.; Kaskel, S.; Dong, R.; Feng, X., Synergistic electroreduction of carbon dioxide to carbon monoxide on bimetallic layered conjugated metal-organic frameworks. *Nat Commun*. **2020**, 11, 1409.

(285) Evans, A. M.; Parent, L. R.; Flanders, N. C.; Bisbey, R. P.; Vitaku, E.; Kirschner, M. S.; Schaller, R. D.; Chen, L. X.; Gianneschi, N. C.; Dichtel, W. R., Seeded growth of single-crystal two-dimensional covalent organic frameworks. *Science*. **2018**, 361, 52.

(286) Falcaro, P.; Buso, D.; Hill, A. J.; Doherty, C. M., Patterning techniques for metal organic frameworks. *Adv Mater*. **2012**, 24, 3153-3168.

(287) Howarth, A. J.; Peters, A. W.; Vermeulen, N. A.; Wang, T. C.; Hupp, J. T.; Farha, O. K., Best Practices for the Synthesis, Activation, and Characterization of Metal-Organic Frameworks. *Chem. Mater*. **2017**, 29, 26-39.

(288) Wang, F.; Liu, Z.; Yang, C.; Zhong, H.; Nam, G.; Zhang, P.; Dong, R.; Wu, Y.; Cho, J.; Zhang, J.; Feng, X., Fully Conjugated Phthalocyanine Copper Metal-Organic Frameworks for Sodium-Iodine Batteries with Long-Time-Cycling Durability. *Adv Mater*. **2019**, e1905361.

(289) Feldblyum, J. I.; McCreery, C. H.; Andrews, S. C.; Kurosawa, T.; Santos, E. J.; Duong, V.; Fang, L.; Ayzner, A. L.; Bao, Z., Few-layer, large-area, 2D covalent organic framework semiconductor thin films. *Chem Commun (Camb)*. **2015**, 51, 13894-13897.

(290) Matsumoto, M.; Valentino, L.; Stiehl, G. M.; Balch, H. B.; Corcos, A. R.; Wang, F.; Ralph, D. C.; Mariñas, B. J.; Dichtel, W. R., Lewis-Acid-Catalyzed Interfacial Polymerization of Covalent Organic Framework Films. *Chem*. **2018**, 4, 308-317.

(291) Medina, D. D.; Rotter, J. M.; Hu, Y.; Dogru, M.; Werner, V.; Auras, F.; Markiewicz, J. T.; Knochel, P.; Bein, T., Room temperature synthesis of covalent-organic framework films through vapor-assisted conversion. *J Am Chem Soc*. **2015**, 137, 1016-1019.

(292) Patterson, J. P.; Abellán, P.; Denny, M. S.; Park, C.; Browning, N. D.; Cohen, S. M.; Evans, J. E.; Gianneschi, N. C., Observing the Growth of Metal-Organic Frameworks by in Situ Liquid Cell Transmission Electron Microscopy. *J Am Chem Soc*. **2015**, 137, 7322-7328.

(293) Jones, C. G.; Martynowycz, M. W.; Hattne, J.; Fulton, T. J.; Stoltz, B. M.; Rodriguez, J. A.; Nelson, H. M.; Gonen, T., The CryoEM Method MicroED as a Powerful

1 Tool for Small Molecule Structure Determination. *ACS Cent Sci.* **2018**, *4*, 1587-1592.

2 (294) Li, R. L.; Flanders, N. C.; Evans, A. M.; Ji, W.;

3 Castano, I.; Chen, L. X.; Gianneschi, N. C.; Dichtel, W. R.,

4 Controlled growth of imine-linked two-dimensional

5 covalent organic framework nanoparticles. *Chem Sci.*

6 **2019**, *10*, 3796-3801.

7 (295) Li, H.; Chavez, A. D.; Li, H.; Li, H.; Dichtel, W. R.;

8 Bredas, J. L., Nucleation and Growth of Covalent Organic

9 Frameworks from Solution: The Example of COF-5. *J Am*

10 *Chem Soc.* **2017**, *139*, 16310-16318.

11 (296) Brillson, L. J., An Essential Guide to Electronic

12 Material Surfaces and Interfaces *Wiley*. **2016**.

13 (297) Assour, J. M.; Harrison, S. E., Electrical

14 conductivity of metal-free and copper phthalocyanine

15 crystals. *J. Phys. Chem. Solids.* **1965**, *26*, 670-672.

16 (298) Pham, H. Q.; Le, D. Q.; Pham-Tran, N.-N.;

17 Kawazoe, Y.; Nguyen-Manh, D., Electron delocalization

18 in single-layer phthalocyanine-based covalent organic

19 frameworks: a first principle study. *RSC Advances.*

20 **2019**, *9*, 29440-29447.

21 (299) Guldi, D. M.; Ramey, J.; Martinez-Diaz, M. V.; de

22 la Escosura, A.; Torres, T.; Da Ros, T.; Prato, M.,

23 Reversible zinc phthalocyanine fullerene ensembles.

24 *Chem Commun (Camb)*. **2002**, 2774-2775.

25 (300) Mandal, A. K.; Mahmood, J.; Baek, J.-B., Two-

26 Dimensional Covalent Organic Frameworks for

27 Optoelectronics and Energy Storage. *ChemNanoMat*.

28 **2017**, *3*, 373-391.

29 (301) Shimizu, D.; Osuka, A., Porphyrinoids as a

30 platform of stable radicals. *Chem Sci.* **2018**, *9*, 1408-1423.

31 (302) Blicke, F. F., The Mannich Reaction. *Organic*

32 *Reactions*. **2011**, 303-341.

33 (303) Dong, R.; Han, P.; Arora, H.; Ballabio, M.;

34 Karakus, M.; Zhang, Z.; Shekhar, C.; Adler, P.; Petkov, P.

35 S.; Erbe, A.; Mannsfeld, S. C. B.; Felser, C.; Heine, T.;

36 Bonn, M.; Feng, X.; Cánovas, E., High-mobility band-like

37 charge transport in a semiconducting two-dimensional

38 metal-organic framework. *Nat. Mater.* **2018**, *17*, 1027-1032.

39 (304) Sun, L.; Park, S. S.; Sheberla, D.; Dinca, M.,

40 Measuring and Reporting Electrical Conductivity in

41 Metal-Organic Frameworks: Cd<sub>2</sub>(TTFTB) as a Case

42 Study. *J Am Chem Soc.* **2016**, *138*, 14772-14782.

43 (305) Walsh, A.; Butler, K. T.; Hendon, C. H., Chemical

44 principles for electroactive metal-organic frameworks.

45 *MRS Bulletin*. **2016**, *41*, 870-876.

46 (306) Murase, R.; Ding, B.; Gu, Q.; D'Alessandro, D. M.,

47 Prospects for electroactive and conducting framework

48 materials. *Philos Trans A Math Phys Eng Sci.* **2019**, *377*,

49 20180226.

50 (307) Mukherjee, D.; Manjunatha, R.; Sampath, S.;

51 Ray, A. K., Phthalocyanines as Sensitive Materials for

52 Chemical Sensors. **2017**, 165-226.

53

54 (308) Fan, F.-R.; Faulkner, L. R., Phthalocyanine thin

55 films as semiconductor electrodes. *J Am Chem Soc.*

56 **1979**, *101*, 4779-4787.

57 (309) Koo, W.-T.; Jang, J.-S.; Kim, I.-D., Metal-Organic

58 Frameworks for Chemiresistive Sensors. *Chem.* **2019**, *5*,

59 1938-1963.

60 (310) Catlow, C. R.; Davidson, M.; Hardacre, C.;

1 Hutchings, G. J., Catalysis making the world a better

2 place. *Philos Trans A Math Phys Eng Sci.* **2016**, 374.

3 (311) Elizarova, G. L.; Matvienko, L. G.; Lozhkina, N.

4 V.; Maizlish, V. E.; Parmon, V. N., Homogeneous catalysts

5 for dioxygen evolution from water. Oxidation of water

6 by trisbipyridylruthenium(III) in the presence of

7 metallophthalocyanines. *React Kinet Catal L.* **1981**, *16*,

8 285-288.

9 (312) Mamuru, S. A.; Ozoemena, K. I., Heterogeneous

10 Electron Transfer and Oxygen Reduction Reaction at

11 Nanostructured Iron(II) Phthalocyanine and Its

12 MWCNTs Nanocomposites. *Electroanalysis*. **2010**, *22*,

13 985-994.

14 (313) Zheng, F.; Xiang, D.; Li, P.; Zhang, Z.; Du, C.;

15 Zhuang, Z.; Li, X.; Chen, W., Highly Conductive Bimetallic

16 Ni-Fe Metal Organic Framework as a Novel

17 Electrocatalyst for Water Oxidation. *ACS Sustain. Chem.*

18 *Eng.* **2019**, *7*, 9743-9749.

19 (314) Zagal, J. H.; Páez, M. A.; Silva, J. F., Fundamental

20 Aspects on the Catalytic Activity of Metallomacrocyclics

21 for the Electrochemical Reduction of O<sub>2</sub>. **2006**, 41-82.

22 (315) Miner, E. M.; Fukushima, T.; Sheberla, D.; Sun,

23 L.; Surendranath, Y.; Dinca, M., Electrochemical oxygen

24 reduction catalysed by Ni<sub>3</sub>(hexaminotriphenylene)2.

25 *Nat Commun.* **2016**, *7*, 10942.

26 (316) Yoshimoto, S.; Tada, A.; Suto, K.; Itaya, K.,

27 Adlayer Structures and Electrocatalytic Activity for O<sub>2</sub>

28 of Metallophthalocyanines on Au(111): In Situ

29 Scanning Tunneling Microscopy Study. *J. Chem. Phys B*.

30 **2003**, *107*, 5836-5843.

31 (317) Qing, X.; Shi, J.; Xu, P.; Xu, J.; Qiao, J., The Oxygen

32 Reduction Reaction Catalyzed by Carbon-Supported

33 Copper Phthalocyanine Tetrasulfonic Acid (CuPcTS/C)

34 by High Temperature Treatment. *ECS Transactions*.

35 **2013**, *58*, 1347-1352.

36 (318) Meshitsuka, S.; Ichikawa, M.; Tamaru, K.,

37 Electrocatalysis by metal phthalocyanines in the

38 reduction of carbon dioxide. *J. Chem. Soc.* **1974**, 158.

39 (319) Grodkowski, J.; Dhanasekaran, T.; Neta, P.;

40 Hambright, P.; Brunschwig, B. S.; Shinozaki, K.; Fujita, E.,

41 Reduction of Cobalt and Iron Phthalocyanines and the

42 Role of the Reduced Species in Catalyzed

43 Photoreduction of CO<sub>2</sub>. *The Journal of Physical*

44 *Chemistry A*. **2000**, *104*, 11332-11339.

45 (320) Han, N.; Wang, Y.; Ma, L.; Wen, J.; Li, J.; Zheng,

46 H.; Nie, K.; Wang, X.; Zhao, F.; Li, Y.; Fan, J.; Zhong, J.; Wu,

47 T.; Miller, D. J.; Lu, J.; Lee, S.-T.; Li, Y., Supported Cobalt

48 Polyphthalocyanine for High-Performance

49 Electrocatalytic CO<sub>2</sub> Reduction. *Chem.* **2017**, *3*, 652-664.

1 (321) Zagal, J. H.; Griveau, S.; Ozoemena, K. I.;  
2 Nyokong, T.; Bedioui, F., Carbon nanotubes,  
3 phthalocyanines and porphyrins: attractive hybrid  
4 materials for electrocatalysis and electroanalysis. *J  
5 Nanosci Nanotechnol.* **2009**, 9, 2201-2214.

6 (322) Yoshida, T.; Kamato, K.; Tsukamoto, M.; Iida, T.;  
7 Schlettwein, D.; Wöhrle, D.; Kaneko, M., Selective  
8 electroacatalysis for CO<sub>2</sub> reduction in the aqueous  
9 phase using cobalt phthalocyanine/poly-4-  
10 vinylpyridine modified electrodes. *J. Electroanal. Chem.*  
11 **1995**, 385, 209-225.

12 (323) Lin, S.; Diercks, C. S.; Zhang, Y.-B.; Kornienko, N.;  
13 Nichols, E. M.; Zhao, Y.; Paris, A. R.; Kim, D.; Yang, P.;  
14 Yaghi, O. M.; Chang, C. J., Covalent organic frameworks  
15 comprising cobalt porphyrins for catalytic CO<sub>2</sub>  
16 reduction in water. *Science.* **2015**, 349, 1208-1213.

17 (324) Kilby, J. S., Invention of the integrated circuit.  
18 *IEEE Transactions on Electron Devices.* **1976**, 23, 648-  
19 654.

20 (325) Olson, G. B., Computational Design of  
21 Hierarchically Structured Materials. *Science.* **1997**, 277,  
22 1237-1242.

23 (326) Erucar, I.; Keskin, S., High-Throughput  
24 Molecular Simulations of Metal Organic Frameworks for  
25 CO<sub>2</sub> Separation: Opportunities and Challenges.  
26 *Frontiers in Materials.* **2018**, 5.

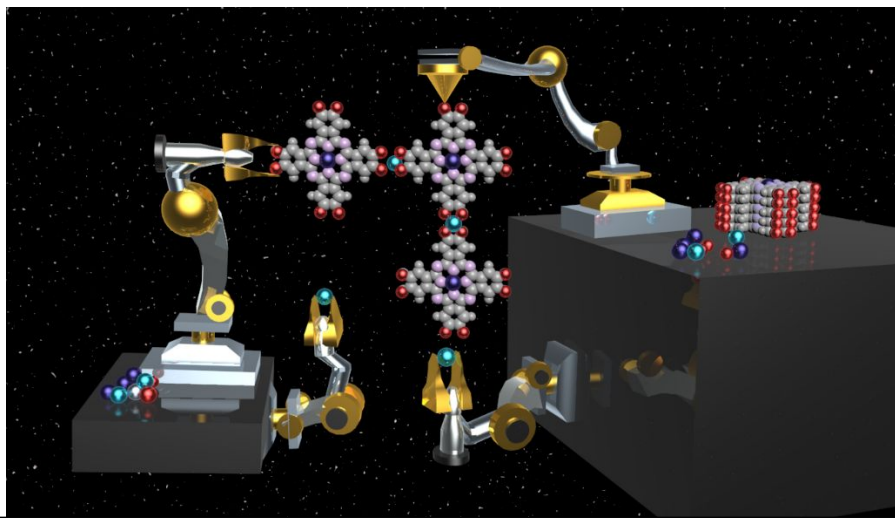
27 (327) Sholl, D. S.; Lively, R. P., Defects in Metal-  
Organic Frameworks: Challenge or Opportunity? *The  
28  
29  
30  
31  
32  
33  
34  
35  
36  
37  
38  
39  
40  
41  
42  
43  
44  
45  
46  
47  
48  
49  
50  
51  
52  
53  
54  
55  
56  
57  
58  
59  
60* *Journal of Physical Chemistry Letters.* **2015**, 6, 3437-  
3444.

(328) Hobbs, J. K.; Humphris, A. D. L.; Miles, M. J., In-Situ Atomic Force Microscopy of Polyethylene Crystallization. 1. Crystallization from an Oriented Backbone. *Macromolecules.* **2001**, 34, 5508-5519.

(329) Hirschle, P.; Preiß, T.; Auras, F.; Pick, A.; Völkner, J.; Valdepérez, D.; Witte, G.; Parak, W. J.; Rädler, J. O.; Wuttke, S., Exploration of MOF nanoparticle sizes using various physical characterization methods – is what you measure what you get? *CrystEngComm.* **2016**, 18, 4359-4368.

(330) Nannenga, B. L.; Gonen, T., The cryo-EM method microcrystal electron diffraction (MicroED). *Nature Methods.* **2019**, 16, 369-379.

(331) Pambudi, F. I.; Anderson, M. W.; Attfield, M. P., Unveiling the mechanism of lattice-mismatched crystal growth of a core-shell metal-organic framework. *Chem Sci.* **2019**, 10, 9571-9575.



1  
2  
3  
4  
5  
6  
7  
8  
9  
10  
11  
12  
13  
14  
15  
16  
17  
18  
19  
20  
21  
22  
23  
24  
25  
26  
27  
28  
29  
30  
31  
32  
33  
34  
35  
36  
37  
38  
39  
40  
41  
42  
43  
44  
45  
46  
47  
48  
49  
50  
51  
52  
53  
54  
55  
56  
57  
58  
59  
60